IMPERIAL COLLEGE LONDON

DEPARTMENT of MEDICINE

DIVISION of BRAIN SCIENCES

# The role of serotonergic and dopaminergic mechanisms and their interaction in levodopa–induced dyskinesias

A thesis submitted for the degree of Doctor of Philosophy

Andreas–Antonios Roussakis

# Table of contents

# Abstract

Long–term levodopa treatment in Parkinson's disease (PD) is commonly associated with troublesome levodopa–induced dyskinesias (LIDs). Striatal serotonergic terminals amid the degenerating dopaminergic ones are proposed to play an important role in LIDs by taking up exogenous levodopa and releasing dopamine in an unregulated fashion. However, to date, the underlying mechanisms of LIDs are not fully understood.

By using single photon emission computed tomography (SPECT) with $^{123}$I–Ioflupane and positron emission tomography (PET) with $^{11}$C–DASB and $^{11}$C–PE2I, the clinical studies conducted for this thesis aimed (a) to estimate the role of striatal dopamine transporter (DAT) availability in early PD as a prognostic marker for LIDs, (b) to explore whether striatal DAT availability changes over time are related to the appearance of LIDs, (c) to estimate the role of striatal serotonin-to-dopamine transporter (SERT–to–DAT) binding ratios to LIDs, and (d) to look for a relation between the changes in striatal SERT, DAT and SERT–to–DAT binding ratios over time and the appearance of LIDs.

The main findings are as follows: (a) in early PD, striatal DAT availability alone does not predict the appearance of future LIDs, (b) at later stages, the occurrence of LIDs may be dependent on the magnitude of DAT decline in the putamen, (c) the SERT–to–DAT binding ratio in the putamen is increased in PD patients as compared to controls, and within PD, it is higher in patients with LIDs as compared to nondyskinetic patients, (d) as PD continues to progress, putaminal serotonergic

terminals remain relatively unchanged in comparison to the dopaminergic ones and the aforementioned imbalance (as reflected by the binding ratio) increases over time. These findings provide fundamental insight in the pathophysiology of LIDs and have direct implications for further research towards novel therapeutics in PD dyskinesia.

# Declaration of originality and Preface

I hereby declare that this thesis and work described within, is my personal work except where specifically stated or referenced. This work was conducted at the Centre for Neuroinflammation and Neurodegeneration within the Division of Brain Sciences, at the Medical School of Imperial College in London.

This thesis has not been submitted for any other degree, diploma or other qualification at any other academic institution.

I have no interests to disclose.

This thesis is 50310 words long (including 10170 words as bibliography and appendices and a 298 words long abstract) and contains 17 tables, 37 figures and graphs, 2 boxes and 37 equations.

Andreas-Antonios Roussakis

# Copyright declaration

Andreas-Antonios Roussakis

# Acknowledgements

# Statement of contribution

This thesis comprises a series of studies that may be part of larger research projects in terms of funding and ethics applications. I had a significant contribution in the majority of them including the design, setup and of course the conduct of these studies.

Specifically, for the REC Ref. 12/LO/0414 project (*Chapters 3, 4,* and *5*) I wrote and submitted all the documentation needed for the application to the West London Research Ethics Committee, the Imperial College Joint Research Compliance Office (JRCO) and the Administration of Radioactive Substances Advisory Committee (ARSAC). I also wrote all the additional documentation needed for these applications, including the IRAS forms, the participant information sheet and consent forms, the letter to General Practitioners and the web–based advertisements. I liaised with the REC, the JRCO, the National Institute for Health Research Clinical Research Network (NIHR CRN) and ARSAC committees until the project received favourable approvals and continued liaising with them, whereas it was necessary.

I was liaising closely with the Nuclear Medicine department, the management office of the Research Imaging department of the Imperial College Healthcare NHS Trust and Imanova Ltd to ensure that the projects will be conducted as per protocol. I continuously ensured compliance with Good Clinical Practice throughout the conduct

of the studies and my licence to practice medicine in the UK was successfully revalidated by the General Medical Council.

I have managed the identification of potential participants and have actively recruited study subjects. I conducted initial face–to–face and phone-based pre–screening interviews with all subjects interested in the imaging studies. I explained to potential participants the background and rationale of each study and the study procedures. I obtained written informed consent whereas screening was successful, based on the review of the relevant inclusion/exclusion criteria.

I have been responsible of the medical governance of the study. I reviewed results from the magnetic resonance imaging (MRI) scans and any significantly clinical incidental findings were appropriately treated and communicated to the General Practitioners and the Consultant Neurologist of participant's direct care. I conducted all SPECT scanning and the majority of PET and MRI scanning briefly including venous cannulation, radioligand administration and inspection of scanning procedures. I run all SPECT imaging analysis and I collaborated in the analysis of a part of the PET imaging data with Mr Nick Lao–Kaim. I run all statistical analyses, including between group comparisons and correlations between imaging and clinical data.

I provided the initial interpretation of the findings of each study and coordinated the review and the subsequent discussion with all the collaborators.

# Peer–reviewed publications contributing to this thesis

*Original research articles*

1. **Roussakis AA**, Politis M, Towey D and Piccini P. Serotonin–to–dopamine transporter ratios in Parkinson disease: Relevance for dyskinesias; 2016; *Neurology; 86(12):1152-8.*

2. **Roussakis AA**, Politis M, Towey D and Piccini P. Longitudinal study of presynaptic dopaminergic mechanisms in Parkinson's disease: Relevance for dyskinesias; *in preparation*

3. **Roussakis AA**, Lao-Kaim N*, Martín–Bastida A, Valle-Guzman N, Kefalopoulou Z, Paul–Visse G, Widner H, Politis M, Foltynie T, Barker RA, Piccini P. Increased serotonin–to–dopamine transporter ratios in Parkinson's disease dyskinesias: a longitudinal study. *in preparation*

4. Rolinski M, Griffanti L, Piccini P, **Roussakis AA**, Szewczyk-Krolikowski K, Menke RA, Quinnell T, Zaiwalla Z, Klein JC, Mackay CE, Hu MT. Basal ganglia dysfunction in idiopathic REM sleep behaviour disorder parallels that in early Parkinson's disease. *Brain*. 2016; 139(Pt 8):2224-34.

5. Li W, Lao-Kaim NP, **Roussakis AA**, Martín-Bastida A, Valle-Guzman N, Paul G, Loane C, Widner H, Politis M, Foltynie T, Barker RA, Piccini P. ^{11}C-PE2I

and ^{18}F-Dopa PET for assessing progression rate in Parkinson's: A longitudinal study. Mov Disord. 2018; 33(1):117-127.

*Review article*

1. **Roussakis AA**, Piccini P, Politis M. Clinical utility of DaTscan™ ([123]I -Ioflupane Injection) in the diagnosis of Parkinsonian Syndromes. 2013; *Degenerative Neurological and Neuromuscular Disease*

*Conferences and scientific meetings of special interest*

a) **Roussakis AA** and Piccini P. Predictor value of Dopamine Transporter (DAT) availability at time of diagnosis for clinical disease's progression in Parkinson's disease. Parkinson's UK annual meeting, York, UK, 2014 (*poster presentation*)

b) **Roussakis AA**, Politis M, Towey D and Piccini P. Parkinson's disease progression is associated with increased putaminal serotonin to dopamine transporter ratio: relevance for dyskinesias. American Academy of Neurology annual meeting, Washington DC, USA, 2015 (*dual oral presentation and poster presentation*)

c) **Roussakis AA**, Politis M, Towey D and Piccini P. Serotonin-to-dopamine transporter ratios in the striatum of patients with Parkinson's disease: impact on Levodopa–induced dyskinesia. Association of British Neurologists annual meeting, Harrogate, UK, 2015 (*poster presentation*)

d) **Roussakis AA**, Politis M, Towey D and Piccini P. Levodopa induced dyskinesias: increased serotonin to dopamine transporter ratios in the putamen of Parkinson's disease patients. European Academy of Neurology annual meeting, Berlin, Germany, 2015 (*oral and poster presentation*)

*e)* Li W, Lao–Kaim N, **Roussakis AA**, Martín–Bastida A, Politis M, Valle–Guzman N, Kefalopoulou Z, Paul G, Widner H, Foltynie T, Barker R, Piccini P. Comparison of $^{11}$C–PE2I and $^{18}$F–Dopa PET for assessing progression and severity in patients with Early Parkinson's disease.  NECTAR annual meeting, Lund, Sweden, 2015 (*oral presentation*)

*f)* **Roussakis AA**, Lao–Kaim N, Martin–Bastida A, Valle–Guzman N, Kefalopoulou Z, Paul G, Widner H et al. ,Increased serotonin–to– dopamine transporter ratios in Parkinson's disease dyskinesias: a longitudinal study. European Academy of Neurology annual meeting, Copenhagen, Denmark, 2016 (*oral presentation*)

*g*) **Roussakis AA**, Lao-Kaim N, Martin-Bastida A, Valle-Guzman N, Politis M, Foltynie T, Barker R, Piccini Pet al., 2017, Serotonin-to-dopamine transporter ratios in Parkinson's dyskinesias: The longitudinal study, 21st International Congress of Parkinson's Disease and Movement Disorders, (*poster presentation*)

*h*) **Roussakis AA**, Towey D, Piccini P. Changes over time in striatal DAT availability in Parkinson's: relevance to levodopa-induced dyskinesias. European Academy of Neurology annual meeting, Amsterdam, Netherlands, 2017 (*e– presentation*)

# Overview of Chapters

*Chapter 1* introduces Parkinson's disease dyskinesias through a clinical overview of Parkinson's disease and our current understanding on dyskinesias centred on evidence from previous studies. The rationale, aims and hypotheses of the studies presented in this thesis are included at the end of this chapter.

*Chapter 2* contains the methodology used for the studies of this thesis including details relevant to the recruitment of participants and clinical evaluations performed to both Parkinson's disease patients and controls, the technical methodology details relative to PET and SPECT imaging and finally the details of the statistical analyses.

In *Chapter 3*, I present a SPECT study in Parkinson's disease, in which I investigated whether DAT availabilities in the striatum at diagnosis can predict the onset of dyskinesia.

*Chapter 4* contains a longitudinal SPECT study of ^{123}I–Ioflupane in relation to dyskinesias in Parkinson's disease.

In *Chapter 5*, by using PET with ^{11}C–DASB and SPECT with ^{123}I–Ioflupane, I investigated the role of SERT over DAT availabilities in the striatum in relation to dyskinesias.

*In Chapter 6*, I report a longitudinal PET study of the role of the SERT, DAT and SERT–to–DAT binding ratios in the striatum of Parkinson's disease patients with and without dyskinesias.

*Chapter 7* includes the discussion of findings for the above studies in the context. At the end of this chapter, I have included the limitations and recommendations for future work.

# List of tables

# List of figures and graphs

# List of boxes

# Glossary of abbreviated terms

| abbreviated name | full name |
|---|---|
| | |
| 5–HT1a……………………… | type 1a serotonin receptor |
| 5–HT1b…….………………. | type 1b serotonin receptor |
| AADC…………………….... | aromatic L-amino acid decarboxylase |
| AIMS…………….………… | abnormal involuntary movements |
| ANOVA……………………. | analysis of variance |
| BDI…………….…………… | Beck's depression inventory |
| BP……………………….….. | *in vitro* binding potential |
| BP′……………….………….. | modified binding potential |
| BP$_{ND}$…………………….…… | nondisplaceable binding potential |
| CT…………………………... | computed tomography |
| DAT……………….……….... | dopamine transporter |
| DBS…………………….…… | deep brain stimulation |
| DD$_{diagn}$……………….………. | disease duration from diagnosis |
| DV………………………….. | distribution volume |
| DVR……………….………... | distribution volume ratio |
| FPB……………….………… | filter back projection |
| GPi………………………….. | globus pallidus internus |
| HAM–D……………….…….. | Hamilton rating scale for depression |
| LCIG………………….…….. | intestinal levodopa/carbidopa gel |
| LED$_{Dag}$……………….……….. | dopamine receptor agonist equivalent dose |
| LED$_{Ldopa}$…………….………… | levodopa equivalent dose |
| LED$_{Total}$……………….……… | total dopaminergic–levodopa equivalent dose |
| LIDs……………….………… | levodopa–induced dyskinesias |
| MMSE…………….………… | mini mental state examination |
| MNI…………………….…….. | Montreal Neurological Institute |
| MRI……………….………… | magnetic resonance imaging |

| | |
|---|---|
| MRI$_R$………………………..……… | MRI images registered to MNI template |
| NMDA………………………... | N-methyl-D-aspartate |
| OSEM…………………………. | ordered subset expectation maximisation |
| PET……………………………. | positron emission tomography |
| REM…………………………… | rapid eye movement |
| ROI……………………………. | region of interest |
| SBR……………………………. | specific binding ratio |
| SPM…………………………… | statistical parametric mapping |
| SD……………………………… | standard deviation |
| SERT…………………………... | serotonin transporter |
| SPECT………………………… | single photon emission computed tomography |
| SRTM…………………………. | simplified reference tissue model |
| STN…………………………… | subthalamic nucleus |
| UPDRS………………………… | unified Parkinson's disease rating scale |
| VOI…………………………… | volume of interest |

# 🖝 Chapter 1 – Introduction

## 1.1 Parkinson's disease – A brief overview

Parkinson's disease is a chronic neurodegenerative movement disorder which was firstly described as "paralysis agitans" by the English Surgeon James Parkinson back in 1817 in the popular "Essay on the shaking palsy" (Parkinson. 1817). It was only later renamed Parkinson's disease by the French Neurologist Jean–Martin Charcot (Charcot. 1877).

Parkinson's disease also known as idiopathic or primary Parkinsonism refers to the most common Parkinsonian syndrome. The term Parkinsonian syndrome or Parkinsonism refers to the main motor symptoms of the disease. Parkinsonism may be therefore primary (idiopathic Parkinsonism or of unknown aetiology), secondary due to vascular load in the basal ganglia, drug–induced, or psychogenic; although in some atypical cases Parkinsonism is linked to a genetic background (familiar Parkinsonism). Nonetheless, in most cases, the cause of Parkinsonism remains unknown.

It is thought that approximately 1 in 500 people are affected by Parkinson's disease; that is a population of approximately 127,000 people in the UK who live with this movement disorder. The prevalence rate of Parkinson's has been estimated to 31 among 10,000 males and 24 among 10,000 females, while the highest prevalence rate was among those aged over 80 years (Parkinson's UK. 2009). Parkinson's disease is the second most common neurodegenerative disorder after dementia. Based on the UK National Statistics Office 2009 data, mathematical prediction modelling, suggested

that Parkinson's disease prevalence rate in the UK will reach a 26.7% increase of the above figures by 2020 (Parkinson's UK. 2009).

## 1.2 Neuropathological features of Parkinson's disease

Severe loss of melanised neurons and the presence of intraneuronal Lewy bodies in the substantia nigra pars compacta (Fearnley and Lees. 1991) are believed to be the most important hallmarks of Parkinson's disease pathology. In particular, neuronal loss begins in the lateral ventral nigral tier which is the most affected anatomical region throughout the course of Parkinson's disease.

The loss of dopaminergic neurons in the midbrain is progressive and shows different patterns of neurodegeneration in Parkinson's disease (Damier et al., 1999). Nonetheless, the nigral damage is always accompanied by extranigral pathology including many cortical and subcortical regions. In that sense, regional selectivity of Lewy body pathology in Parkinson's disease is believed to reflect disease–specific neurodegenerative mechanisms. Braak and colleagues systematised Parkinson's disease-related intraneuronal pathology proposing that brain pathology begins in the medulla obloganta/pontine tegmentum and frequently in the anterior olfactory nucleus. Lewy body pathology continues on an ascending route in which the substantia nigra and other midbrain regions become progressively involved, until it finally appears in the neocortex and other forebrain regions (Braak et al., 2003). It is therefore proposed that Parkinson's–related pathology propagates in a stereotypic

pattern and that Lewy body pathology reaches the nigra not early on but at stage 3 (of Braak's staging system).

The above staging system refers to a topographic Lewy body pathology distribution rather than a classification of Parkinson's–related dysfunction of the affected brain regions. Newer techniques, including *in vivo* imaging in humans have enabled a dynamic approach to study molecular and cellular pathological mechanisms in living humans with Parkinson's. Hence, *in vivo* imaging of the human brain is able to reflect the distribution of dysfunction across dopaminergic and non–dopaminergic terminals and explore the relation of such dysfunction to clinical characteristics and severity of Parkinson's symptoms. However, the impact of *in vivo* clinical studies will rely on the ability to efficiently translate the evidence of their findings to clinical practice and novel therapeutics.

## 1.3 Diagnosis of Parkinson's disease

James Parkinson described clinically the "paralysis agitans" in his Essay (Parkinson. 1817) and characterised its symptoms as tremor at rest, slowness, shuffling gait, flexed posture, festination, falls, soft speech, dysphagia and "saliva trickling from the mouth" in a group of six patients. In addition, he noted the slow progression of the disease over time.

The diagnosis of idiopathic Parkinsonism still remains clinical. The cardinal motor symptoms of Parkinson's disease as we describe them today include tremor at rest,

bradykinesia, rigidity and postural instability. Nonetheless, clinical presentation of Parkinson's patients varies among individuals. Clinical presentation of patients with a probable diagnosis of Parkinson's disease is not always typical during the diagnostic process and to this end, a correct clinical diagnosis requires to refer to Parkinson's disease as a distinct clinical entity. The Queen Square Brain Bank diagnostic criteria are most commonly used for the clinical diagnosis of idiopathic Parkinson's disease (Hughes et al., 1992). Similarly, a correct clinical diagnosis of Parkinson's disease can be assisted by the diagnostic criteria proposed by the National Institute of Neurological disorders and stroke (Gelb et al., 1999).

## 1.4 Motor and non–motor symptoms

The tremor in Parkinson's disease (also described as pill–rolling tremor), is typically present at rest while it decreases on activation of movements. Typically, Parkinsonian–type tremor is unilateral in early disease and is commonly affecting the extremities. The frequency and intensity of tremor varies among individuals and is related to physical activity, levels of anxiety, and the effect of several agents such as caffeine, nicotine, and a-adrenergic blockers. An estimated 30% of Parkinson's patients have minimal or no resting tremor; commonly described as "akinetic–rigid" type of Parkinson's disease in comparison to "tremulous" Parkinson's. On neurological examination, tremor is typically present at rest, while absence of tremor can be noted when the hands and legs are examined in posture and in action.

Bradykinesia [<Greek βραδὺς (bradys=slow) + κίνησις (kinesis=movement, motion)]] refers to the slowness of movement. Bradykinesia can be general and can be accompanied by a lack of spontaneous movements. On neurological examination, bradykinesia can be detected in the extremities and can vary from mild to severe. In advanced disease, the term akinesia refers to the absence of movement. Bradykinesia can be also presented as micrographia (smaller handwriting), hypomimia (reduced facial mimic), hypophonia (soft speech), and reduced blink rate. Rigidity refers to muscle stiffness.

Rigidity can be detected in the neck, shoulders, upper and lower limbs. On neurological examination, cogwheel rigidity is the combination of tremor and "lead–pipe" rigidity most commonly in patient's wrist and arm, while it is felt by the examiner as resistance to passive movement. Postural instability is a common symptom in advanced disease which eventually leads to loss of postural reflexes, impaired balance and falls with consecutive injuries.

Parkinson's disease presents also with a range of non–motor symptoms (Chaudhuri et al., 2011) which may precede the development of the movement disorder. Common non–motor symptoms include rapid eye movement (REM) sleep behavioural disorder, insomnia, fatigue, weight loss, pain, reduced (or absence of) olfaction [namely hyposmia (or anosmia respectively)], apathy, depression, anxiety, constipation, orthostatic hypotension, erectile dysfunction, sexual dysfunction and reduced libido for females, excessive sweating, dysphagia, drooling, mild cognitive

impairment, and dementia. The most common motor and non–motor symptoms of

Parkinson's disease are listed in box 1.

Box 1 – List of the most common motor and non–motor symptoms of Parkinson's disease

| motor symptoms | bradykinesia<br>tremor at rest<br>rigidity<br>postural instability |
|---|---|

| autonomic dysfunction | orthostatic hypotension, hyperhidrosis, urinary urgency and nocturia, sexual dysfunction, weight loss |
|---|---|
| cognition | cognitive impairment, dementia |
| neuropsychiatric symptoms | depression, apathy, anxiety, distress, hallucinations, delusions, illusions |
| sensory symptoms | musculoskeletal pain, peripheral pain, hyposmia and anosmia, ageusia |
| sleep disturbances | REM behaviour disorder, excessive daytime somnolence, insomnia, restless legs syndrome, non–REM parasomnias |
| other | constipation, fatigue, dysphagia, excessive sialorrhea |

The Unified Parkinson's disease rating scale (UPDRS) is the most commonly used

clinical rating scale for assessing severity of Parkinson's disease symptoms and signs

(Fahn et al., 1987; Goetz et al., 2007).

Parkinson's disease is a progressive movement disorder and the Hoehn & Yahr clinical staging scale is widely used to classify progression clusters within a group of Parkinson's disease patients (Hoehn and Yahr. 1967). A 2010 study looked into a large cohort of Parkinson's disease patients and calculated the median time taken to transit from one Hoehn &Yahr stage to the next stage. Longer age at disease onset, longer disease duration and more severe disease at baseline were associated with a faster progression rate through Hoehn &Yahr stages (Zhao et al., 2010).

## 1.5 Pharmacotherapy in Parkinson's disease

Pharmacological research for treating Parkinson's disease before the definition of Parkinson's disease pathology had comprised several agents including mercury, ergot of rye, belladonna, chloroform, strychnine, phosphorus, a variety of alkaloids, synthetic antimuscarinics, amphetamines, and antihistamines (Fahn. 2015).

The breakthrough came with the discovery of striatal dopamine deficiency in Parkinson's by Oleh Hornykiewicz in 1960. Hornykiewicz and Ehringer demonstrated 90% loss of dopamine in the striatum of patients with Parkinson's disease while no loss was found in a group of patients with Huntington's disease (Ehringer and Hornykiewicz. 1960). Hornykiewicz and colleagues reported that dopamine was also significantly reduced in the substantia nigra in Parkinson's disease as compared to normal controls, while dopamine reductions in the striatum and nigra of Parkinson's disease brains were more pronounced as compared to the serotonin and noradrenalin ones (Bernheimer et al., 1961; Hornykiewicz. 1963). A few years later, the Greek–

American physician George Cotzias introduced levodopa in therapeutics of Parkinson's disease with two publications in the New England Journal of Medicine (Cotzias et al., 1967; Cotzias et al., 1969). Since the introduction of gradually increasing doses of levodopa by Cotzias, levodopa and younger than levodopa drugs including dopamine receptor agonists, mono–amino–oxidase and catechol–O–methyltransferase inhibitors have been thoroughly studied for long term efficacy and are currently widely accepted for treating Parkinson's disease symptoms.

## 1.6 Common side effects related to dopaminergic agents

Nonetheless, dopaminergic drugs are not panacea. In absence of medicines which slow down the progression of the disease, pharmacotherapy strategies practically require continuous increases of administered levodopa. Levodopa is undoubtedly an efficient drug for the management of Parkinson's disease motor symptoms since its introduction in the 1960s; however, long–term dopaminergic treatment is commonly associated with the occurrence of several complications including motor fluctuations and troublesome dyskinesias. The most common side effects induced by levodopa and dopamine receptor agonists are listed in box 2 (British National Formulatory, 2015a; 2015b).

Box 2 – List of the most common side effects of levodopa and dopamine receptor agonists

| | |
|---|---|
| levodopa | nausea, vomiting, confusion, hallucinations and delusions, motor fluctuations, **dyskinesias**, dopamine dysregulation syndrome, mood swings, sleepiness, fainting, dizziness on standing up quickly, heart palpitations, agitation |
| dopamine receptor agonists | nausea, vomiting, confusion, hallucinations and delusions, impulsive and compulsive behaviour including binge eating or compulsive eating and subsequent weight gain, hypersexuality and compulsive sexual behaviour, dopamine dysregulation syndrome, gambling and uncontrollable excessive shopping or spending, punding, pathological internet use, sudden onset of sleep and somnolence, peripheral oedema |

## 1.7 Levodopa–induced dyskinesias: phenomenology

Cotzias'es chronic clinical trial of levodopa comprised high administered doses of the drug which then induced several side effects including nausea, vomiting and "neurologic side effects consisted of involuntary movements ranging from fleeting to severe." (Cotzias et al., 1969). These involuntary movements, currently described by the Parkinson's disease society as levodopa–induced dyskinesias (LIDs) are the most common side effects induced by levodopa in the long term.

Dyskinesias are choreic involuntary movements most commonly linked to peaks of levodopa in the plasma. Peak dose LIDs occur while levodopa is reaching its therapeutic effects i.e. patients are in "on" dopaminergic medication state; however, LIDs may be unpredictable and therefore intrusive with common daily activities. The severity of dyskinesias varies per individual patient from mild to severe; from a patient's perspective, dyskinesias can be hardly noticeable, bearable or restrictive. The severity of dyskinesias is dependent on the administered levodopa dose; an average daily dose ≥600mg has been linked with the appearance of LIDs (Fahn et al., 2005), while the risk of dyskinesia increases in a dose–dependent manner (Olanow et al., 2013).

The occurrence of LIDs has been linked with the duration of levodopa treatment (Schrag and Quinn. 2000). Approximately 40–50% of Parkinson's disease patients treated with levodopa daily experience motor fluctuations and dyskinesias within four years of treatment. As the duration of levodopa treatment increases to a decade, more than 90% of Parkinson's disease patients eventually experience dyskinesias (Ahlskog and Muenter. 2001). Hence, in advanced disease, most patients have a high daily intake of levodopa and indeed a high risk to experience dyskinesias. Studies on clinical risk factors for the development of dyskinesias have linked the occurrence of LIDs to a young age of disease onset (Kostic et al., 1991; Wickremaratchi et al., 2011), higher daily administered doses (Olanow et al., 2013) and to the initial administered daily dose (Grandas et al., 1999).

If a Parkinson's patient with a history of LIDs temporarily abstains from levodopa, he/she enters into an "off" dopaminergic medication state. During that "off" state, this individual will typically be bradykinetic and rigid. While in that "off" state, no exogenous levodopa should be present in their striatal terminals and he/she should not experience LIDs. However, if levodopa is re-introduced to this patient, he/she will eventually get into an "on" dopaminergic medication state. While in that "on" state, bradykinesia and rigidity should be improved by exogenous levodopa and in that "on" state, exogenous levodopa may trigger peak dose LIDs once again. The above clinical observations suggest that the onset of peak dose LIDs is an irreversible event in the course of Parkinson's that it is linked to permanent changes made in the brain.

## 1.8 An overview of available anti–dyskinetic treatments

As Parkinson's disease progresses and levodopa needs are increasing, the management of LIDs can become problematic in clinical practice. Hence, there is a great need to understand the pathophysiology of LIDs towards developing novel targeted therapeutics. Currently, advanced Parkinson's disease patients with LIDs may benefit from available treatments such as continuous intestinal levodopa infusion and surgical treatment with deep brain stimulation (DBS), while in earlier stages of Parkinson's, the pharmaceutical management of LIDs merely involves treatment with the amantadine. Nonetheless, the underlying mechanisms in Parkinson's dyskinesia are not fully understood. As a result, available therapeutics for managing LIDs are not adequately effective, while preventive treatments for LIDs are not available.

## 1.8.1 Continuous intestinal levodopa infusion

Experimental studies suggest that motor complications of long–term levodopa treatment can be reduced by continuous administration of levodopa and on this basis, continuous infusion of intestinal levodopa/carbidopa gel (LCIG) has been introduced in clinical practice in Europe, Canada and Australia and more recently in the US.

LCIG has shown an increase of the time during the day that patients are in "on" dopaminergic medication state and have no dyskinesias (Olanow et al., 2014; Pickut et al., 2014; Buongiorno et al., 2015; Timpka et al., 2016). In follow–up studies, LCIG has been shown to be equally safe and effective in managing troublesome dyskinesias (Olanow et al., 2014; Cáceres–Redondo et al., 2014). Nonetheless, a recent study proposed that long term LCIG treatment may in fact worsen the rate at which dyskinesias occur, despite the fact that troublesome LIDs were found proportionally reduced (Buongiorno et al., 2015). It could be therefore proposed that LCIG may reduce the troublesome dyskinesias in advanced disease, however, it remains unclear whether efficacy sustains in long term.

Currently, LCIG is indicated in advanced disease for patients with severe motor fluctuations and dyskinesias, in whom available combinations of Parkinson's medication have not been individually efficient. However, LCIG is suitable for only a modest percentage of Parkinson's disease patients, as LCIG requires a percutaneous endoscopy gastrostomy tube, which may be impractical and unwelcome by the patients.

## 1.8.2 Surgical treatment of dyskinesia

Non–pharmacological management of significant dyskinesias ultimately refers to DBS which involves the implantation of a neuro–stimulator that sends electrical impulses in selected brain nuclei, most commonly the subthalamic nucleus (STN) and globus pallidus internus (GPi) (Deep-Brain Stimulation for Parkinson's Disease Study Group et al., 2001).

LIDs have consistently improved in studies with STN DBS (Østergaard et al., 2002; Russmann et al., 2004; Simonin et al., 2009; Kim et al., 2015), which usually allows a reduction in the dose of administered levodopa. Nonetheless, STN DBS can even induce dyskinesia, as levodopa administration has been found able to induce LIDs after STN implantation (Elia et al., 2012). Nevertheless, anti–dyskinetic effects of DBS have been shown to sustain in long term after STN implantation, which has been proposed to induce a stabilisation of striatal synaptic function and neuronal networks (Simonin et al., 2009). Studies in GPi DSB have shown that levodopa needs are significantly reduced post DBS implantation with subsequent reductions in dyskinesia (Krack et al., 1998; Deep–Brain Stimulation for Parkinson's Disease Study Group, 2001). It could proposed, that improvements in dyskinesia may be greater in GPi DBS as compared to STN implantation, as in STN DBS, the occurrence of LIDs seems to be still dependent on administered levodopa doses (Russmann et al., 2004). Although it is quite interesting that LIDs are fairly improved by GPi and STN DBS implantations, DBS applies for a limited number of patients, it requires an invasive

neurosurgery implantation, and clinical follow–up may be available only in a limited number of clinical settings.

## 1.8.3 Amantadine

A common pharmaceutical approach for managing LIDs in clinical practice includes the use of amantadine, an anti–viral agent which has been shown to clinically improve LIDs (Verhagen Metman et al., 1998; Metman et al., 1999; Snow et al., 2000; Wolf et al., 2010; Ory–Magne et al., 2014; Pahwa et al., 2015). Amantadine is believed to act as an N-methyl-D-aspartate (NMDA) glutamate receptor antagonist; however, a dominant mechanism of action related to dyskinesias remains unknown. Following levodopa administration, NMDA glutamate receptors' activity, has been shown to be increased in the caudate, putamen and precentral gyrus of dyskinetic patients in comparison to non–dyskinetic patients; while no between–group differences were observed in the same cohort, when Parkinson's disease patients were assessed during an "off" dopaminergic medication state (Merello et al., 1999). Nonetheless, amantadine may also lose efficacy within a few months of continuous treatment and it is unknown whether amantadine's beneficial effects sustain in advanced disease.

Recently, an extended release preparation of the drug has been shown to be tolerable and efficient in improving LIDs (Ahmed et al., 2011) similarly to the observations for the standard release preparation. Hence, evidence from the above studies encourages the use of amantadine for managing dyskinesias and that glutamate neurotransmission may play a role in the development of LIDs. However, clinical

trials with another agent sharing NMDA glutamate characteristics, namely memantine, have been inconclusive for memantine's effect in improving consistently LIDs (Varanese et al., 2010; Wictorin et al., 2016). As amantadine treatment is mainly based on empirical evidence from clinical practice, further research will need to provide robust evidence for the role of NMDA glutamate receptor antagonists in LIDs.

## 1.9 Understanding dyskinesia pathophysiology

To date, there is significant evidence suggesting that the underlying pathophysiology of LIDs is relative to impaired dopaminergic neurotransmission in the striatum; however, the exact mechanisms are complex and not fully understood. Recent evidence has extended the above findings to non–dopaminergic sites within the striatum including the involvement of serotonergic terminals in the development of LIDs.

## 1.9.1 An overview of neurotransmission and neurotransmitter transporters

Neurotransmitters (such as dopamine, serotonin, adrenaline, noradrenaline, histamine, glutamate, aspartic acid, γ-aminobutyric acid, acetylcholine and glycine) enable the intracellular communication in the central nervous system. They transmit chemical signals from a neuron to another neuron, glial cell or muscle and are believed to act locally. The principles of physiological neurotransmission in the central nervous system are common among different neurotransmitters.

Neuronal pathways serve to connect relatively distant neurons and subsequently enable intraneuronal communication. The neurons of these pathways have axons that run the entire length of the pathway. The vehicle on each of these pathways is a neurotransmitter. Neurotransmitters are synthesised and stored in synaptic vesicles inside the neurons and are then transmitted via projecting neuraxons to synaptic destinations. Once released into the synapse, neurotransmitter are believed to activate postsynaptic receptors which are highly selective for the released neurotransmitter (Figure 1). At a presynaptic level, membrane neurotransmitter transporters ($Na^+$ / $Cl^-$ dependent transporters) reuptake the neurotransmitter which has been released and not uptaken in a postsynaptic manner. Thus, the transmission in the synapse may terminate by reuptake into the neurons or by active transport to glial cells, as well as by diffusion or by enzymatic catabolism.

Neurotransmitter transporters can be classified in two main families: plasma membrane transporters responsible for high affinity uptake of neurotransmitters from the extracellular space into the neuronal cytoplasm, and vesicular transporters responsible for neurotransmitter transport from the cytoplasm into secretory vesicles. Molecular cloning has identified two classes of plasma membrane transporters. They are both dependent on the Na+ intracellular/extracellular gradient for their activity but they differ in their dependence on extracellular Cl-. One family requires both Na+ and Cl- and includes the transporters for dopamine, noradrenaline, and serotonin as well as the transporters for γ–aminobutyric acid, glycine, and proline. The other family, which includes transporters for excitatory amino–acids glutamate and

aspartate transport into glial and neuronal cells does not involve co–transport of Cl-
but requires the co–transport of H+ and exchange for K+. Transport into secretory
vesicles involves the exchange of luminal H+ for cytoplasmic transmitters and seems
to involve two distinct families of proteins. One includes the vesicular transporters of
all monoamines and the transporter for acetylcholine; this family uses primarily H+
exchange. The other family relies more on the positive charge inside secretory vesicles
and includes γ–aminobutyric and glycine transporters.
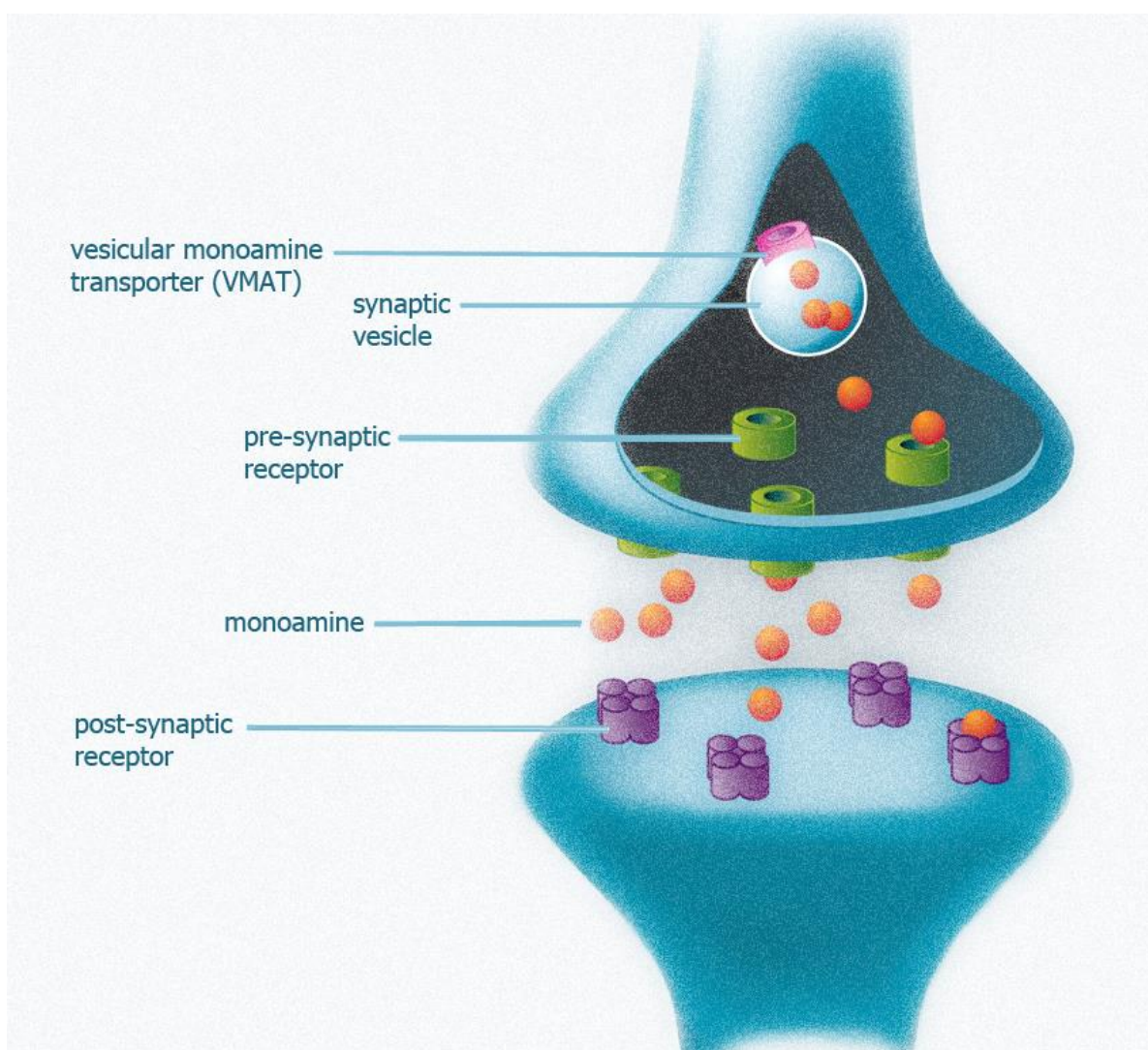


Figure 1 – Schematic illustration of monoamine neurotransmission

The coding of neurotransmitters, their receptors and transporters is highly dynamic and variable among pathological conditions. Parkinson's disease pathophysiology has been typically linked to altered dopaminergic neurotransmission; i.e. altered function of neurons primarily involved in the transmission of dopamine. Nonetheless, such alterations are not structural and are known to extend in the course of Parkinson's disease also to non–dopaminergic terminals, including serotonergic and noradrenergic neurons.

## 1.9.2 Dopamine and levodopa

Dopamine (Table 1 and Figure 2) is a monoamine that is involved in several pathways of neuronal communication and plays a major role in reward–motivated behaviour and the motor control. Dopamine is synthesised by decarboxylation of its precursor L-3,4,dihydroxy-phenylalanine (levodopa) (Figure 3). Levodopa (Table 2 and Figure 4) is synthesised by hydroxylisation of L-tyrosine (Figure 3). Dopamine can be further metabolised to synthesise other neurotransmitters including norepinephrine and epinephrine.

There are at least five dopamine receptor subtypes that have been identified in humans. The dopaminergic receptors are divided mainly in two groups; D1–like receptors (including D1 and D5) and D2–like receptors (including D2, D3 and D4 subtypes). D1 and D2 subtypes are the most common dopamine receptors and are highly expressed in the neurons of the striatum. The D2 receptors are functionally diverse; the D2 subtype is in high concentrations in the postsynaptic membrane of the

nigrostriatal terminals but they are also expressed as autoreceptors on axon terminals. The dopamine transporter (DAT) is a transmembrane protein which actively reuptakes synaptic dopamine that has not been uptaken postsynaptically. In humans, dopamine is transmitted via four major pathways from one brain region to another. Dopamine in the nigrostriatal pathway connects the substantia nigra to the dorsal striatum. It is believed that the dopamine nigrostriatal pathway is involved in the control of voluntary movement.

Table 1 – Summarised characteristics of dopamine

| Chemical name | 4-(2-aminoethyl)benzene-1,2-diol |
|---|---|
| Other name(s) | dopamine, DA, 3,4-Dihydroxyphenethylamine |
| Chemical formula | C8H11NO2 |
| Molecular weight | 153.17 g/mol |
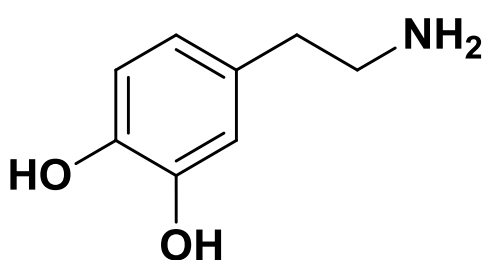


Figure 2 – Chemical structure of dopamine

Levodopa (L-3,4,dihydroxyphenylalanine) is the amino-acid precursor of dopamine. It is further processed to dopamine by decarboxylation catalysed by aromatic L-amino

acid decarboxylase (AADC). AADC is not exclusively expressed in dopaminergic neurons; it catalyses several different decarboxylation reactions including 5-hydroxytryptophan to serotonin and L-histidine to histamine. (Figure 3)
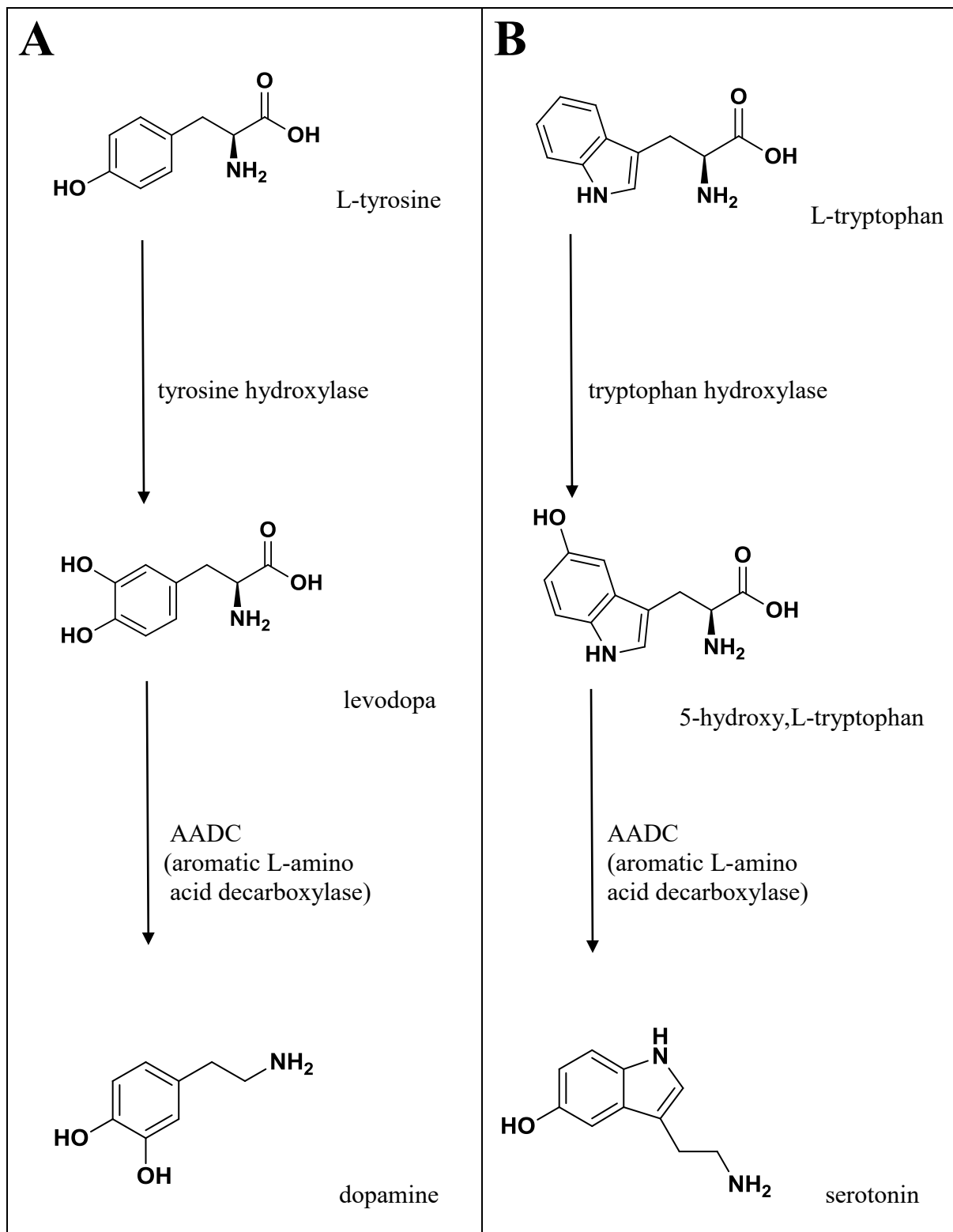


Figure 3 – Biosynthesis pathway of dopamine (A) and serotonin (B)

Levodopa crosses the blood–brain barrier, whereas dopamine itself cannot. Systemic *per os* administration of levodopa is almost completely absorbed. Nonetheless, exogenously administered levodopa is also metabolised within the peripheral nervous system. In clinical practice, it is given as either co–careldopa (levodopa and carbidopa) or as co–beneldopa (levodopa and benserazide). Both carbidopa and benserazide are extracerebral dopa–decarboxylase inhibitors and are co–administered with levodopa aiming to reduce the peripheral conversion of levodopa to dopamine, thereby aiming to limit side effects induced by peripheral actions of levodopa such as nausea, vomiting, and cardiovascular effects. Effectively, co–administration of levodopa and extracerebral dopa–decarboxylase inhibitor achieve elevated brain dopamine concentrations with lower doses of levodopa, on the assumption that levodopa decarboxylation occurs exclusively in the brain.

Table 2 – Summarised characteristics of levodopa

| Chemical name | (S)-2-Amino-3-(3,4-dihydroxyphenyl)propanoic acid |
|---|---|
| Other name(s) | levodopa, LD, L-dopa, L-3,4-dihydroxyphenylalanine |
| Chemical formula | $C_9H_{11}NO_4$ |
| Molecular weight | 197.19 g/mol |
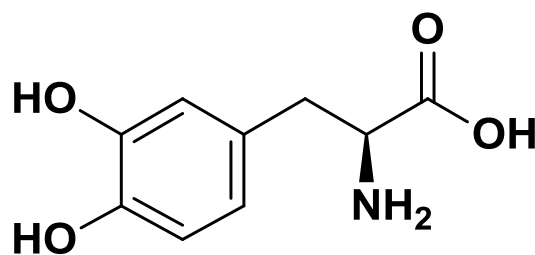
Figure 4 – Chemical structure of levodopa

### 1.9.3 Dopamine transporter (DAT)

The DAT is a presynaptic membrane transporter responsible for the uptake of dopamine from the extracellular space back into the neuronal cytoplasm and may thus terminate dopamine transmission. DAT's structure is characterised by 12 helical transmembrane loops, which consist of 20 to 24 amino acids, a large second hydrophilic extracellular loop with two to four potential glycosylation sites and intracellular localisation of both N– and C– terminals (Giros et al., 1993; Worrall et al., 1994; Nelson et al., 1998). The gene encoding human DAT is a 64–kilobase gene (SLC6A3) that is localised on chromosome 5 (Giros et al., 1991; Shimada et al., 1991).

The reuptake of dopamine is being controlled by phosphorylation and dephosphorylation of DAT (Pristupa et al., 1998; Masson et al., 1999). DAT's expression varies per anatomical brain region. DAT's distribution coincides with established dopaminergic innervation including several brain regions such as substantia nigra, dorsal and ventral striatum and ventral mesencephalon. Since DAT is present exclusively in dopamine synthesising neurons (Ciliax et al., 1995; Freed et al., 1995), the DAT can be therefore considered a specific marker of dopaminergic

terminals integrity and to a second level to dopaminergic neurons' function in certain brain regions. Hersch and colleagues (Hersch et al., 1997) have observed that in striatal terminals DAT is not concentrated in active synaptic zones but is distributed widely in axons and axon membranes, which suggests that DAT probably functions to regulate extracellular dopamine levels throughout the striatum.

## 1.9.4 Serotonin transporter (SERT)

Likewise DAT, the serotonin transporter (SERT) is a presynaptic membrane transporter responsible for the uptake of serotonin from the extracellular space back into the neuronal cytoplasm. SERT is a 630 amino acid long receptor, whose structure is characterised by 12 helical transmembrane domains. The reuptake of serotonin is mediated by phosphorylation and dephosphorylation of SERT. The gene encoding human SERT is a 24–kilobase gene (SLC6A4) that is localised on chromosome 17 at 17q11.2 (Blakely et al., 1991; Hoffman et al., 1991; Blakely et al., 1997).

The majority of SERTs are localised at presynaptic cell membranes or along axons (Zhou et al., 1998). SERT is highly expressed in the hypothalamus, thalamus, amygdala, putamen, caudate, and hippocampus while lower SERT concentrations are found in the prefrontal cortex and the cerebellum (Cortés et al., 1988; Laruelle et al., 1988; Kish et al., 2005). Likewise DAT, SERT can be therefore considered a specific marker of serotonergic terminals' integrity for certain brain regions.

## 1.9.5 Preclinical and clinical studies

To date, there is significant evidence suggesting that the underlying pathophysiology of LIDs is closely related to impaired dopaminergic neurotransmission in the striatum. More recently, preclinical and clinical studies have suggested that non–dopaminergic sites within the striatum may be also related to LIDs; however, the exact mechanisms are complex and not fully understood.

Studies in the animal model of Parkinson's disease as well as in humans have looked primarily into dopaminergic mechanisms as responsible for the development of LIDs due to synaptic dopamine depletion and the progressive decrease of dopamine storage capacity (Leenders et al., 1986). Several studies have indicated that the progressive loss of dopaminergic terminals in the striatum is related to the development of LIDs (Tedroff et al., 1996; de la Fuente–Fernández et al., 2001; de la Fuente–Fernández et al., 2004; Pavese et al., 2006). ^{11}C–raclopride, which specifically binds to postsynaptic D2, D3 dopaminergic receptors, has been validated as a PET radioligand for *in vivo* quantification of synaptic dopamine release in humans. An interesting PET imaging study with ^{11}C–raclopride showed that, in advanced disease, the same amount of exogenous levodopa may induce different dopamine release in the synapse, as compared to early diagnosed patients (Tedroff et al., 1996). Moreover, de la Fuente–Fernández and colleagues showed that standard doses of administered levodopa induces dramatic swings of dopamine levels in the striatum of dyskinetic patients as compared to a group of Parkinson's patients without LIDs (de la Fuente–Fernández et al., 2004). In the same context, increases of synaptic dopamine levels in

the striatum correlated positively with higher dyskinesias scores (Pavese et al., 2006). In addition, oscillations in the synaptic dopamine levels have been shown to precede the appearance of LIDs (de la Fuente–Fernández et al., 2001) and to be associated with a younger age at disease onset and a longer disease duration (Sossi et al., 2006).

Though LIDs are by definition induced by exogenous levodopa, evidence from studies in dyskinesias induced by dopaminergic medicines other than levodopa should be also introduced here. In early Parkinson's, monotherapy with either standard release ropinirole (Rascol et al., 2000), pramipexole (Holloway et al., 2004), cabergolide (Bracco et al., 2004), bromocriptine (Montastruc et al., 1994) or pergolide (Oertel et al., 2006) have been described to induce dyskinesias. Nonetheless, long–term monotherapy with any of the above drugs showed a lower incidence of dyskinesias as compared to long–term treatment with levodopa only. This may be due to the fact that ropinirole, pramipexole, cabergolide, bromoctiptine as well as pergolide have longer half-lives (ropinirole: approximately 6 hours; pramipexole: approximately 8.5-12 hours; cabergolide: approximately 63-69 hours; pergolide: approximately 27 hours) compared to levodopa (half-life of approximately 1-3 hours), thus resulting into more stable plasma concentrations. In addition, in all of the above longitudinal clinical trials, the onset of dyskinesia was delayed in the group of patients who were on dopamine receptor agonist monotherapy as compared to the patients who were treated with levodopa only.

It could be therefore proposed that in early Parkinson's, long-acting agents such as dopamine receptor agonists maintain stable plasma concentrations (as opposed to levodopa) and therefore provide continuous stimulation of the dopamine receptors. In contrast, shorter-acting agents such as levodopa can have fluctuating plasma levels and subsequently lead to intermittent dopamine receptors' stimulation. It should be also noted that the firing neuronal rate is proposed to be reduced in the basal ganglia in LIDs (Papa et al., 1999) as well as in apomorphine-induced choreic movements (Levy et al., 2001). Toning firing that provides a continuous supply of dopamine is proposed to have an abnormal pattern in Parkinson's patients with LIDs (Li et al., 2015) and give place to burst firing that leads to sudden release of high concentration of dopamine into the synapse. Hence, the large fluctuations in striatal dopamine levels may also be due to the changes in the neuronal firing rate.

Based on the above notions, monotherapy with the very short-acting apomorphine (half-life of approximately 40 minutes) in *de novo* Parkinson's should lead to fluctuating plasma levels and intermittent dopamine receptors' stimulation and possibly trigger the onset of dyskinesias sooner than longer–acting drugs. Nonetheless, to my knowledge, there is no study that has tried apomorphine as monotherapy in *de novo* Parkinson's patients and has directly compared its safety and efficacy to longer-acting dopamine receptor agonists or to levodopa. In fact, the comparison of apomorphine monotherapy to pergolide monotherapy in the primate model of Parkinson's, showed that dyskinesia induced–by–apomorphine was not different in severity to dyskinesia induced by the longer acting pergolide (Maratos et

al., 2003). Moreover, this study in the primate model of Parkinson's showed that apomorphine-induced dyskinesia was significantly less pronounced compared to dyskinesia induced by levodopa only (Maratos et al., 2003). Furthermore, in moderate-to-advanced Parkinson's, the reduction of dosing frequency of levodopa (standard–release multiple dosing over long–acting reduced dosing of the same amount of oral levodopa) did not trigger the onset of LIDs in patients with stable response (Hinson et al., 2009). Based on the above findings, it could be argued that dosing frequency may indeed play a role in the onset of dyskinesias, however, dosing frequency may not be closely related to the severity of dyskinesia, once LIDs are primed.

Taken together, evidence from all the above studies support that the occurrence of LIDs in advanced disease depends heavily on the way striatal dopamine release is regulated in the synapse. However, the exact mechanisms that regulate dopamine release in advanced disease and relate the non–continuous stimulation of the dopamine receptors to the occurrence of LIDs are not clearly understood.

Several preclinical studies have provided further evidence that striatal *serotonergic* terminals may be also related to LIDs. Serotonergic terminals are able to uptake exogenously administered levodopa and convert it into dopamine, as they express AADC (Figure 3). Serotonergic terminals are also able to store dopamine in synaptic vesicles and release it into the synapse in an activity–dependent manner (Ng et al., 1970; Ng et al., 1971; Tanaka et al., 1999; Maeda et al., 2005; Kannari et al., 2006). It could be argued that serotonergic neurons mediate dopamine release in the striatum

in response to highly administered levodopa intake as a compensatory mechanism for the reduced dopamine release. Nonetheless, striatal serotonergic terminals lack presynaptic auto–regulatory mechanisms as they do not express the DAT (reviewed by Piccini. 2003b). It has been therefore proposed that, when exogenous levodopa levels are increased, serotonergic terminals release dopamine in an uncontrolled manner as compared to the physiological release (Carta et al., 2007; Bézard et al., 2013; Politis et al., 2014). Although dopamine release could take place also in noradrenergic terminals, in these neurons (the noradrenergic ones), dopamine rapidly undergoes hydroxylation to norepinephrine. Thus, the noradrenergic terminals are most likely unable to release significant amounts of dopamine from levodopa.

Based on the evidence from the above studies, several agents with direct serotonergic action have been studied Parkinson's patients with dyskinesias and the animal model of Parkinson's disease. Chemical and pharmacological blockade of striatal serotonergic function has been shown to significantly reduce the abnormal involuntary movements (AIMS) in the animal model of Parkinson's disease (Carta et al., 2007; Bézard et al., 2013; Muñoz et al., 2008; Conti et al., 2014). The combined pharmaceutical blockage of types 1a and 1b of serotonin receptors (5–HT1a and 5–HT1b) prior to levodopa administration has been shown in the rats to diminish AIMS without affecting the effects of levodopa (Muñoz et al., 2008). In humans, the mechanisms underlying the development of LIDs are more complex. Both buspirone (Politis et al., 2014) and eltoprazine (Svenningsson et al., 2015), which are serotonin–receptor partial agonists have shown anti–dyskinetic effects when administered prior

to levodopa without counteracting levodopa's main effects. The role of buspirone in attenuating LIDs was further supported by PET imaging findings that buspirone administration normalised levels of dopamine release in the striatum (Politis et al., 2014). However, the above studies have not shown evidence for long term safety and efficacy.

Serotonergic markers have been detected in terminal stages of Parkinson's disease progression (Kish et al., 2008); in advanced stages of Parkinson's, patients have shown to have reduced SERT density in the putamen (as reflected by $^{11}$C–DASB BPND) as compared to controls, while these losses were not found in the early stages of the disease (Politis et al., 2010). Hence, if the serotonergic terminals are indeed involved in the development of LIDs, it remains unclear which is the exact mechanism of their involvement and if there is a relation with the progressive decline of the dopaminergic striatal terminals. A recent PET imaging study looked into midbrain–SERT availability over striatal–DAT density in early disease. The above study showed that imbalanced SERT–over–DAT binding ratios do not predict the development of LIDs, however, it proposed that this may occur at later stages of Parkinson's disease progression (Suwijn et al., 2013).

## 1.10 Rationale

In the studies described in this thesis, I intended to further explore the role of both striatal dopaminergic and serotonergic terminals in relation to the appearance of Parkinson's disease dyskinesia. In advanced Parkinson's, patients fail to maintain a stable rate of dopamine release in the synapse. This has been proposed to be due to the striatal dopaminergic terminals, which progressively lose their capacity to store and release dopamine in a controlled manner. I thereby intended to study the dopaminergic neurotransmission at a presynaptic level by assessing the striatal DAT availabilities in Parkinson's disease patients with and without LIDs. As striatal serotonergic terminals are proposed to be related in Parkinson's disease dyskinesias, I also intended to study the integrity of serotonergic terminals (through striatal SERT availabilities) in relation to striatal DAT and the occurrence of LIDs.

Brain PET and SPECT imaging techniques are most powerful to study the *in vivo* distribution of certain biological molecules including the DAT and SERT in the human brain. ^{123}I–Ioflupane has been validated for use in clinical practice as it can demonstrate striatal dopaminergic dysfunction and support a clinical diagnosis of idiopathic Parkinson's disease cases. ^{123}I–Ioflupane is a SPECT radioligand with high *in vivo* affinity for the DAT and much lower for the norepinephrine transporter and the SERT. ^{123}I–Ioflupane has a high specific to non–specific binding, high reversibility and good uptake in the striatum. ^{11}C–DASB has been validated for assessing SERT availability in several PET studies in humans. ^{11}C–DASB has high affinity (Ki: 1.10 nM) for the SERT and excellent *in vitro* selectivity over the other monoamine

transporters: the norepinephrine transporter and the DAT (Wilson et al., 2000b). ^{11}C–DASB has high specific to non–specific binding (Ginovart et al., 2001), good reversibility and high uptake in the striatum (Houle et al., 2000). In addition, ^{11}C–DASB reaches binding equilibrium relative to non–specific binding within a reasonable amount of time (Houle et al., 2000). ^{11}C–PE2I is a newer PET radioligand for assessing DAT availability in humans. ^{11}C–PE2I has high affinity (Ki: 17 nM) for the DAT and very good *in vitro* selectivity over the other monoamine transporters: the norepinephrine transporter and the SERT (>30–fold) (Hall et al., 1999). ^{11}C–PE2I has high specific to non–specific binding (Halldin et al., 2003; Jucaite et al., 2006), good reversibility and high uptake in the striatum (Halldin et al., 2003; Ribeiro et al., 2007; Seki et al., 2010). In addition, ^{11}C–PE2I reaches binding equilibrium relative to non–specific binding within a reasonable amount of time (Halldin et al., 2003).

## 1.11 Aims of the studies conducted for this thesis

a) To estimate the role of striatal DAT availability in Parkinson's disease as a prognostic marker for the appearance of future LIDs.

b) To explore whether striatal DAT availability changes over time in Parkinson's disease are related to the appearance of LIDs.

c) To estimate the role of striatal SERT–to–DAT binding ratios in Parkinson's disease in relation to LIDs.

d) To assess the changes over time in striatal SERT, DAT and SERT–to–DAT binding ratios in Parkinson's disease in relation to the development of LIDs.

# Chapter 2 – Methodology

## 2.1 Ethical approval

The studies described in *Chapters 3, 4* and *5* were reviewed and approved by the West London Research Ethics Committee (REC Ref. 12/LO/0414). The study described in *Chapter 6* was submitted under the REC Ref. 12/EE/0096, Transeuro Consortium. Alongside with the Ethics Committees, all research projects were reviewed and approved by the Imperial College Joint Research Compliance Office and the Administration of Radioactive Substances Advisory Committee, UK. Administration of ionising radiation was performed following appropriate training in accordance with the Ionising Radiation for Medical Exposure Regulations. All members of staff who worked during this project with ionising radiation, including sealed radioactive sources, unsealed radioactive sources and naturally radioactive materials were appropriately trained and registered with the Safety Department of Imperial College London. Personal dosimetry body and finger badges were worn during all activities that involved ionising radiation in accordance to Ionising Radiations Regulations 2000.

## 2.2 Screening of potential participants and subject recruitment

Parkinson's disease patients were recruited from Movement Disorders Clinics. During their participation in the study, Parkinson's patients were regularly followed up in six–month intervals by Movement Disorders Specialists as part of their clinical care. Controls were recruited by publicity posters and by web–based adverts hosted by the Michael J Fox Trial finder. Each participant who showed interest in the research study was given an information sheet with details on the research project and was invited

for a face–to–face consultation in a clinical outpatient setting at Imperial College/Imperial College Healthcare NHS Trust. Participants were offered the opportunity to ask questions and receive appropriate answers. My personal contact details were given to each participant for further information and discussion. All participants of the studies described in this thesis provided informed written consent in accordance to the Declaration of Helsinki. A hard copy of the signed consent form was given to each participant, to their general practitioner attached to an information letter, while a third copy was filed in the study's master file.

Screening appointments consisted of a review of participants' past medical history, family and medication history, a physical examination and the completion of validated and non–validated clinic–behavioural questionnaires. The name and dose of each medication was recorded and the levodopa equivalent daily doses ($LED_{Dag}$, $LED_{Ldopa}$, and $LED_{Total}$) were calculated. A full medical history was obtained from each participant including past medical conditions, hospital admissions, past surgical operations and relevant medication history. These details were recorded and were subsequently cross–checked with information from participants' medical notes and clinical letters to their general practitioners. A clinical diagnosis of Parkinson's disease was confirmed following the Queen Square Brain Bank diagnostic criteria for idiopathic Parkinson's disease (Hughes et al., 1992) for the patients who participated in the studies described in this thesis – see Appendix I. Parkinson's patients were asked to provide details of the time they had their first motor symptom, time of diagnosis, time of initiating each anti–parkinsonian medication, and details of

previous exposure to ionising radiation for clinical and/or research purposes. Participants who declared that they were exposed to ionising radiation for any reason during the past 12 months from their screening visit were excluded for participation in this study. Women of child bearing potential, were tested for pregnancy with urine β–human chorionic gonadotropin pregnancy tests. None of the female participants of the study was pregnant or was breast–feeding during their participation in the study.

## 2.3 Clinical data

### 2.3.1 Evaluation of motor symptoms

Clinical evaluation of motor and non–motor symptoms' severity was performed using the UPDRS (Goetz et al., 2007) – see Appendix II. In particular, Parkinson's disease severity was performed using the III part of the UPDRS form (motor symptoms) and the Hoehn & Yahr staging scale (Hoehn and Yahr. 1967) – see Appendix III.

### 2.3.2 Calculation of disease duration

Disease duration from diagnosis ($DD_{diagn}$) was calculated as the difference (in years) from diagnosis time to corresponding time. $DD_{diagn}$ was defined based on the date of each individual participants' diagnosis of Parkinson's disease at the Movement Disorders Clinics.

### 2.3.3 Calculation of levodopa equivalent doses

The $LED_{Total}$, $LED_{Ldopa}$ and $LED_{Dag}$ doses were calculated in mg for each individual participant following the formulas (as in Politis et al., 2014) shown in Appendix IV.

## 2.3.4 Evaluation of LIDs

The presence of LIDs was assessed within 1 hour after the patients had taken their usual levodopa dose (range of single levodopa dose: 100–200mg). For the evaluation of LIDs, I have used the IV part of the UPDRS scale (Goetz et al., 2007), the AIMS scale (Guy. 1976), and the Rush dyskinesia rating scale (Goetz et al., 1994) – see Appendices II, V and VI, respectively. The severity of LIDs was scored using the AIMS scale for every 15 minutes for the next 120 minutes.

## 2.3.5 Evaluation of depression

Patients with a history of depression were excluded from this study. All participants were assessed for having (or not) depression through clinical history and by using either the validated questionnaire of the Hamilton scale for depression (HAM–D) (Hamilton. 1960; Leentjens et al.,. 2000a) or the validated Beck's Depression Inventory (BDI) (Beck et al., 1961; Leentjens et al., 2000b). HAM–D scores above 7 and BDI scores above 10 was an exclusion criterion. The HAM–D scale is in Appendix VII. The BDI questionnaire is in Appendix VIII.

## 2.3.6 Evaluation of cognitive impairment

Patients with a history of dementia were excluded from this study. All participants were assessed through clinical history and whereas possible, by using the validated questionnaire of mini mental examination state (MMSE) (Folstein et al., 1975). MMSE scores below 26 was an exclusion criterion. The MMSE questionnaire is in Appendix IX.

## 2.4 Principles of brain PET and SPECT technology and kinetic modelling

Brain PET and SPECT imaging enable three–dimensional visualisation of biological compounds and quantification of physiological processes in the human brain. The study of distribution, density and activity of certain biological compounds in the brain and their interactions can be achieved by the use of an appropriate PET/SPECT radioligand (or radioactive tracer), which is a metabolically active compound labelled with a radioactive isotope and a PET–CT/SPECT–CT scanner, which is a computed tomography (CT) scanner sensitive to detect radioactivity. PET/SPECT scans are carried out on an outpatient basis. Each radioligand is subject to distribution, accumulation to target tissue, metabolism and clearance. Accumulation of the radioligand in certain brain regions reflects molecular interaction between the radioligand and the specific receptor of the target tissue. Thus, a brain PET/SPECT imaging study can be regarded as the visualisation of distribution, density and activity of a radioligand in certain brain regions. Subsequently, the quantification of brain PET and SPECT imaging data reflects the magnitude of selective uptake of the radioligand by rich–in–receptor brain regions.

Each ligand has unique pharmacokinetics and characteristics and therefore unique applications in clinical imaging studies. A radioligand is synthesised to have stability of labelling. A brain radioligand should be able to cross the blood–brain barrier by passive diffusion and access the biological target rapidly. After entering the brain, the radioligand should have the least possible amount of metabolites. Ideally, radioligand

metabolites that are formed in the brain should be cleared rapidly and plasma metabolites should have high polarity so that they cannot re-enter the brain. Undoubtedly, a radioligand should have high affinity and selectivity to a specific biological compound along with low non–specific binding in regions that do not contain the biological compound of interest (Heiss and Herholz. 2006). The time–course of uptake and clearance of a radioligand can be measured using appropriate tracer kinetic modelling. The principles of tracer kinetic modelling for the quantification of *in vivo* distribution of a radioligand originate from *in vitro* binding studies. The following paragraphs contain the fundamental concepts of tracer kinetic modelling for the reversibly binding radioligands which are most commonly used in brain PET and SPECT imaging studies including the ones presented in this thesis.

The radioligand is injected intravenously to the examinee while γ–rays are emitted from the decay of the radioisotope for a certain amount of time; eg. $^{11}$C has a half–life of approximately 20 minutes, $^{123}$I of 13.2 hours, $^{18}$F of 110 minutes, and $^{15}$O of only two minutes. Typically, SPECT radioligands have isotopes with longer half–lives as compared to the PET ones, which are commonly injected minutes after their production. Hence, SPECT radioligands with long half–lives can get rid of non–specific binding and reach equilibrium over several hours. This may have been an advantage of SPECT over the short–acting radioisotopes commonly used in PET, however, PET is widely accepted as much more selective and sensitive (Heiss and Herholz. 2006).

The PET subject is placed within a field of view of the PET–CT scanner where a number of detectors can register incident γ–photons. After injection, the radioactive ligand is circulated around the body and localises temporarily according to its specific biochemistry. The radioisotope of the PET ligand decays via positron emission during which a nuclear proton decays to a neutron, a positron and a neutrino. As emitted positrons travel a short distance within human tissue, they start to interact with electrons either by annihilation or by the formation of a positronium (either ortho– or para–positronium). Positron as well as para–positron annihilation generates two 511 keV photons which are anti–parallel. Hence, the decay of the PET radioisotope is the ultimate source of anti–parallel photons which are travelling in opposite directions.

Each pair of these anti–parallel photons are coincident since they occur at the same time and are products of the same annihilation. The PET combines incident photons as time pulses and if these time pulses fall within a short time window, they are regarded as coincident. The two emitted photons must be determined during pre-determined time window to be counted as true coincidence event. However, in practice, most of the photons are lost because of their absorption in body tissues. This loss of detection of true coincidence events is called attenuation and it is lower in the surface of the body than deeper in the body, quite low in the lungs and deeper in high density tissue such as bones. Attenuation can lead to severe artefacts. Hence, by performing attenuation correction, the PET detectors are capable of registering the two coincident photons that correspond to the same annihilation, thus detecting the position, within the camera's field of view, at which a positron emission occurred.

With this procedure, in PET, positional information is registered without the presence of physical collimator. This procedure, known as electronic collimation, offers improved sensitivity and uniformity of the point source response function.

In SPECT technology, that requires the presence of a physical collimator, positional information is gained from emitted photons independent to each other. Single photons emitted from the SPECT radioisotope first encounter the physical collimator of the γ–camera. The collimator absorbs photons that are not travelling perpendicular (or within a certain acceptable angle) to the face of the SPECT detector. A collimator that has larger holes is more sensitive in detecting γ rays, however, this leads to poorer resolution. On the other hand, if the collimator holes are smaller, this would provide greater resolution but poorer sensitivity. The γ–camera rotates around the SPECT subject and obtains directional information from incident photons. However, travelling photons which are not "normal" or "nearly normal" to the collimator face are not reaching the detector. As a result, SPECT has lower detector efficiency and provides less quantitative accuracy as compared to PET (discussed in Heiss and Herholz. 2006).

The raw data collected during PET/SPECT scanning undergo processing by the scanner computer and are stored as sinograms. Once raw PET/SPECT data are acquired, they are transformed to an imaging workstation, where they are tomographically reconstructed to actual PET/SPECT images. Image reconstruction can be performed using several algorithms, most commonly through filter back

projection (FBP) or some form of iterative algorithm such as the ordered subset expectation maximisation (OSEM) method. Correction can be applied for attenuation, scatter as well as partial volume effect while post-reconstruction filtering can be applied to remove excess noise. Typically, the attenuation is measured by acquisition of a separate transmission scan while the patient is in the scanner just before the injection of the radioligand. Transmission scans are usually using an external source of radioactivity (such as $^{68}$Ge/$^{68}$Ga). Prior to the transmission scan, another scan called the blank scan is being performed using the same radioactive source for which the participant is not required to be in the scanner. Attenuation correction factors are computed utilising the transmission and the blank scans.

Brain PET and SPECT imaging technology and radioligand synthesis have shown great progress over the past decades. Improvements in computer–based methodology have enhanced image resolution and quantification of PET and SPECT data, while novel radioligands are more selective to the pathology of the studied disease. Continued research in multimodal imaging including PET–CT and PET–MRI will improve the understanding of neurodegeneration and neuroinflammation, validate *in vivo* diagnostics, and may provide biomarkers to monitor disease–modifying therapies.

Hence, the above advances may encourage the use of these Nuclear Medicine techniques as both research and clinical tools to assess the integrity of brain cells,

explore the mechanisms of underlying neuropathology and monitor progressive neurological disorders.

## 2.4.1 Principles from *in vitro* binding studies

All modelling approaches in radioligand binding for PET and SPECT studies assume a compartmental system. To determine the complex dynamics of receptor binding *in vivo*, the radioligand behaviour is divided into virtual compartments in order to extract the compartment of specific binding.

In an *in vitro* environment, tissue homogenates are incubated with the radioligand in buffer solution (McGonigle and Molinoff. 1994). An *in vitro* system can be therefore regarded as a system of two compartments: the first compartment refers to the buffer solution in the test tube and the second one refers to the receptor–rich tissue. Once the radioligand is put into the test tube, the radioligand molecules move from the buffer compartment into the tissue compartment by binding to the receptors. Unbound ligand (L) and reversible receptor (R) react to form a ligand-receptor (LR) complex:

$$L+R \rightleftharpoons LR \qquad\qquad \text{(Equation 1).}$$

Reversible radioligands reach equilibrium concentrations over time when no net transfer of radioligands occurs between the two compartments. At equilibrium, the forward reaction (L+R→LR) is balanced by the backward unbinding reaction (LR→L+R) and the aforementioned reversible reaction (equation 1) is characterised

by the *in vitro* on–rate ($k_{on}$) and off–rate ($k_{off}$) constants. The rate of a chemical reaction is directly proportional to the concentrations of the reactants (law of mass action). The radioligand equilibrium association ($K_A = k_{on}/k_{off}$) and dissociation constants ($K_D = k_{off}/k_{on}$) relate the concentrations [L], [R] and [LR]. Mathematically, $k_{on}$[L][R]= $k_{off}$[LR], $K_A$ = [LR]/[L][R] and $K_D$ = [L][R]/[LR]. In *in vitro* conditions, the total number of receptors ($B_{max}$) is equal to the sum of [R] + [LR]. Following that, $K_D$ = [L]·($B_{max}$–[LR])/[LR]. Rearranging this equation,

$$[LR] = B_{max} \cdot [L]/([L] + K_D) \qquad \text{(Equation 2).}$$

The kinetic description of the radioligand–receptor reaction is based on the principles of the Michaelis–Menten equation for enzymatic reactions. This equation is the equilibrium solution to a differential equation that describes the change per unit time (the rate) of the quantity of radioligand bound to the receptors. In an *in vitro* binding study, increasing amounts of radioligand can be added in the solution several times until a standard concentration of receptors is saturated. A saturation curve can be then drawn by plotting the concentrations of the radioligand–receptor complex against the increasing amounts of the radioligand. By applying nonlinear regression analysis, both $B_{max}$ and $K_D$ can be then estimated. Nonetheless, to apply the above principles to *in vivo* binding that imaging techniques require, multiple scans would be needed i.e. multiple radioligand doses, which would make such a clinical study impractical. In fact, in PET and SPECT imaging studies only a very small amount of radioligand is being administered i.e. concentrations [L], [R] and [LR] are all very small.

## 2.4.2 Binding Potential

Binding potential (BP) is a term that was introduced by Mintun to clarify the linear role of the receptor density ($B_{max}$) and radioligand binding affinity ($1/K_D$) (Mintun et al., 1984; Innis et al., 2007). For the purposes of an *in vivo* imaging study, the very small concentration of the targeted receptors [R] can be regarded "equal" to $B_{max}$. Strictly speaking for the *in vivo* very small radioligand concentrations, $[R] \approx B_{max}$. Following that and rearranging equation 2, the quotient of [LR], [L] can be written as:

$$[LR]/[L] = B_{max}/K_D \qquad \text{(Equation 3)}$$

and

$$BP = B_{max}/K_D \qquad \text{(Equation 4).}$$

According to equation 4, the affinity of the radioligand and the $K_D$ are inversely related i.e. the lower the $K_D$ value (lower concentration), the higher the affinity of the radioligand (affinity = $1/K_D$). Therefore, the "Mintun equation of BP" can be alternatively written as:

$$BP = B_{max} \times \text{(affinity)} \qquad \text{(Equation 5).}$$

It should be noted, that:

1.$B_{max}$ denotes here the maximum available receptor density *in vitro*.

2.In an *in vivo* environment, some receptors are occupied by endogenous molecules while the rest of the receptors are either in a low affinity state or compartmentalised; hence, $B_{avail}$ denotes the density of the available receptors to bind *in vivo*.

## 2.4.3 Compartmental modelling for *in vivo* binding studies

When specific binding refers to *in vivo* binding, the environment is different to that of *in vitro* binding assays. Hence, for *in vivo* studies, the concept of "Mintun's BP" is extended and further definitions are introduced in the following sections of this chapter. Brain regions containing the under–study receptors have at least three compartments: just after the tracer is being administered intravenously, the radioligand will get into arterial plasma (first compartment), it will then cross the blood–brain barrier (second compartment, also known as the first tissue or nondisplaceable compartment), and it will then reach the cerebral region that is rich–in–receptors (third compartment) (Ichise et al., 2001).

Hence, the *in vivo* system has an open first compartment in which the radioligand clears over time. Furthermore, delivery of the radioligand through the first to the second and third compartments depends on regional cerebral blood flow. Moreover, in *in vivo* studies, there may be brain regions that are devoid of receptors (so called reference regions) which do not have the third compartment. In the *in vivo* environment there is also a non–specific binding compartment which refers to the compartment that exchanges with the free compartment. In practice, for the majority of radioligands, the non–specific binding and free compartments are treated as a

70

single compartment. The principles that apply *in vitro* can be extended to the *in vivo* environment, however, this is based on certain assumptions (Ichise et al., 2001):

1. The radioligand in the system comes from arterial plasma only (single source).

2. The radioligand crosses the blood–brain barrier back and forth freely by diffusion.

3. The exchange of radioligand between the compartments is described by fundamental kinetics.

4. Non–specifically bound radioactivity in the free (second) compartment equilibrates rapidly with free radioactivity in the tissue.

5. Un-metabolised parent radioligand in plasma equilibrates rapidly with plasma protein so that the free fraction is constant over time.

6. The nondisplaceable distribution volume (DV – see definition below in 2.4.5) of the free compartment in the receptor–containing tissue is identical to the corresponding DV in the receptor–free tissue.

Hence, to determine the dynamics of receptor binding *in vivo*, a three–compartmental model can be applied consisting of the freely exchangeable in plasma ligand, the non–specifically bound (+free) ligand in tissue and the specifically–bound ligand in tissue (Figure 5).

## 2.4.4 Principles of radioligand kinetic properties for *in vivo* binding

For each brain tissue, the radioligand can be either specifically–bound to receptors (B), non–specifically bound (NS) or free (F) (reviewed by Innis et al., 2007). The

radioactivity concentrations of the B, NS, and F components of the radioligand change over time; hence, the mathematical expression of the total radioactivity concentration of the radioligand in brain tissue ($C_{TISSUE}$) over time (t) is the following function:

$$C_{TISSUE}(t) = C_B(t) + C_{NS}(t) + C_F(t) \qquad \text{(Equation 6)}.$$

Because the non–specifically bound ($C_{NS}$) and the free concentration ($C_F$) are regarded as a whole (under assumption 4), the $C_{TISSUE}(t)$ equation can be written as:

$$C_{TISSUE}(t) = C_B(t) + C_{F+NS}(t) \qquad \text{(Equation 7)}$$

$$\Rightarrow C_B(t) = C_{TISSUE}(t) - C_{F+NS}(t) \qquad \text{(Equation 8)}.$$

To quantify the above concentrations, this would require several measurements i.e. the conduct of several scans to measure cerebral uptake, clearance of the ligand, assessment of the ligand concentration in plasma as well as of the ligand radiometabolites. However, by conducting an imaging study, only two sets of measures are available for extraction: one is the total radioactivity concentration in brain tissue ($C_{TISSUE}$) and the other one the arterial plasma concentration ($C_P$). The assessment of the variations of the radioligand concentrations over time requires an input (delivery) function, which describes the concentrations of the free radioligand in plasma as a function of time. The radioactive concentrations of the ligand in the arterial plasma at time (t), $C_P(t)$, can be obtained by measuring the radioligand concentrations in arterial blood samples and $C_{TISSUE}(t)$ can be the concentration of the

ligand as measured directly at time (t) within a given region of interest. The interaction among the three compartments described above and the differential equations that associate these compartments over time are shown in Figure 5 and equations below.
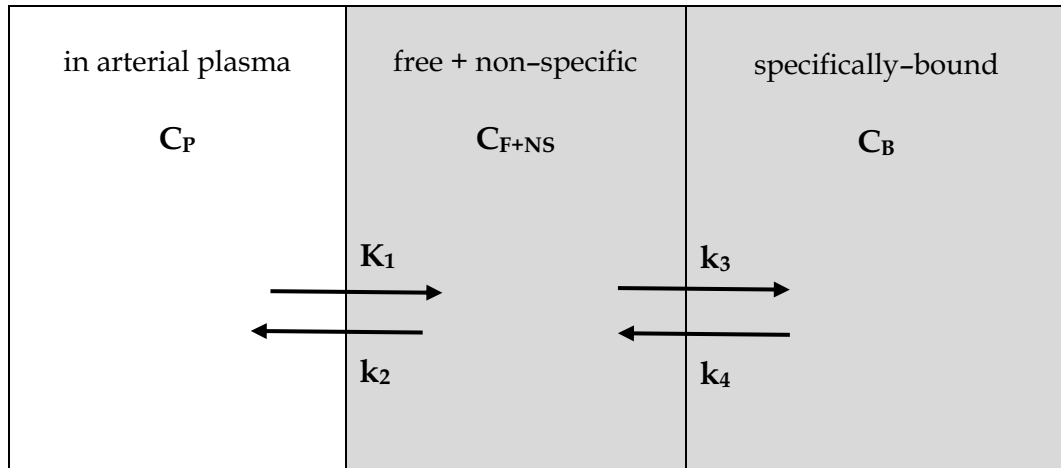


Figure 5. Standard compartmental model for reversible receptor–binding radioligands.
Grey denotes the intracerebral compartments. $C_P$, $C_{F+NS}$, $C_B$ denote time–dependent local activity of the tracer in arterial blood, free and bound tracer in the tissue, respectively. $K_1$, $k_2$, $k_3$ and $k_4$ denote the transfer rate kinetic constants.

The system can be described by the following differential equations, in which the radioactivity concentrations of the compartments ($C_P$, $C_{F+NS}$, $C_B$) are associated over time (Ichise et al., 2001):

$$d_{F+NS}(t)/dt = K_1 C_P(t) + k_4 C_B(t) – k_2 C_{F+NS}(t) – k_3 C_{F+NS}(t) \qquad \text{(Equation 9)}$$

$$dC_B(t)/dt = k_3 C_{F+NS}(t) – k_4 C_B(t) \qquad \text{(Equation 10)}$$

where,
$C_P$ is the metabolite–corrected plasma concentration (kBq/ml)
$C_{F+NS}$ is the concentration of the free (+ non–specifically bound) ligand in the tissue (kBq/ml)
$C_B$ is the specifically–bound concentration of the ligand in the tissue (kBq/ml)
$K_1$ is the rate constant for transfer from plasma to free compartment (ml/cm3 · min)
$k_2$ is the rate constant for transfer free compartment to plasma (ml/ml · min)
$k_3$ is the rate constant for transfer from free to bound compartment (ml/ml · min)
$k_4$ is the rate constant for transfer from bound to free compartment (ml/ml · min).

## 2.4.5 Principles from clinical pharmacology

In clinical pharmacology, the DV refers to the volume of blood (or plasma) that would be required to account for the amount of drug in the entire body. For example, if the concentration of a drug in plasma is 100ng/ml and 10mg of the drug are in the entire body, then its DV would be 10mgx1ml/100ng=100L. *In vivo* imaging with radioligands adapts this concept so that the target region is regarded as a particular organ rather than the entire body and secondly, the target is expressed as the amount of radioligand in a volume of tissue (i.e. a concentration) (Innis et al., 2007). The free fraction of the radioligand in plasma ($f_1$) is the fraction of the ligand that is not bound to plasma proteins at equilibrium i.e. the exchangeable portion of the free ligand. Similarly, the free fraction of the radioligand in tissue ($f_2$), is the fraction of the ligand in tissue that is available for specific binding. Hence, the equilibrium DV of a compartment is expressed as the ratio of the concentration of the ligand that is distributed in the compartment relative to the free concentration in plasma ($f_1C_P$) at equilibrium. For instance, if the concentration of the ligand in the striatum (tissue compartment) at equilibrium is 100kBq/cm$^3$ and 5kBq/ml in arterial plasma, then the DV$_{STRIATUM}$ = 20ml/cm$^3$ i.e. 20ml of free radioligand in the plasma would be required for the radioligand in 1 cm$^3$ in the striatum (Innis et al., 2007).

## 2.4.6 Modified Binding Potential

Earlier above, BP was introduced as equal to $B_{max}/K_D$ (equation 4). In most clinical applications though, no attempt is made to calculate $B_{max}$ and $K_D$ separately, and BP as the ratio of the two is acceptable (Mintun et al., 1984; Heiss and Herholz. 2006). In

the case of negligible occupancy of receptors by the ligand and co-injected cold (unlabelled) ligand, the BP can be calculated from measured parameters of a kinetic study (Meyer and Ichise. 2001) as:

$$BP = K_1k_3/k_2k_4f_1 \hspace{5cm} \text{(Equation 11).}$$

Because accurate measurement of $f_1$ in plasma is problematic, a measure closely related to BP is being used i.e. "modified BP" or BP' (Heiss and Herholz. 2006). This assumes that non-specific binding (as considered by the $f_2$) in tissue is constant and can be disregarded. Under this assumption, BP' can be directly calculated from $k_3$ and $k_4$ as follows:

$$BP' = f_2B_{max}/K_D = k_3/k_4 \hspace{4cm} \text{(Equation 12).}$$

Full kinetics to determine $B_{max}$ and $K_D$ are usually too complicated for clinical routine use. Therefore, equilibrium approaches are applied to determine receptor specific binding.

## 2.4.7 Reference tissue compartmental model

Although arterial plasma is the gold standard input (delivery) function, the process for obtaining it is usually difficult to implement in clinical studies and often can be replaced by reference tissue. Modelling for reference region as input function includes both a rich-in-receptor region of interest as well as a reference region that is assumed to be devoid of the studied receptors.

## 2.4.7.1 Three compartment model (two tissue compartment) – kinetics

The reference tissue compartment model is based on the following differential equations (see details in Lammertsma et al., 1996):

$$dC_{F+NS}(t)/dt = K_1C_P(t) + k_4C_B(t) - k_2C_{F+NS}(t) - k_3C_{F+NS}(t) \qquad \text{(Equation 13)}$$

$$dC_B(t)/dt = k_3C_{F+NS}(t) - k_4C_B(t) \qquad \text{(Equation 14)}$$

where,
$C_P$ is the metabolite–corrected plasma concentration (kBq/ml)
$C_{F+NS}$ is the concentration of the free (+ non–specifically bound) ligand in the tissue (kBq/ml)
$C_B$ is the specifically–bound concentration of the ligand in the tissue (kBq/ml)
$K_1$ is the rate constant for transfer from plasma to free compartment (ml/ml · min)
$k_2$ is the rate constant for transfer from free to plasma compartment (ml/ml · min)
$k_3$ is the rate constant for transfer from free to specifically–bound tissue (ml/ml · min)
$k_4$ is the rate constant for transfer from specifically–bound tissue to free compartment (ml/ml · min).

In practice, $[C_B]$ and $[C_{F+NS}]$ cannot be measured but only the total concentration of

the tissue as:

$$C_{TISSUE}(t) = C_B(t) + C_{F+NS}(t) \qquad \text{(Equation 15).}$$

From equations 13 and 14, it is possible to derive a relationship between $C_{TISSUE}$ and

metabolite–corrected plasma concentration $C_P$ as a function of time as:

$$C_{TISSUE}(t) = aC_P(t)*\exp(-ct) + bC_P(t)*\exp(-dt) \qquad \text{(Equation 16)}$$

where,
$a = r \cdot (k_3+k_4 - c)$,
$b = r \cdot (d-k_3-k_4)$,
$c = (s-p)/2$,
$d = (s+p)/2$,
$p = \sqrt{(s^2-q)}$,
$q = 4k_2k_4$,
$r = K_1/p$,
$s = k_2+k_3+k_4$,
* = convolution integral.
However, with PET, a macroscopic region of interest (ROI) will be sampled that will

contain a significant contribution from intravascular activity in the "early phase" after

a bolus injection of the ligand. This background signal will depend on the plasma concentration, but on all activity within the intravascular space i.e. the whole blood concentration $C_a$. A blood volume component $V_b$ should therefore be taken into account in the measured ROI concentration, $C_{ROI}$, as follows:

$$C_{ROI}(t) = C_{TISSUE}(t) - V_b\{C_a(t) - C_{TISSUE}(t)\} \qquad \text{(Equation 17).}$$

Rearranging the above equation:

$$C_{ROI}(t) = (1 - V_b)C_{TISSUE}(t) + V_bC_a(t) \qquad \text{(Equation 18).}$$


From the equations 16 and 18, $K_1$, $k_2$, $k_3$, $k_4$ and $V_b$ can be obtained using standard nonlinear regression analysis. And, from $k_3$, $k_4$, the BP' can be obtained as equal to $k_3/k_4$ (Lammertsma et al., 1996). Previous equations have been derived for negligible non–specific binding of the ligand. However, if the kinetics of non–specific binding are fast, the previous equations are still valid, because the rapid exchange between free and non–specific pools effectively increases the free compartment. If non–specific kinetics are slower, the $k_3/k_4$ ratio will contain a non–specific component.


## 2.4.7.2 Two compartment model (single tissue compartment) – kinetics

The details of this model can be found in the article of Lammertsma and colleagues (Lammertsma et al., 1996). Briefly, a relationship between $C_{TISSUE}$ and metabolite–corrected plasma concentration $C_P$ as a function of time can be described for the single–tissue compartment model as follows:

$$C_{TISSUE}(t) = K_1C_P(t)*exp(-k_2t) \qquad \text{(Equation 19)}$$

where,
$K_1$ is the rate constant for transfer from plasma to tissue compartment (ml/ml·min)

$k_2$ is the rate constant for transfer from tissue to plasma compartment (ml/ml·min).

A blood volume component $V_b$ is related to the whole blood concentration $C_a$. Hence, similarly to above, $V_b$ needs to be taken into account to describe the measured ROI concentration:

$$C_{ROI}(t) = (1 - V_b)C_{TISSUE}(t) + V_bC_a(t) \qquad \text{(Equation 20)}.$$

In this case, the parameters $K_1$, $k_2$ and $V_b$ can be obtained using standard nonlinear regression analysis. From $K_1$ and $k_2$, the DV of the ligand ($DV_d$) can be calculated as:

$DV_d = K_1/k_2$ (Lammertsma et al., 1996).

## 2.4.7.3 The reference tissue model – kinetics

The details of the reference tissue model kinetics can be found in the article of Lammertsma and colleagues (Lammertsma et al., 1996). Briefly, application of the above equations to the reference tissue model gives the following equations:

$$dC_{REF}(t)/dt = K'_1C_P(t) - k'_2C_{REF}(t) \qquad \text{(Equation 21)}$$

$$dC_{F+NS}(t)/dt = K_1C_P(t) + k_4C_B(t) - k_2C_{F+NS}(t) - k_3C_{F+NS}(t) \qquad \text{(Equation 22)}$$

$$dC_B(t)/dt = k_3C_{F+NS}(t) - k_4C_B(t) \qquad \text{(Equation 23)}$$

where,
$C_{REF}$ is the concentration in the reference region (kBq/ml)
$C_P$ is the metabolite–corrected plasma concentration (kBq/ml)
$C_{F+NS}$ is the concentration of the free (+ non–specifically bound) ligand in the tissue (kBq/ml)
$C_B$ is the specifically–bound concentration of the ligand in the tissue (kBq/ml)
$K_1$ is the rate constant for transfer from plasma to free compartment (ml/ml ·min)
$k_2$ is the rate constant for transfer from free to plasma compartment (ml/ml ·min)
$k_3$ is the rate constant for transfer from free to specifically–bound tissue (ml/ml ·min)
$k_4$ is the rate constant for transfer from specifically–bound tissue to free compartment (ml/ml ·min)

$K'_1$ is the rate constant for transfer from plasma compartment to reference tissue (ml/ml · min)

$k'_2$ is the rate constant for transfer from reference tissue to plasma compartment (ml/ml · min).

As mentioned earlier, in practice, $C_{TISSUE}(t) = C_B(t) + C_{F+NS}(t)$ (Equation 7). Taken the above equations together, it is now possible to derive a relationship between $C_{TISSUE}$ and $C_{REF}$. This contains six parameters: $K_1$, $k_2$, $k_3$, $k_4$, $K'_1$ and $k'_2$ but not $C_B$, $C_{F+NS}$ or $C_P$. However, the plasma constants $K_1$ and $K'_1$ enter only as a ratio $R_1 = K_1/K'_1$ which accounts for any differences in delivery to the region of interest and the reference tissue. By assuming that the DV of the non–specifically bound ligand in both the region of interest and reference tissues is the same ($K'_1/k'_2 = K_1/k_2$), it should be $k'_2 = k_2/R_1$. Hence,

$$C_{TISSUE}(t) = R_1[C_{REF}(t) + aC_{REF}(t)*exp(-ct) + bC_{REF}(t)*exp(-dt)] \quad \text{(Equation 24)}$$

where,

$a = (k_3+k_4 - c) \cdot (c - r)/p$,

$b = (d-k_3-k_4) \cdot (d - r)/p$,

$c = (s+p)/2$,

$d = (s - p)/2$,

$p = \sqrt{(s^2-q)}$,

$q = 4k_2k_4$,

$r = k_2/R_1$,

$s = k_2+k_3+k_4$,

$* =$ convolution integral.

By replacing $k_4$ by $k_3/BP'$, and by using standard nonlinear regression analysis, equation 24 can be used to obtain the best estimates of the four parameters ($R_1$, $k_2$, $k_3$ and BP) from the measured tissue concentrations $C_{TISSUE}(t)$ and $C_{REF}(t)$ without the need for measuring $C_P(t)$ (Lammertsma et al., 1996).

It should be noted, that this equation takes into account differences in delivery between specific and reference tissue ($R_1$) and that it does not assume that $C_{REF}(t)$ equals $C_{F+NS}(t)$.

## 2.4.8 Simplified reference tissue model

An alternative three–parameter reference tissue model is proposed by Lammertsma and Hume (Lammertsma and Hume. 1996) based on the original four–parameter reference tissue model. The reference tissue compartmental model is based on the following differential equations:

$$dC_{REF}(t)/dt = K'_1C_P(t) - k'_2C_{REF}(t) \hspace{2cm} \text{(Equation 25)}$$

$$dC_{F+NS}(t)/dt = K_1C_P(t) + k_4C_B(t) - k_2C_{F+NS}(t) - k_3C_{F+NS}(t) \hspace{0.5cm} \text{(Equation 26)}$$

$$dC_B(t)/dt = k_3C_{F+NS}(t) - k_4C_B(t) \hspace{2cm} \text{(Equation 27)}$$

where,
$C_{REF}$ is the concentration in the reference region (kBq/ml)
$C_P$ is the metabolite–corrected plasma concentration (kBq/ml)
$C_{F+NS}$ is the concentration of the free (+ non–specifically bound) ligand in the tissue (kBq/ml)
$C_B$ is the specifically–bound concentration of the ligand in the tissue (kBq/ml)
$K'_1$ is the rate constant for transfer from plasma compartment to reference tissue (ml/ml · min)
$k'_2$ is the rate constant for transfer from reference tissue to plasma compartment (ml/ml · min).

If the tracer kinetics in the target region are such that it is difficult to distinguish between free and specific compartments, the reference tissue model can be simplified further. This refers to the situation where the time–radio activity curve of the ROI can be fitted to a single tissue compartment model with plasma input (see above), without significant improvement when a two–tissue compartment model is used. In this case,

equation 25 is still valid, however, equations 26 and 27 can be replaced by a single equation:

$$dC_{TISSUE}(t)/dt = K_1 C_P(t) - k_{2a} C_{TISSUE}(t), \qquad \text{(Equation 28)}$$

where, $k_{2a}$ (1/min) is the apparent rate constant for transfer from specific compartment to plasma. If equation 28 provides a good representation of the tracer kinetics, the corresponding total DV of the tracer should be the same as that derived from equations 26 and 27. Hence,

$$K_1/k_{2a} = (K_1/k_2) \cdot (1+BP') \qquad \text{(Equation 29)}.$$

Combining the above equations, the following equation can be derived:

$$C_{TISSUE}(t) = R_1 C_{REF}(t) + \{k_2 - R_1 k_2/(1+BP'\} C_{REF}(t)^* \exp\{-k_2 t/(1+BP')\} \quad \text{(Equation 30)}.$$

In contrast to the four–parameter reference tissue model shown earlier, the simplified reference tissue model (Lammertsma and Hume. 1996) contains three parameters ($R_1$, $k_2$, and BP').

## 2.4.9 Determination of specific binding using the Simplified Reference Tissue Model

At equilibrium, there is no net transfer of the radioligand between the compartments. The equilibrium approaches to determine receptor binding compare the target region containing the receptor of interest and a reference region. The DV of the target region and the DV of the reference region can be measured as tissue activity [$C_B$]. Theoretically, both regions are different with respect to [$C_B$] but both should contain

the same activity of free ligand [$C_{F+NS}$]. Hence, the closest to BP would be BP' (see more in Innis et al., 2007).

Combining the principles that apply for *in vitro* studies and the clinical pharmacology terminology for DVs and the fact that BP' refers to specific binding; in imaging, "specific binding in tissue" should be calculated taking into account the nondisplaceable and total uptake of the radioligand in tissue. Hence, BP' should be related to the different DVs and to the ratio between tissue and free ligand activity as follows:

$$BP' = (DV_{REC}/DV_{REF}) - 1 = C_{TISSUE}/C_{F+NS} - 1 \qquad \text{(Equation 31)}$$

where, $DV_{REC}$ refers to the distribution volume of the ligand in target tissue and $DV_{REF}$ in the reference region, respectively.

Because it is often difficult to achieve actual equilibrium, an approximation is used from a graphic representation of kinetic data, the Logan plot (Logan et al., 1996), in which: when the integral of regional activity over current regional activity is plotted versus the integral of plasma activity over regional activity, the slope of the curve approximates the regional tracer DV. By comparing the slopes for $DV_{REC}$ and $DV_{REF}$, the BP' can be then calculated (Logan et al., 1996). If it can be assumed that $k_2$ is not changed by the experiment in either the target or the reference region, it is possible to avoid the use of plasma input function and a transformed time axis involving the integral of tissue activity in the reference region can be used. However, although the linear part of this plot approximates BP', this convenient variant of the Logan plot

(Logan et al., 1996) must be used with caution because the results might be biased by changes in blood flow. Since the fitting in the Logan plot approach can be done by simple linear regression, this method is well suited for generation of parametric images.

The DV of specifically–bound ligand in tissue ($DV_B$) should be therefore equal to:

$$DV_B = DV_{TISSUE} - DV_{ND} \qquad \text{(Equation 32)}$$

where, $DV_{TISSUE}$ is the DV of total ligand uptake in tissue relative to concentration of ligand in plasma and $DV_{ND}$ is distribution volume of free and non–specifically bound ligand in tissue relative to the ligand concentration in plasma. The term $DV_{TISSUE}/DV_{ND}$ is the distribution volume ratio (DVR) (Innis et al., 2007). Hence,

$$BP_{ND} = DVR - 1 \qquad \text{(Equation 33).}$$

$BP_{ND}$ values represent the ratio of specifically–bound radioligands to nondisplaceable ones in tissue at equilibrium. $BP_{ND}$ does not require arterial plasma concentrations and under equilibrium circumstances and certain assumptions, can be calculated "directly" from brain data using an appropriate reference tissue method. $BP_{ND}$ can be "indirectly" calculated from DVs with arterial plasma concentrations as $DV_{TISSUE}/DV_{ND} - 1$ (Innis et al., 2007). $BP_{ND}$ refers to *in vivo* measurement and reflects an approximation to *in vitro* BP which is truly equal to $B_{max}/K_D$. $BP_{ND}$ is unitless and it is the typical outcome measure in reference tissue methods as it directly compares the concentration of the radioligand in a rich–in–receptor region to that in a receptor–

free region. Its use depends heavily on the assumptions that nondisplaceable uptake is independent of subject groups or treatment effects. The advantages of the reference tissue model is that is least invasive, it reduces the complexity of scanning protocol and the imaging data analyses. In addition, there is no requirement for the labour–intensive measurements of labelled radiometabolites (Lammertsma and Hume. 1996).

## 2.4.10 Determination of specific binding using the Peak Equilibrium Model

The above principles and assumptions have been applied in both ^{123}I–β-CIT (Laruelle et al., 1994) and ^{123}I–Ioflupane SPECT protocols (Booij et al., 1997) proposing that quantification of specific to non–specific DAT binding in the striatum can be obtained without the use of arterial data. The longer half-life of [123]I (approximately 13.2 hours) as opposed to the PET isotopes such as [11]C (approximately 20 mins) allows to study the kinetics of uptake for several hours post–injection. The regional specific to non–specific binding ratios method assumes equal non– specific uptake in the striatum and the occipital cortex. The binding ratio has been shown to be a reliable estimate of Mintun's BP (= $B_{max}/K_D$).

DAT–specific imaging through SPECT was primarily developed to aid the clinical diagnosis of Parkinson's and Parkinson's plus syndromes. Its application needs to meet certain criteria for making the conduct of clinical SPECT studies easy to implement in clinical practice as well as for making their interpretation simple enough. In clinical practice, DAT–specific imaging *in vivo* studies typically refer to ^{123}I–Ioflupane SPECT imaging. Acquired SPECT data are usually reconstructed at a

nuclear medicine workstation in order to become available at the local site for visual assessment and reporting. Over the past few years, ^{123}I–Ioflupane SPECT imaging has become increasingly available across various clinical sites; its use has got extended from the clinical purposes and forming the grounds for imaging studies in Parkinson's. The great diagnostic value of ^{123}I-Ioflupane SPECT has therefore guided the methodology studies on DAT–specific binding around semi–quantification methods, given that this radioligand allows imaging through SPECT without the use of arterial line data. Semi–quantification methods of ^{123}I–Ioflupane allow to calculate specific binding ratios (SBR) that equal counts/voxel in rich–in–receptor binding sites over counts/voxel measured in non–specific reference regions, the latter being assumed to be devoid of dopaminergic neurons. Essentially, regional SBRs can be viewed as a robust outcome measure to reflect the density of DAT in certain regional terminals. The SBR calculation requires the definition of ROI(s)/VOI(s) and of the reference region.

For certain radioligands including the ^{123}I–β-CIT and ^{123}I–Ioflupane, the SBR can be regarded as equal to $BP_{ND}$, when the specific binding time activity curve reaches a peak. In this simulation, the major assumption is that $C'_{F+NS}(t)$ in the reference region is the same as $C_{F+NS}(t)$ in the specific binding region. This assumption is not the same as if $V'_{F+NS}=V_{F+NS}$ (Ichise et al., 2001). Indeed, as the radioligand moves from the free compartment to the specific compartment in the specific binding region, this assumption is unlikely to be entirely true. However, for some radioligands, the

assumption is sufficiently valid to derive adequate BP (Farde et al., 1989; Ichise et al., 2001). Hence, because,

$$C_{TISSUE}(t) = C_{F+NS}(t) + C_B(t) + C_P(t)V_b \qquad \text{(Equation 34)}$$

and $\qquad C_{REF}(t) = C'_{F+NS}(t) + C_P(t)V_b \qquad \text{(Equation 35)},$

if $C_{F+NS}(t)=C'_{F+NS}(t)$, then from equations 34, 35, $C_{TISSUE}(t) - C_{REF}(t) = C_B(t)$. Hence, $C_B(t)$ can be plotted and a curve fitted to these data. At the peak of the fitted curve, $dC_B(t)/dt=0$, hence $C_B(t)/C_{F+NS}(t) = k_3/k_4 = BP'$. A variation of this model applies to the case of $^{123}I-\beta$-CIT, in which the radioligand kinetics are so slow that a protracted peak equilibrium is reached 24 hours after injection and only one scan during this prolonged equilibrium is needed to estimate BP' (Laruelle et al., 1994). In other SPECT studies, SBR has been proposed to be a reliable estimate of $BP=B_{max}/KD$ (Farde and von Bahr. 1990; Laruelle et al., 1994, Booij et al., 1997). Hence, it is currently being used to reflect DAT–specific to non–specific binding derived from $^{123}I$–Ioflupane and $^{123}I$–β-CIT SPECT.

## 2.5 Molecular PET and SPECT targets in Parkinson's disease

PET and SPECT imaging techniques offer the potential of visualising *in vivo* the distribution of several biological compounds that have been associated with Parkinson's pathophysiology. A plethora of highly specific radioligands (Table 3) have been validated through PET and SPECT imaging for the study of several aspects of Parkinson's disease including: (a) the study of pathological dopamine neurotransmission, (b) the role of dopaminergic and non–dopaminergic terminals in

Parkinson's disease pathology, (c) the evaluation of diagnostic biomarkers in Parkinson's, (d) the development of molecular markers for studying Parkinson's disease progression (e) the study of Parkinson's disease related neuroinflammation and (f) the assessment of the efficacy of experimental treatments including novel neuro–modulating compounds and invasive restorative therapy. A schematic way to view dopamine neurotransmission in Parkinson's could be a study of the dopamine transmission at three sites: presynaptic, synaptic and postsynaptic.

Table 3 – List of dopaminergic radioligands validated for use in humans

| Short name of radioligand | Molecular target | Potential uses in studying Parkinson's disease | References |
|---|---|---|---|
| presynaptic dopaminergic membrane | | | |
| $^{123}$I–Ioflupane, $^{11}$C–β–CIT | dopamine transporter | reuptake of dopamine/ integrity of dopaminergic neurons and function | Booij et al., 1997 |
| $^{18}$F–CFT, $^{18}$F–WIN35,428 | | | Laakso et al., 1998 |
| $^{11}$C–methylphenidate | | | Volkow et al., 1996 |
| $^{11}$C–nomifensine | | | Brooks et al., 1990 |
| $^{11}$C–PE2I | | | Halldin et al., 2003 |
| dopamine | | | |
| $^{18}$F–Fdopa | aromatic L-amino acid decarboxylase | intraneuronal uptake of levodopa/ integrity of dopaminergic neurons | Garnett et al., 1983 |
| $^{11}$C-DTBZ | vesicular monoamine transporter–type 2 | synaptic vesicles function/ integrity of dopaminergic neurons and function | Koeppe et al., 1999 |
| $^{18}$F-Fluoropropyl-DTBZ | | | Lin et al., 2010 |
| postsynaptic dopaminergic membrane | | | |
| $^{11}$C-raclopride, $^{3}$H-raclopride | dopamine D2 receptors | dopamine transmission and release/ integrity of dopaminergic neurons and function | Hall et al., 1988 |
| $^{123}$I–iodobenzamide | | | Meyer et al., 2008 |
| $^{11}$C–SCH23390 | dopamine D1 receptors | | Farde et al., 1987 |
| $^{11}$C(+)–PHNO | dopamine D2 and D3 receptors | | Willeit et al., 2006 |
| $^{18}$F–Fallypride | | | Mukherjee et al., 2002 |
| $^{18}$F–desmethoxyfallypride | | | Siessmeier et al., 2005 |

The targets for each of the above sites are consecutively the presynaptic membrane, dopamine itself, and the postsynaptic dopaminergic membrane. Among the available PET and SPECT radioligands that have been designed to target dopaminergic transmission, the studies conducted for this thesis included SPECT imaging with ^{123}I–Ioflupane, and PET imaging with ^{11}C–DASB and ^{11}C–PE2I.

## 2.5.1 ^{123}I–Ioflupane

Table 4 – Summarised characteristics of ^{123}I–Ioflupane

| Chemical name | N-(3-Fluoropropyl)-2β-carbomethoxy-3β-(4-[123I]iodophenyl)nortropane |
|---|---|
| Abbreviated name(s) | ^{123}I–Ioflupane, ^{123}I–FP–CIT, ^{123}I–β–CIT–FP |
| Chemical formula | C18H23FINO2 |
| Molecular weight | 427.28 g/mol |
| Target | Dopamine transporter (DAT) |
| Imaging method used | Single photon emission computed tomography (SPECT) |
| Source of radioactive signal | [123]I |
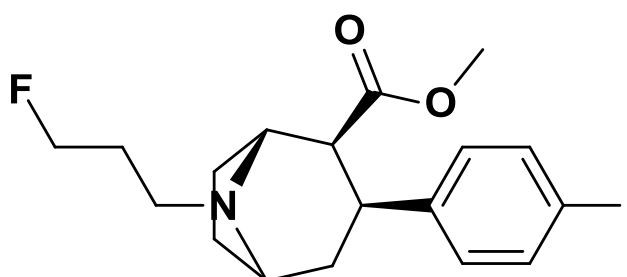


Figure 6 – Chemical structure of ^{123}I–Ioflupane

N-(3-Fluoropropyl)-2β-carbomethoxy-3β-(4-[123I]iodophenyl)nortropane (^{123}I–Ioflupane or ^{123}I–β–FP–CIT) is a cocaine analogue labelled with ^{123}I; it is synthesised by the trialkyltin nonradioactive precursor SnFP–CT which is prepared from nor–β–CIT (Neumeyer et al., 1994).

[123]I–Ioflupane is a SPECT radioligand with high *in vivo* affinity for the DAT (Booij et al., 1997; Booij et al., 1998). The main metabolic product of ^{123}I–Ioflupane is FP–CIT acid, a polar compound that is unable to cross the blood–brain barrier. The other metabolites include nor–β–CIT and free iodine. 48 hours post injection, about 60% of the injected radioactivity is excreted in the urine, while faecal excretion is estimated to be lower at approximately 14% (Booij et al., 1998). Ioflupane labelled with ^{11}C or ^{125}I rapidly reaches high concentrations in the human striatum as suggested by autoradiography in humans and through ^{11}C–β–FP–CIT PET in the cynomolgus monkey (Lundkvist et al., 1995). ^{123}I–Ioflupane has been suggested to have some affinity also for extrastriatal SERT sites in humans (Booij et al., 2007; Koopman et al., 2012). However, the affinity of ^{123}I–Ioflupane for the SERT has been proposed quite weak as compared to the affinities of less specific compounds such as β–CIT (Lee JY et al., 2014). The effective dose of ^{123}I–Ioflupane for adults and elderly in the striatum is 185 MBq/4.35 mSv (per 70 kg individual) (Kuikka et al., 1994; Booij et al., 1998; European Medicines Agency. 2011).

[123]I–Ioflupane has been granted a marketing authorisation by the European Medicines Agency (European Medicines Agency. 2011) valid throughout the European Union in

July 2000 (renewed in July 2010) and by the US Food and Drug Administration (Food and Drug Administration. 2011) for the United States in January 2011. ^{123}I–Ioflupane is indicated for assessing the loss of functional dopaminergic neuron terminals in the striatum in patients with clinically uncertain Parkinsonian syndromes which include Progressive Supranuclear Palsy, Multiple System Atrophy, dementia with Lewy bodies, drug–induced Parkinsonism and small vessel diseases other than idiopathic Parkinson's disease. In clinical practice, SPECT with ^{123}I–Ioflupane can be reported as normal or abnormal through subjective visual rating of the ^{123}I–Ioflupane signal (Figure 7). The examiner of the ^{123}I–Ioflupane SPECT must observe the images and judge the extent of ligand specific binding in the striatum based on background signal, which is assumed to be devoid of dopaminergic neurons.
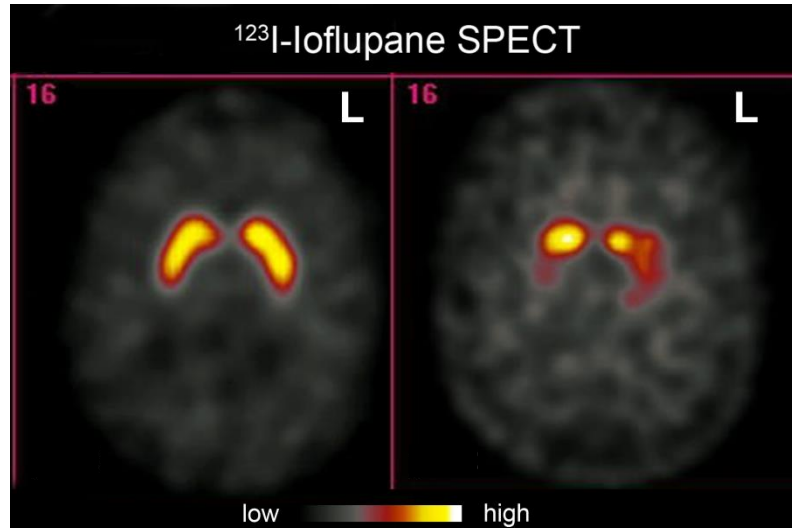


Figure 7 – Representative images (in the axial plane) of ^{123}I–Ioflupane specific to non–specific binding in the striatum in a control (left) and a patient with idiopathic Parkinson's disease (right)
L: left; colour scale represents ^{123}I–Ioflupane specific to non–specific binding (from high to low)

As a result, visual evaluation of DAT SPECT signalling can vary greatly based on the examiner's expertise and knowledge (Scherfler and Nocker. 2009). ^{123}I–Ioflupane SPECT is indicated to discriminate between Parkinsonian syndromes and Essential Tremor cases. It is also indicated to assist in the differential diagnosis between probable dementia with Lewy bodies and Alzheimer's disease. Hence, whereas the main diagnostic question refers to the integrity of the striatal dopaminergic function, ^{123}I–Ioflupane SPECT imaging can be used to investigate such integrity *in vivo* (Towey et al., 2011). ^{123}I–Ioflupane SPECT can be particularly useful in early stages of Parkinson's disease, where bradykinesia and rigidity may not manifest and a clinical presentation is not typical.

## 2.5.2 ^{11}C–DASB

Table 5 – Summarised characteristics of ^{11}C–DASB

| Chemical name | [(11) C]-3-amino-4-(2-dimethylaminomethyl-phenylsulfanyl)-benzonitrile |
|---|---|
| Abbreviated name(s) | [11]C –DASB |
| Chemical formula | C16H17N3S |
| Molecular weight | 283.69 g/mol |
| Target | Serotonin transporter (SERT) |
| Imaging method used | Positron emission tomography (PET) |
| Source of radioactive signal | [11]C |
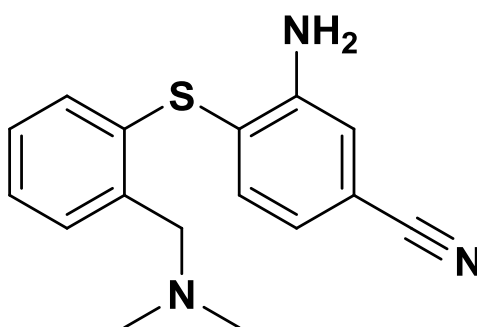
Figure 8 – Chemical structure of ^{11}C–DASB

[11]C–DASB or [11C]-3-amino-4-(2-dimethylaminomethyl-phenylsulfanyl)-benzonitrile labelled is synthesised by alkylation of its N-normethyl secondary amine precursor using [11C] iodomethane into the derived diphenyl-sulfid-molecule (Wilson et al., 2000a; Wilson et al., 2000b).

[11]C–DASB is a PET radioligand with high *in vivo* affinity and reversibility for the SERT and greater specific binding relative to non–specific binding. DASB has some affinity also for the norepinephrine transporter and the DAT. Binding affinities Ki (nm) of DASB for the SERT, the norepinephrine transporter, and the DAT are 0.97, 6,000, and 1,180 nm respectively (Wilson et al., 2000a; Wilson et al., 2000b; Houle et al., 2000; Ginovart et al., 2001; Ichise et al., 2003). The effective dose of ^{11}C–DASB has been calculated at 0.0070 mSv/MBq (26 mrem/mCi) for a 70–kg–standard man (Lu et al., 2004). About 12% of the injected radioactivity is excreted in the urine. It has been proposed most ^{11}C–DASB–derived activity is secreted via the gastrointestinal tract given the amount of activity noted in the liver and gallbladder (Lu et al., 2004). ^{11}C–DASB has a good uptake in the human brain (Houle et al., 2000; Ginovart et al., 2001) and a good specific binding relative to non–specific binding (Ginovart et al., 2001;

92

Ichise et al., 2003). ^{11}C–DASB has a good uptake in the hypothalamus, thalamus and the striatum, and lower uptake in the occipital cortex, the frontal cortex, and the cerebellum (Ginovart et al., 2001).

## 2.5.3 ^{11}C–PE2I

Table 6 – Summarised characteristics of ^{11}C–PE2I

| Chemical name | [^{11}C]N-(3-iodoprop-2E-enyl)-2β-carbomethoxy-3β-(4-methyl-phenyl)nortropane |
|---|---|
| Abbreviated name(s) | ^{11}C-PE2I, ^{11}C-LBT-999 |
| Chemical formula | C19H24INO2 |
| Molecular weight | 425.30 g/mol |
| Target | Dopamine transporter (DAT) |
| Imaging method used | Positron emission tomography (PET) |
| Source of radioactive signal | [11]C |
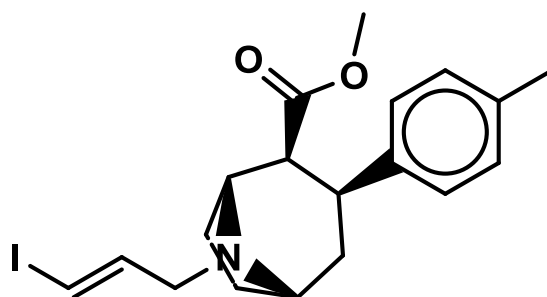


Figure 9 – Chemical structure of ^{11}C–PE2I

[11C]N-(3-iodoprop-2E-enyl)-2β-carbomethoxy-3β-(4-methyl-phenyl)nortropane    or

11C–PE2I is a cocaine analogue that is structurally related to β–CIT and FP–CIT

compounds. 11C–PE2I is a PET radioligand with high affinity for the DAT *in vitro* (Ki:

17 nM) and with much lower affinity (>30–fold) for the norepinephrine transporter

and the SERT (Emond et al., 1997; Chalon et al., 1999; Hall et al., 1999).

11C–PE2I has shown fast kinetics and favourable metabolism in the rhesus (Varrone et

al., 2011) and the cynomolgus monkey (Halldin et al., 2003). 11C–PE2I has a good

uptake in the human brain (Halldin et al., 2003; Ribeiro et al., 2007) and a good specific

binding relative to non–specific binding (Halldin et al., 2003; Jucaite et al., 2006). 11C–

PE2I has a good uptake in the putamen, caudate and lower uptake in the frontal

cortex, temporal cortex and the cerebellum (Halldin et al., 2003; Jucaite et al., 2006).

The effective dose of 11C–PE2I has been calculated at 0.0064 mSv/MBq which gives an

average effective dose of approximately 1.4 mSv per 11C–PE2I PET scan (Ribeiro et al.,

2007). Most of the 11C–PE2I–derived radioactivity is excreted via the urinary tract,

while activities that remain in the liver and the gallbladder are proposed to be smaller

(Ribeiro et al., 2007).

## 2.6 Tomography scanners

Each cohort of participants of the studies of this thesis underwent scanning on the

same scanner (see methods in each chapter for details). Part of the 11C–DASB PET

scans was acquired using a Siemens ECAT Exact HR (model 962) PET tomography

scanner (Brix et al., 1997), which has a total axial field of view of 155mm. Part of the ^{11}C–DASB PET scans was acquired on a Siemens Biograph TruePoint HI–REZ 6 PET/CT tomography scanner (Figure 10), which has a total axial field of view of 162mm. ^{11}C–PE2I PET scans were acquired on Siemens Biograph TruePoint HI–REZ 6 PET/CT tomography scanner. ^{123}I–Ioflupane SPECT scans were acquired using a Siemens Symbia T16 SPECT–CT tomography scanner. Part of the MRI scans was acquired using a Siemens MAGNETOM Avanto 1.5–Tesla MRI system. Part of the MRI scans was acquired using a Siemens MAGNETOM Trio 3–Tesla MRI system.



Figure 10 – Siemens Biograph TruePoint HI–REZ 6 PET/CT tomography scanner

## 2.7 Supply of radioligands

[11]C–DASB solution for intravenous injection was partly supplied by Hammersmith Imanet plc, London, UK and partly by Imanova Ltd, London, UK (see methods sections in each chapter for details). ^{123}I–Ioflupane was fully supplied as DaTSCAN™

solution for intravenous injection by GE Healthcare Ltd, Little Chalfont, Buckinghamshire, UK. ^{11}C–PE2I was fully supplied by Imanova Ltd, London, UK.

## 2.8 Scanning procedures

Patients were positioned supine such that the transaxial plane was parallel to the bicommissural line. Movement was minimised using memory foam padding and video monitoring utilised to aid detection and subsequent repositioning. Participants were instructed to fast from 8am on the day of the scan and to avoid the consumption of alcohol and caffeine–containing beverages for at least 12 hours before scanning. All Parkinson's disease patients who at the time of scanning were treated with dopaminergic agents were asked to withdraw from medication 18 hours for standard release and 48 hours for prolonged release medications prior to any procedure involving ionising radiation and this was defined as the "off" dopaminergic medication state. None of the participants in the studies described in this Thesis was treated with any drugs with direct action on the serotonergic system.

### 2.8.1 PET scanning procedures

A low CT transmission scan (0.36 mSv) of the brain was acquired prior to each PET scan for attenuation correction. Subjects were in a resting state during scanning time. PET radioligand volumes were prepared to 10ml using normal saline solution. A mean activity dose of 450 MBq was administered to each individual participant undertaking a ^{11}C–DASB PET scan. A mean activity dose of 350 MBq was administered to each individual undertaking a ^{11}C–PE2I PET scan. PET radioligands

were administered intravenously as single bolus injections followed immediately by 10ml normal saline flush. Administration was at a rate of 1ml/s. Dynamic emission ^{11}C–DASB, ^{11}C–PE2I PET data were acquired continuously for 90 minutes post–injection.

## 2.8.2 SPECT scanning procedures

[123]I–Ioflupane was injected intravenously as single bolus injection. A mean activity dose of 185MBq was administered to each individual undertaking a ^{123}I–Ioflupane SPECT scan. For the administration of ^{123}I–Ioflupane, thyroid gland blockade was performed by administering potassium iodide tablets 60mg twice daily for three consecutive days, starting 24 hours prior to the SPECT scan day, in accordance to the clinical protocol of the Nuclear Medicine department of Imperial College Healthcare NHS Trust. ^{123}I–Ioflupane SPECT data were acquired continuously while participants were at rest for approximately 45 minutes (acquisition parameters: 128 views with 128x128 matrix and 1.45 zoom with 30 seconds per view in step–and–shoot mode; 15% energy window centred on the 159 keV photopeak of ^{123}I; 2 million total counts). ^{123}I–Ioflupane SPECT data were acquired 180 minutes after intravenous bolus injection of ^{123}I–Ioflupane in line with the clinical protocol of the Nuclear Medicine department of Imperial College Healthcare NHS Trust.

## 2.8.3 MRI scanning procedures

T1–weighted (repetition time = 1900ms, echo time = 3.53ms, flip angle = 15°, inversion time = 1100ms and 1mm isotropic) MRI sequences were obtained with Siemens

MAGNETOM Avanto 1.5–Tesla MRI scanner. T1–weighted volumetric (repetition time = 2300ms, echo time = 2.98ms, flip angle = 9°, time to inversion = 900ms and 1mm isotropic) MRI sequences were obtained with Siemens MAGNETOM Trio 3–Tesla MRI scanner. One whole brain MRI scan lasted 301 seconds, and participants were instructed to remain as still as possible. Prior to any imaging data analysis, all MRI scans were visually reviewed by the MRI Radiology Clinic of Imperial College Healthcare NHS Trust, to exclude ischaemic disease in the basal ganglia.

## 2.9 Analysis of imaging data

The first two paragraphs introduce definitions and terminology used in sections 2.9.3–2.9.6, and the latter paragraphs include the details of the performed analyses of PET and SPECT imaging data.

### 2.9.1 Image registration (or image fusion, matching or warping)

When two brain images are being registered, this refers to the geometric alignment of two (or more) images. The term coregistration refers to intrasubject registration (alignment of two or more images of the same subject) and the term realignment refers to motion correction within the same subject. The term normalisation refers to inter-subject registration that is when several population groups are being studied. The first image is commonly termed as static (or baseline or reference image), while the second image is named as transformed (or source image, repeat or floating image). The image similarity measure (alternatively termed as objective or cost function) refers to the criterion being used to register the two brain images. The geometrical transformation

that maps the features of one image to the features of the other image is termed as transformation (also known as deformation field, displacement field or warp) (Crum et al., 2004). The transformations can be classified variously depending and numerous criteria have been proposed (Oliveira and Taveres. 2014). In brain image registration, mapping is typically as 3D–image to another 3D–image (dimensional classification). When classification refers to the transformation elasticity, image registration can be termed as rigid, affine or non–rigid, projective or curved. Hence, rigid transformation, all points of the image preserve their distances i.e. the image is only rotated and translated (six parameters rigid body transformation). When this transformation gets extended to include not only rotation and transformation but also scaling and shear, this is termed as affine. Affine transformations map parallel lines to parallel lines. In contrast, non–rigid transformations map straight lines to curves (reviewed by Holden. 2008). The terms linear and non–linear are commonly used in literature to denote affine and non–rigid transformations, though this is not mathematically correct (Crum et al., 2004; Oliveira and Tavares. 2014). A quantification analysis approach for each individual was used to quantify reconstructed tomographic PET imaging data. Estimation of $BP_{ND}$ was calculated from DVs as $DV_{TISSUE}/DV_{ND} - 1$ (Innis et al., 2007) for each of the following ROIs. To determine the local distribution of PET radioligands in the brain, I defined the ROIs anatomically.

## 2.9.2 Definitions of ROIs

Regions of interest (ROIs) and volumes of interest (VOIs) are widely used in most imaging modalities. A simple approach in quantitatively analysing an image, is by

quantifying the mean intensity in an ROI. The ROI as a region can be a specific organ or a subregion of that such as a lesion in the brain. The shape, size and anatomical location of the ROI can be either defined by the person who performs the analysis from a selection of predefined shapes or drawn manually having an irregular shape.

A ROI is commonly defined in a single image plane (Figure 11) and can be extended to multiple contiguous planes to form a VOI. The VOI is therefore used to define a group of voxels (and/or partial voxels) and the average or total signal within the volume gives some measure of the tissue or organ contained within it. These need to be processed further, either by comparing to a normal range/cut–off or by combining it with data from another volume. VOI sizes typically range from individual voxels up to sub–organ or organ sized volumes. The shapes can be defined manually or automatically using some form of edge detection/region growing algorithm. Often standard sized VOIs will be defined based on templates or structural images. VOIs can be placed manually or automatically. Automatic positioning of VOIs can be based on image registration, edge detection or image maximum/minimum values.

One advantage of using VOI data is that the counts/signal in the VOI will often directly represent a clinically relevant physical value, or can be used to create such a figure. For example, the counts within a VOI on $^{123}$I–Ioflupane SPECT images is proposed to be proportional to the number of DAT sites within that volume. If a dynamic sequence of images has been acquired, the ROI that has been defined can be then applied to the same region on all images to generate a time activity curve. These

curves are region–specific and show the concentration of the radioligand over time. This time–dependent data set can be then used with a compartmental model to determine biologically meaningful parameters and to construct parametric images.

In the PET studies of this thesis, the ROIs were left and right caudate and putamen nuclei. The reference region was the cerebellum. ROIs were drawn manually based on anatomical borders on the axial section that were defined as follows guided by the Duvernoy three-dimensional sectional atlas (Duvernoy. 1999) using Analyze medical imaging software Version 11.0 (Biomedical Imaging Resource, Mayo Clinic).

For the *caudate*: the anterior border was defined by the lateral ventricle, the posterior border by the internal capsule, the medial border by the lateral ventricle and fornix and the lateral border by the external capsule. For the *putamen*: the anterior border was defined by the anterior limb of the internal capsule, the posterior border by the posterior limb of the internal capsule, the medial border by the external medullary lamina and the lateral border by the external capsule/claustrum. For the *cerebellum*: The anterior border was defined by the inferior semilunar lobule, the posterior border and the lateral border by the transverse sinus and the medial border was defined by the cerebellar falx.
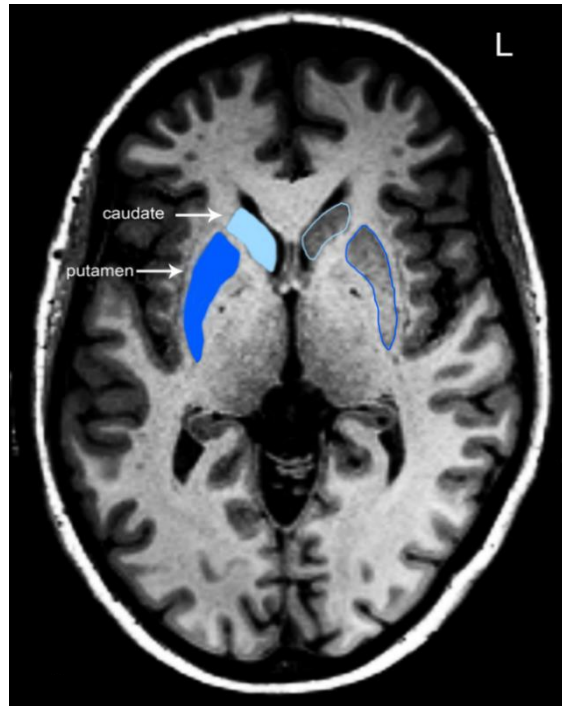
Figure 11 –Caudate and putamen nuclei

Caudate and putamen nuclei are outlined/filled in light blue and dark blue colours, respectively, and annotated in white letters on MRI T1–weighted image in the axial plane; L: left

## 2.9.3 Analysis of ^{11}C–DASB PET imaging data acquired on Siemens ECAT Exact HR PET tomography scanner

[11]C–DASB PET data were analysed employing the SRTM (Lammertsma and Hume. 1996; Gunn et al., 1997) to calculate regional $BP_{ND}$ values. Cerebellar grey matter was used as the reference region based on the assumption that the cerebellum is devoid of serotonergic innervation (Ginovart et al., 2001).

Data were binned into a dynamic series of 28 temporal frames. The dynamic images were reconstructed with the standard Siemens settings using an FBP (direct inversion Fourier transform) algorithm on a 128x128 matrix, zoom 2mm and smoothed using a

3D transaxial Gaussian image filter (full width at half approx. = 5 ? 6 mm). Corrections were applied for attenuation, decay, randoms and scatter.

Following reconstruction of the dynamic ^{11}C–DASB PET image volume, an ADD image was created from the entire dynamic data set using an in–house software package (c_wave). The term *ADD* is not an acronym but is an alternative term for the so–called *summed* or *integrated* images. A template of high–contrast ROIs was defined directly on that ADD image and the ROIs were then applied to the dynamic dataset in order to obtain regional time activity curves and assess whether there was any movement. To correct for intra–scan head movement, dynamic PET images were corrected using a frame-by-frame realignment procedure (reference frame = frame 13) (Montgomery et al., 2006). Frame 13 was chosen as the reference frame because this offered good signal-to-noise ratio and a signal distribution containing features present in both early and late frames. Motion correction did not include adjustment of the attenuation map. The fact that some of the Parkinson's patients were clinically categorised as dyskinetic, did not have an impact on PET scanning, as during each PET scan, all Parkinson's patients were in an "off" dopaminergic medication state i.e. voluntary as well as involuntary movements were quite limited. PET scan record notes also confirmed that no large movement occurred.

Subject MRIs were manually centred on the anterior commissure and then aligned to the bicommisural line in Analyze software. Sufficient alignment to the bicommisural line was checked in transverse, sagittal and coronal planes. Re-orientated MRIs were

then coregistered to the summed (ADD) PET images with normalised mutual information (Studholme et al., 1999) in SPM software (Statistical Parametric Mapping, Wellcome Trust Centre for Neuroimaging, London, UK). Coregistration was visually assessed once completed to see if landmarks are coregistered with a degree of accuracy. Following coregistration, the ROIs were drawn manually on the coregistered MRI in Analyze guided by the Duvernoy three-dimensional sectional atlas (Duvernoy. 1999). Manual delineation of the striatal ROIs was made on the axial plane followed by checks on the coronal plane. ROIs were standardised for volume throughout participants and were manually defined for left and right caudate, and left and right putamen. In c_wave, five consecutive slices were selected on the ADD image to best represent the cerebellum. The reference region was drawn manually in Analyze on the ADD image including cerebellar grey matter and avoiding inclusion of the vermix.

Each object map was then applied to the dynamic images to generate time activity curves using Analyze software. ^{11}C–DASB $BP_{ND}$ values were calculated for each individual for the caudate and the putamen for both hemispheres using c-wave. The average caudate and average putamen specific binding was calculated per individual as the mean caudate $BP_{ND}$ and mean putamen $BP_{ND}$ values, respectively.

## 2.9.4 Analysis of ^{123}I–Ioflupane SPECT imaging data

The European guidelines for DAT imaging (Darcourt et al., 2010) state that semi–quantitative analysis may be useful and that it should include standardised ROIs and

have a normal range preferably based on age–matched controls. Whereas a semi–quantitative analysis approach is used, they recommend the use of either occipital cortex or the cerebellum as reference regions to assess non–specific binding (Darcourt et al., 2010). For the SPECT studies of this thesis, a semi–quantification analysis approach for each individual was used for the ^{123}I–Ioflupane SPECT imaging data. Acquired SPECT data were transferred to a HERMES–workstation and reconstructed with attenuation, scatter and resolution corrections. The reconstructed tomographic data were analysed using the commercially available Brain Registration and Analysis Software Suite (BRASS™) software (Radau et al., 2000; Koch et al., 2005) (HERMES medical solutions, Sweden). The software uses automatic image registration to align the examinee's image to the EARL.db template (HERMES medical solutions, Sweden).This template is made of the scans of twenty healthy controls (not related to the controls presented in the studies of this thesis) that have been spatially registered as follows using Hybrid Recon™ software (HERMES medical solutions, Sweden).

SPECT images were reconstructed using the default software OSEM algorithm that incorporates corrections for attenuation (according to the Chang method; attenuation coefficient $\mu=0.12$ cm$^{-1}$; as in Chang. 1978), scatter (according to Monte Carlo simulation; as in Koch et al., 2005 and in Morton et al., 2005) and camera and collimator resolution recovery using Hybrid Recon™ software (HERMES medical solutions, Sweden). Furthermore, SPECT data were corrected for camera–specific image properties as defined by respective phantom measurements. The reconstructed

SPECT images were smoothed using a 3D Gaussian image filter (full width at half maximum = 7 mm).

During automatic fitting with BRASS™, the function used to determine the similarity of the realigned image to the template is the normalised mutual information (Studholme et al., 1999). The normalised mutual information algorithm is the default setting in BRASS™ for ^{123}I–Ioflupane SPECT studies (see also – Holden et al., 2000; Radau et al., 2001; Yokoi et al., 2004).

Following automatic fitting, a series of predefined volumes of interest (VOIs) were defined based on the EARL.db template. The VOIs were then applied to the image being analysed. All scans were inspected visually and, where necessary, manually realigned to fit to the predefined template (Figure 12). SPECT studies with excessive motion were discarded. A volume centred on the occipital cortex was identified and used as an estimate of non–specific binding in counts/voxel ($C_{NS}$). The volume was defined on the template image using MRIcro software (Rorden and Brett. 2000) and then converted into a binary mask. This volume was then used to scale the counts in each voxel ($C_{VOI}$) so that to calculate the specific to non–specific binding ratio ($C_S/C_{NS}$) for that voxel.

The software automatically calculates SBR values for each region as:

$$SBR = C_S/C_{NS} = (Target – Background) / Background \qquad (Equation\ 36).$$

Here, the *Target* value is the counts/voxel for one of the defined regions ($C_{VOI}$), for example the left caudate, and the *Background* value is the counts/voxel from the occipital cortex, the latter being defined as the reference region. Alternatively, for the SPECT studies of this thesis, the above equation can be written as:

$$\text{DAT–specific to non–specific binding} = \frac{(\text{striatal counts} - \text{background counts})}{\text{background counts}} \qquad \text{(Equation 37)}$$
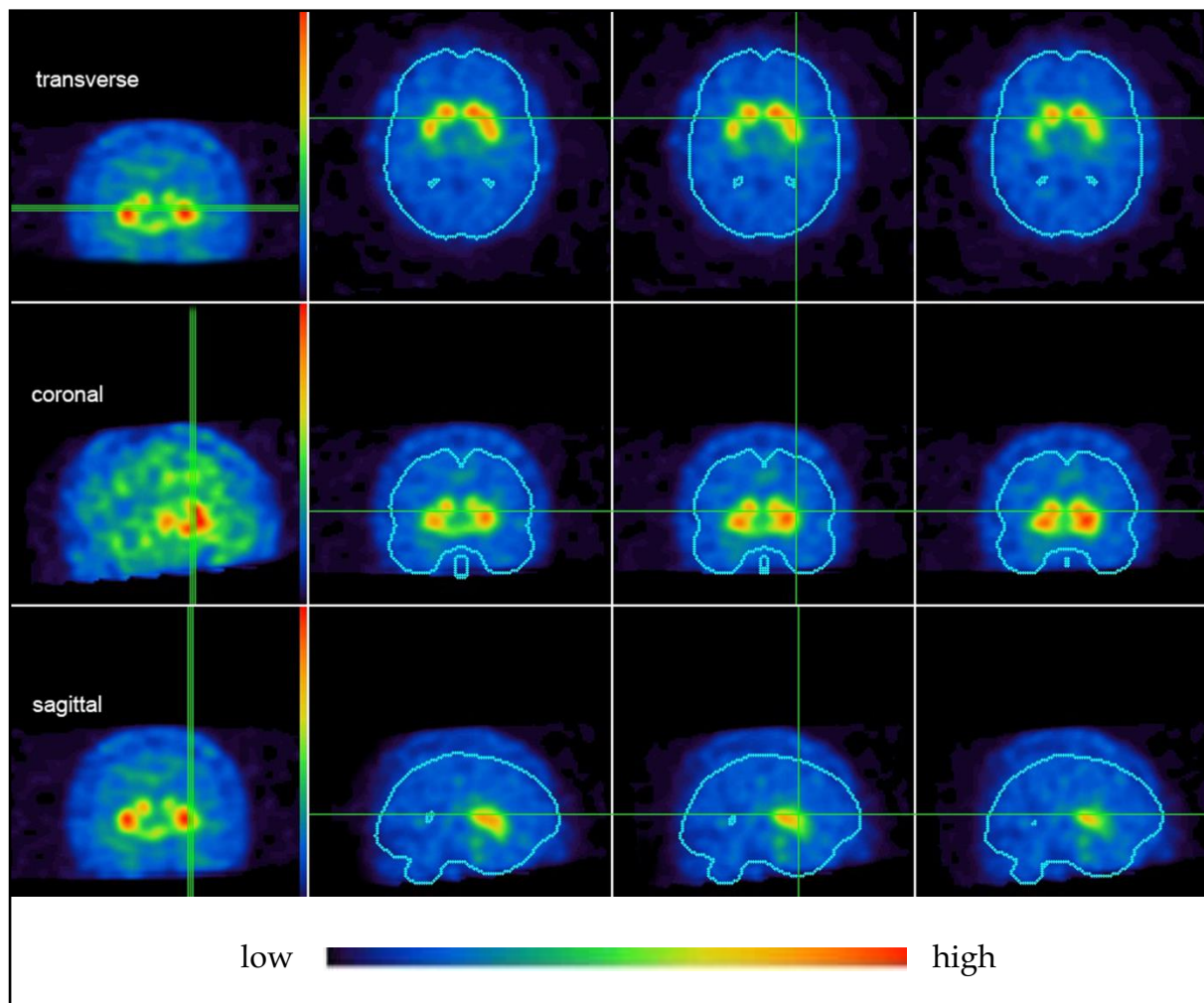


Figure 12 – Pre–processing ^{123}I–Ioflupane SPECT data using BRASS™ software: manual fitting to a predefined template

The figure shows three consecutive slices (green lines) of a ^{123}I–Ioflupane scan in transverse, coronal and sagittal planes. Colour intensity represents density of ^{123}I–Ioflupane specific to non–specific binding (from high to low)

The DAT–specific binding as reflected by the ^{123}I–Ioflupane specific to non–specific binding ratio values was calculated for each caudate and putamen for both hemispheres. The average caudate and average putamen binding was calculated per individual as the mean specific to non–specific binding ratio values for both hemispheres.

## 2.9.5 Analysis of ^{11}C–DASB and ^{11}C–PE2I PET imaging data acquired on Siemens Biograph TruePoint HI–REZ 6 PET/CT tomography scanner

[11]C–DASB and ^{11}C–PE2I PET data were analysed employing the SRTM (Lammertsma and Hume. 1996; Gunn et al., 1997) to calculate regional $BP_{ND}$ values. Cerebellar grey matter was used as the reference region based on the assumption that the cerebellum is devoid of serotonergic (Ginovart et al., 2001) and dopaminergic innervation (Halldin et al., 2003; Jucaite et al., 2006).

Data were binned into a dynamic series of 26 temporal frames. The dynamic images were reconstructed with the standard Siemens settings using an FBP (direct inversion Fourier transform) algorithm on a 128 x 128 matrix, with zoom of 2.6 and 2mm isotropic pixel size and smoothed using a 3D transaxial Gaussian image filter (full width at half maximum = 5mm). Corrections were applied for attenuation, decay, randoms and scatter.

Pre–processing and kinetic modelling for the ^{11}C–DASB and ^{11}C–PE2I PET data was conducted using MIAKAT™ (Molecular Imaging and Kinetic Analysis Toolbox,

version 3.4.2, Imanova Imaging Centre, London, UK; Gunn et al., 2016). Brain extraction was performed on structural MRI images using the FSL BET (Brain Extraction Tool; Analysis Group, FMRIB, Oxford, UK) algorithm (Smith. 2002) in order to delete non–brain tissue. T1–weighted images were then segmented and registered to the MNI template (Mazziotta et al., 1995; Hammers et al., 2003) using 6–parameters rigid–body registration in SPM creating $MRI_R$ images (MRI images registered to MNI template). This term refers to MRI images registered to the MNI template. $MRI_R$ images were then used for manual ROI delineation in Analyze software (Tziortzi et al., 2011). This refers to manual delineation of the striatal ROIs on the axial plane followed by checks on the coronal plane. The $MRI_R$ and ROI map were then downsampled from 1mm to 2mm isotropic voxel sizes.

The cerebellum was defined by using 12-parameters affine registration followed by non–linear warping procedure of the MNI template to the $MRI_R$ images in SPM. The corresponding transformations were applied to an MNI–based regional atlas (Clinical Imaging Centre Atlas v.1.2 GlaxoSmithKline Clinical Imaging Centre, London, UK), as described previously (Tziortzi et al., 2011), in order to transfer the definition of the cerebellum onto the subject's $MRI_R$. Segmentation maps were then used to isolate cerebellar grey matter.

To correct for intra–scan head movement, dynamic PET images were corrected using a frame-by–frame realignment procedure (reference frame = frame 16) and summed to obtain signal-averaged (ADD) images. Frame 16 was chosen as the reference frame

because this offered good signal-to-noise ratio and a signal distribution containing features present in both early and late frames. Motion correction did not include adjustment of the attenuation map. The fact that some of the Parkinson's patients were clinically categorised as dyskinetic, did not have an impact on PET scanning, as during each PET scan, all Parkinson's patients were in an "off" dopaminergic medication state i.e. voluntary as well as involuntary movements were quite limited. PET scan record notes also confirmed that no large movement occurred. ADD images were then coregistered to the $MRI_R$ images using the normalised mutual information algorithm (Studholme et al., 1999). Coregistration was visually assessed once completed to see if landmarks are coregistered with a degree of accuracy. The derived registration parameters were then applied to the motion-corrected dynamic frames so that all images were in register. ROIs maps were then applied to the registered dynamic PET frames to obtain regional time–activity curves.

[11]C–DASB $BP_{ND}$ and ^{11}C–PE2I $BP_{ND}$ values were calculated for each caudate and putamen for both hemispheres, reflective of SERT and DAT specific binding. The average caudate and average putamen specific binding was calculated per individual as the mean caudate $BP_{ND}$ and mean putamen $BP_{ND}$ values, respectively.

## 2.9.6 Calculation of SERT–to–DAT binding ratios

SERT–to–DAT binding ratios (as reflected by ^{11}C–DASB $BP_{ND}$ to ^{123}I–Ioflupane specific binding or ^{11}C–DASB $BP_{ND}$ to ^{11}C–PE2I $BP_{ND}$) for the caudate and the putamen were calculated comprising the average caudate and average putamen uptake values

for each individual participant. SERT–to–DAT binding ratio values were calculated according to the following formulas and refer to different cohorts, hence they were not compared to each other. For the study of *Chapter 5*:

$$\text{SERT/DAT binding ratio} = \frac{\text{11C-DASB BPND}}{\substack{\text{123I-Ioflupane specific to} \\ \text{non-specific binding}}}$$

and for the study in *Chapter 6*:

$$\text{SERT/DAT binding ratio} = \frac{\text{11C-DASB BPND}}{\text{11C-PE2I BPND}} \, .$$

## 2.10 Statistical analyses

The statistical analyses used for the studies in this thesis include both parametric and non–parametric statistical tests. Homogeneity and normality in distribution were tested with Bartlett's and Kolmogorov–Smirnov tests. For multiple comparisons of continuous data that were normally distributed, one–way analysis of variance (ANOVA) was used to compare means and *post hoc* Bonferroni correction was applied, whereas mean values were different. Comparisons between two groups were performed with t–test for independent samples and paired t–test for related samples, where appropriate. For multiple comparisons of values that did not have a normal distribution, the non–parametric Kruskall–Wallis test was used; *post hoc* checked with Dunn's test. Comparisons between two groups were performed with Mann–Whitney U test for independent samples and Wilcoxon signed–rank test for related samples. For sex, being a categorical variable, chi–squared ($\chi^2$) test was performed. The investigation of statistical correlations between clinical and imaging values was performed with the non–parametric Spearman's rank order correlation (r); *post hoc*

correction for multiple testing was performed with Benjamini–Hochberg procedure. The Spearman's correlation test was selected considering the small sample sizes and the level of normality.

The significance (alpha level) was set at $\alpha=0.05$; $p$ values below 0.05 were suggestive of statistical significance. Details of the statistical tests employed for each study are documented in the methods section of each chapter. For all the studies described in this thesis, statistical analyses were performed using the IBM SPSS® Statistics software, Version 22 for Microsoft windows. Graph illustrations were performed using the GraphPad Prism software, Version 6 for Microsoft windows.

# ☞ Chapter 3

# Retrospective analysis of DAT terminals' availability in the striatum of *de novo* Parkinson's disease patients: relevance to dyskinesias

## 3.1 Introduction

The occurrence of LIDs has been linked with the duration of levodopa treatment (Schrag and Quinn. 2000) and with longer disease duration; as the duration of levodopa treatment increases to a decade, more than 90% of Parkinson's disease patients eventually experience dyskinesias (Ahlskog and Muenter. 2001). As striatal DAT availabilities decline progressively in the course of Parkinson's, it could be questioned whether critical DAT decreases in the striatum precede the appearance of LIDs in earlier stages of the disease.

## 3.2 Aim and hypothesis

This study intended to estimate the role of striatal DAT availability, as reflected by ^{123}I–Ioflupane SPECT, as a prognostic marker for the appearance of LIDs. I hypothesised that Parkinson's patients with LIDs had lower striatal DAT availability in earlier stages of the disease as compared to non–dyskinetic patients.

## 3.3 Methods

### 3.3.1 Participants

42 participants with Parkinson's were included in this study. All Parkinson's disease patients had a ^{123}I–Ioflupane SPECT brain scan, at a time they were drug–naïve. Twelve healthy volunteers were included as controls. Parkinson's disease patients were retrospectively selected from the Movement Disorders Clinics of the Imperial College Healthcare NHS Trust, London, UK. All Parkinson's disease patients were recalled to provide informed written consent and were then included in this study.

### 3.3.2 Clinical assessments

A cut–off time point to assess the presence of dyskinesia was five years after the clinical diagnosis of Parkinson's disease. Patients were then divided in two groups depending on whether they had a history of LIDs (dyskinetic group) or not (patients without LIDs). Clinical data were collected retrospectively from medical notes and clinical letters to general practitioners. Missing data and queries were cross checked with individual participants. The following clinical data were recorded for this cohort of Parkinson's disease patients: history of dyskinesia, date of diagnosis, medication history, daily $LED_{Ldopa}$, $LED_{Dag}$ and $LED_{Total}$. Clinical evaluation of motor symptoms' severity and progression was performed using the Hoehn & Yahr staging scale (Hoehn and Yahr. 1967). The severity of Parkinson's disease patients was standardised by enrolling patients who were drug–naïve and had Hoehn & Yahr stage 1 (unilateral involvement). Differences were sought between the two groups for clinical characteristics at both baseline and at the five–year cut–off time points. Parkinson's disease patients with a clinical history of depression and/or cognitive impairment were excluded from this study. Normal controls were screened for depression using the HAM–D scale and for cognitive impairment using the MMSE. See also Sections 2.2 and 2.3.

### 3.3.3 Imaging procedures

All Parkinson's disease patients had a ^{123}I–Ioflupane SPECT brain scan 2.23±2.29 years after clinical diagnosis. All Parkinson's disease patients alongside a ^{123}I–Ioflupane SPECT scan had a 1.5 Tesla T1–weighted MRI scan. See details in *Chapter 2*, Sections 2.6, 2.7, and 2.8.2.

### 3.3.4 $^{123}$I–Ioflupane SPECT imaging data analysis

See details in *Chapter 2*, Sections 2.9 and 2.9.4.

### 3.3.5 Statistical analyses

For multiple comparisons of values that were normally distributed, one–way ANOVA was used to compare means and *post hoc* Bonferroni correction was applied. Comparisons of means of age, DD$_{diagn}$, daily LEDs, and $^{123}$I–Ioflupane specific to non–specific binding between groups (either controls to Parkinson's group or PD LIDs to PD non–LIDs) were performed with t–test for independent samples. Comparisons of Hoehn & Yahr scores between LIDs and non–LIDs groups were performed with Mann–Whitney U test for independent samples. See also Section 2.10 and legends of Tables 7,8 and Figures 13,14 below.

## 3.4 Results

### 3.4.1 Clinical data

At the time of $^{123}$I–Ioflupane SPECT scanning, all Parkinson's disease patients (27M:15F) were drug–naïve. At the five–year cut–off time point, all Parkinson's patients were treated with levodopa for a minimum of two years. Patients were then divided in two groups: 10 Parkinson's disease patients (6M:4F) with a history of LIDs and 32 (21M:11F) who had not developed dyskinesias (non–LIDs). At the time of $^{123}$I–Ioflupane SPECT scanning, there was no difference in age between controls and the Parkinson's disease group of 42 patients; however, between subgroup comparison showed that PD patients who later developed LIDs were younger at $^{123}$I–Ioflupane

SPECT scanning time ($p<0.05$) as compared to those who did not develop LIDs. No statistically significant difference was found between the two Parkinson's groups for disease duration and Hoehn & Yahr staging. At the five–year cut–off time point, the group of Parkinson's disease patients with LIDs had higher Hoehn & Yahr scores (2.50±0.59) as compared to the group of patients without LIDs (2.00±0.47), ($p<0.05$). The dyskinetic group was taking significantly higher $LED_{Ldopa}$ and higher $LED_{Total}$ doses as compared to the non–dyskinetic group ($p<0.001$).

Table 7 - Demographics and clinical characteristics of Parkinson's disease patients

| | normal controls | PD patients | | |
|---|---|---|---|---|
| | | all | PD non–LIDs | PD LIDs |
| No. of participants | 12 | 42 | 32 | 10 |
| [a]Sex | 7M:5F | 27M:15F [ns] | 21M:11F | 6M:4F [ns] |
| at ^{123}I–Ioflupane SPECT time | | | | |
| [b]Age | 61.41±8.64 | 63.95±11.04[ns] | 65.96±9.25 | 57.49±12.87* |
| [b]$DD_{diagn}$ | - | 2.22±2.34 | 2.22±2.52 | 2.21±1.51 [ns] |
| H&Y stage | - | 1 | 1 | 1 |
| Daily $LED_{Total}$ | - | - | - | - |
| 5 years post clinical diagnosis | | | | |
| [b]Age | - | 67.20±11.04 | 68.74±10.05 | 62.28±13.12[ns] |
| $DD_{diagn}$ | - | 5 | 5 | 5 |
| [c]H&Y stage | - | 2.12±0.55 | 2.00±0.47 | 2.50±0.59* |
| [b]Daily $LED_{Total}$ | - | 410.10±234.08 | 355.47±227.41 | 728.90±147.42*** |
| [b]Daily $LED_{Ldopa}$ | - | 332.95±223.38 | 254.22±174.15 | 584.90±155.64*** |
| [b]Daily $LED_{Dag}$ | - | 111.43±155.26 | 101.25±136.77 | 144.00±193.87[ns] |

Data represent mean values ± 1 SD; PD: Parkinson's disease; H&Y: Hoehn & Yahr staging scale in "off" medication state; Age and $DD_{diagn}$ are calculated in years. Daily $LED_{Total}$, $LED_{Ldopa}$, and $LED_{Dag}$ are calculated in mgs; Multiple comparisons were conducted with one–way ANOVA followed by *post hoc* Bonferroni correction; [a]Comparison for differences in sex was performed with chi–squared ($\chi^2$) test; [b]Comparison of means was made with t–test for independent samples; [c]Comparison of Hoehn & Yahr scores between LIDs and non–LIDs groups was performed with Mann–Whitney U test; ns – no statistically significant difference between all PD patients and controls or between PD non–LIDs and PD LIDs groups *denotes statistical significance $p<0.05$ between PD non–LIDs and PD LIDs groups; ***denotes statistical significance $p<0.001$ between PD non–LIDs and PD LIDs groups.

## 3.4.2 Imaging data

The Parkinson's disease cohort showed reduced ^{123}I–Ioflupane specific to non–specific binding (p<0.001) in the caudate and the putamen as compared to controls. Parkinson's patients without LIDs had 43.64% loss in the putamen, while patients with LIDs had 43.97% loss as compared to normal controls. The mean ^{123}I–Ioflupane specific to non–specific binding value in the putamen for the dyskinetic group (1.74 ± 0.46) was not statistically different to the mean putaminal value for the PD non–LIDs group (1.72 ± 0.51; p>0.05). Baseline ^{123}I–Ioflupane specific to non–specific binding values were not statistically different for the caudate between the two groups of patients (2.65 ± 0.81 versus 2.72 ± 0.55; p>0.05).
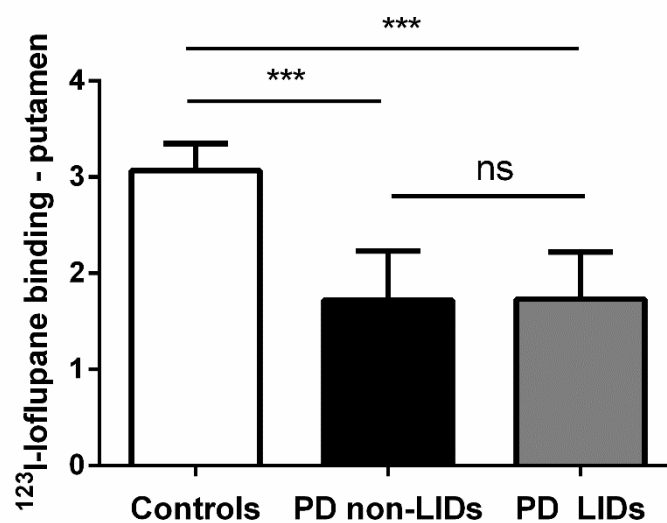


Figure 13 – ^{123}I–Ioflupane specific to non–specific binding in the putamen

[123]I–Ioflupane specific to non–specific binding in the putamen shown in 12 normal controls (white bar), 32 Parkinson's disease (PD) patients without LIDs (non–LIDs) (black bar) and 10 PD patients with LIDs (grey bar). Bars represent mean values + 1 SD. Mean values are calculated as an average for both hemispheres. Comparison of means was made with t–test for independent samples; ns – no statistically significant difference between PD non–LIDs and PD LIDs groups; *** denotes statistical significance p<0.001 between each PD group and the normal controls.
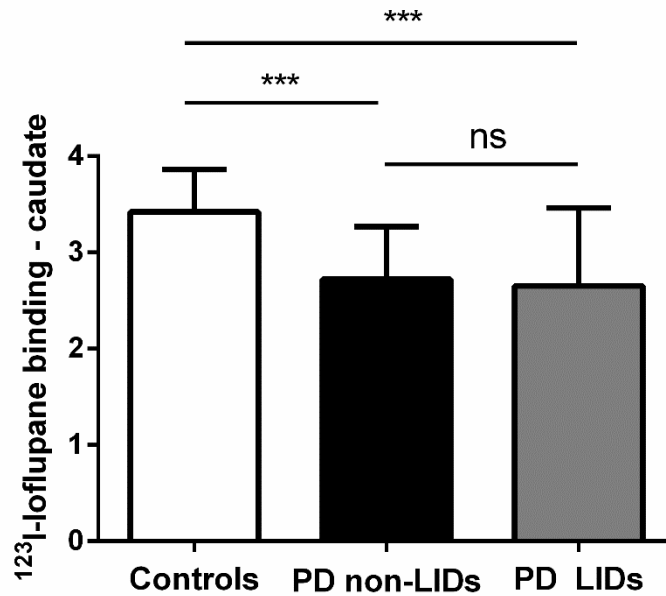
Figure 14 – $^{123}$I–Ioflupane specific to non–specific binding in the caudate

$^{123}$I–Ioflupane specific to non–specific binding in the caudate shown in 12 normal controls (white bar), 32 Parkinson's disease (PD) patients without LIDs (non–LIDs) (black bar) and 10 PD patients with LIDs (grey bar). Bars represent mean values + 1 SD. Mean values are calculated as an average for both hemispheres. Comparison of means was made with t–test for independent samples; ns – no statistically significant difference between PD non–LIDs and PD LIDs groups; *** denotes statistical significance p<0.001 between each PD group and the normal controls.

Table 8 – Mean $^{123}$I–Ioflupane specific to non–specific binding values

|  | normal controls | PD patients | | |
|---|---|---|---|---|
|  |  | all | PD non–LIDs | PD LIDs |
| No. of participants | 12 | 42 | 32 | 10 |
| $^{123}$I–Ioflupane specific to non–specific binding (DAT) | | | | |
| Caudate | 3.42±0.44 | 2.70±0.63*** | 2.72±0.55 | 2.65±0.81ns |
| Putamen | 3.07±0.28 | 1.73±0.51*** | 1.72±0.51 | 1.74±0.46ns |

Data represent mean ± 1 SD; PD: Parkinson's disease. Mean values are calculated as an average for both hemispheres. Multiple comparison was conducted with one–way ANOVA followed by *post hoc* Bonferroni correction. Comparison of means was made with t–test for independent samples; ns – no statistically significant difference between PD non–LIDs and PD LIDs groups; ***denotes statistical significance p<0.001 between all PD patients and the normal controls.
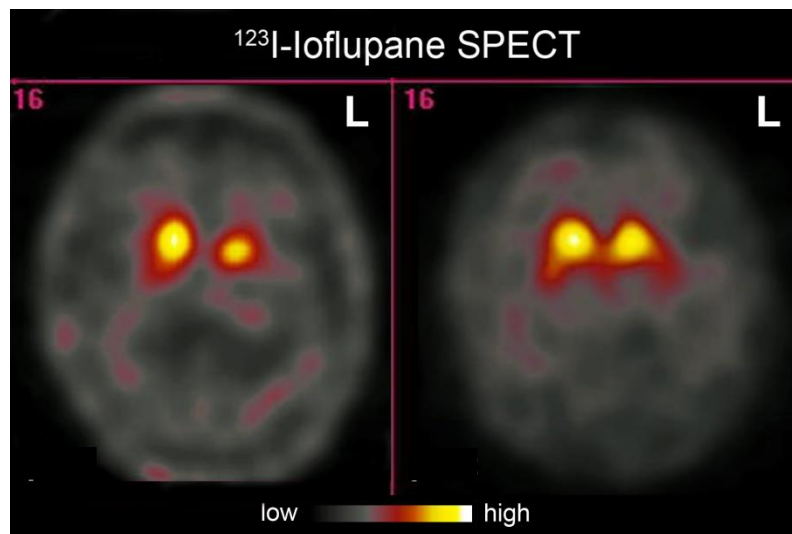
Figure 15 – Representative images (in the axial plane) of $^{123}$I–Ioflupane specific to non–specific binding (DAT) in the striatum in two *de novo* Parkinson's disease patients.

These patients had similar DAT–specific binding in the striatum. Within five years from diagnosis and levodopa therapy, the patient on the left had not developed LIDs, while the patient on the right had become dyskinetic; L: left; colour scale represents $^{123}$I–Ioflupane specific to non–specific binding (from high to low).

## 3.5 Summary of findings

In this study, I investigated whether the magnitude of striatal DAT–specific binding in early untreated Parkinson's disease is related to the appearance of LIDs within five years from diagnosis. I found that at baseline, striatal $^{123}$I–Ioflupane specific to non–specific binding in Parkinson's disease patients who developed LIDs within five years from diagnosis were not significantly different from the patients who had not developed LIDs by that time. The Parkinson's disease patients who became dyskinetic within five years from clinical diagnosis were taking higher doses of levodopa as compared to the non–dyskinetic group (p<0.001). At that time, the two groups were still matched for age, however not for the Hoehn & Yahr staging scores (p<0.05). The

SPECT study described in the current chapter comprised *de novo* Parkinson's patients who were matched for severity and age at diagnosis. At five years from diagnosis, however, the two groups of patients (with and without LIDs) had different disease severity as reflected from the differences in Hoehn & Yahr staging scores ($p<0.05$). The findings from the SPECT study may support the hypothesis that the development of LIDs relatively early (within five years from diagnosis of Parkinson's) may be a sign of faster progression rate.

# ☞ Chapter 4

# Changes over time in striatal DAT availability in relation to the development of dyskinesias

## 4.1 Introduction

Numerous imaging studies in humans have suggested that the density of striatal DAT declines progressively and that this decline is age–related. It has been proposed that the age–related DAT decline in the striatum is associated functionally with age–related postsynaptic alterations relative to the striatal decline of the dopamine D2 receptors (Ishibashi et al., 2009). In Parkinson's, the exact mechanism of striatal DAT decline is not fully understood. In normal controls, it has been proposed that the per–decade DAT decline, as reflected by $^{18}$F–FE–PE2I specific binding, is similar for the caudate and the putamen (Shingai et al., 2014). A recent PET imaging study with $^{18}$F–FP–CIT suggested that age has a critical effect in the $^{18}$F–FP–CIT striatal binding that is smaller in the putamen than in the caudate of Parkinson's disease patients (Lee CS et al., 2014). It could be therefore proposed that in Parkinson's, reduced DAT availabilities in the striatum may be due to both neuronal cell losses and functional changes of the remaining neurons. The study described in *Chapter 3* suggests that striatal DAT density in early *de novo* disease, as reflected by $^{123}$I–Ioflupane, can be highly variable among individuals relative to severity and that it seems unlikely to predict the appearance of LIDs at later stages of the disease. Hence, it could be questioned whether the rate of DAT decline in the striatum of Parkinson's disease patients is related to the occurrence of LIDs.

## 4.2 Aim and hypothesis

In this study, I intended to explore whether striatal DAT availability changes over time are related to the appearance of LIDs. I hypothesise that Parkinson's disease

patients with LIDs have more pronounced striatal reductions of DAT availability over time as compared to non–dyskinetic patients.

## 4.3 Methods

### 4.3.1 Participants

Fifteen Parkinson's disease patients were enrolled in this study. Parkinson's disease patients were retrospectively selected from the Movement Disorders Clinics of the Imperial College Healthcare NHS Trust, London, UK. All Parkinson's disease patients were recalled to provide informed written consent and were then included in this study. At baseline, all the Parkinson's disease patients were drug–naïve. At follow–up time, all Parkinson's disease patients had been treated with levodopa for at least two years. Parkinson's disease patients were then divided in two groups depending on whether they had developed (or not) LIDs.

### 4.3.2 Clinical assessments

Retrospective clinical data were collected from medical notes and clinical letters to general practitioners. Missing data and queries were cross checked with individual participants. The following clinical data were recorded for this cohort of Parkinson's disease patients: history of dyskinesia, date of diagnosis, medication history, $LED_{Ldopa}$, $LED_{Dag}$ and $LED_{Total}$. Clinical evaluation of motor symptoms' severity and progression was performed using the Hoehn & Yahr staging scale (Hoehn and Yahr. 1967). The severity of Parkinson's disease patients at baseline was standardised by enrolling patients who were drug–naïve and had Hoehn & Yahr stage 1 (unilateral

involvement). Differences were sought between the two groups for clinical characteristics at both baseline and at follow–up time points. Parkinson's disease patients with a clinical history of depression and/or cognitive impairment were excluded from this study. See also Sections 2.2, and 2.3.

### 4.3.3. Imaging procedures

All Parkinson's disease patients had two ^{123}I–Ioflupane SPECT brain scans; baseline: $1.19 \pm 1.99$ years after clinical diagnosis and follow–up: $6.31 \pm 2.99$ years from baseline. The times between baseline and follow–up scans were not statistically different between the two groups (p>0.05). All Parkinson's disease patients alongside a ^{123}I–Ioflupane SPECT scan had a 1.5 Tesla T1–weighted MRI scan. See details in *Chapter 2*, Sections 2.6, 2.7 and 2.8.2.

### 4.3.4 ^{123}I–Ioflupane SPECT imaging data analysis

See details in *Chapter 2*, Sections 2.9 and 2.9.4.

### 4.3.5 Statistical analyses

Comparisons of means (age, $DD_{diagn}$, daily LEDs, and ^{123}I–Ioflupane specific to non–specific binding) between LIDs and non–LIDs groups were performed with t–test for independent samples (either baseline only or follow-up only data) and paired t–test for related samples (baseline–to–follow-up). Comparisons of means (^{123}I–Ioflupane specific to non–specific binding) separately for each subgroup were performed with paired t–test for related samples (baseline–to–follow-up). Comparisons of Hoehn &

Yahr scores between LIDs and non–LIDs groups were performed with Mann–Whitney U test for independent samples (either baseline only or follow-up only data). Comparisons of means (Hoehn & Yahr scores) separately for each subgroup were performed with Wilcoxon signed–rank test for related samples (baseline–to– follow-up). See also Section 2.10 and legends of Tables 7–11 and Figures 16–19 below.

## 4.4 Results

## 4.4.1 Clinical data

At follow–up, all Parkinson's disease patients had been treated with levodopa for a minimum of two years. At that time, 8 Parkinson's disease patients have developed LIDs while 7 had no history for LIDs. Retrospectively, the two Parkinson's groups (LIDs, non–LIDs) did not had any significant difference in age disease duration, and Hoehn & Yahr staging – see Table 9 below.

At follow–up, both groups were still matched for age and disease duration. The mean LED$_{Total}$ was significantly higher in the dyskinetic group as compared to the group with stable response (p<0.001). In the dyskinetic group, Hoehn & Yahr scores were much higher at follow-up as compared to their baseline (p<0.001). Follow-up Hoehn & Yahr scores were higher also in the non–dyskinetic group as compared to their baseline values (p<0.001). Between–group comparison at follow-up, showed that Hoehn & Yahr scores were higher in the dyskinetic group as compared to those with stable response (p<0.01) – see Table 10 below.

Table 9 – Demographics and clinical characteristics of Parkinson's patients at baseline

| | PD patients † | |
|---|---|---|
| | PD non–LIDs | PD LIDs |
| No. of PD patients | 7 | 8 |
| [a]Sex | 5M:2F | 3M:5F [ns] |
| [b]Age | 60.75±8.24 | 52.39±9.80 [ns] |
| [b]$DD_{diagn}$ | 1.52±2.53 | 0.94±1.30 [ns] |
| [c]H&Y stage | 1.50±0.46 | 1.75±0.50 [ns] |
| AIMS scale score | - | - |
| Daily $LED_{Total}$ | - | - |

† PD patients were classified as PD non–LIDs or PD LIDs at follow–up time; data shown in this table are baseline data when at that time all PD patients were drug naïve. Data represent mean values ± 1 SD; PD: Parkinson's disease; H&Y: Hoehn & Yahr staging scale in "off" medication state; AIMS: abnormal involuntary movements; Age and $DD_{diagn}$ are calculated in years; [a]Comparison for differences in sex was performed with chi–squared ($\chi^2$) test; [b]Comparison of means was made with t–test for independent samples; [c]Comparison of Hoehn & Yahr scores between LIDs and non–LIDs groups was performed with Mann–Whitney U test; ns – no statistically significant difference between PD non–LIDs and PD LIDs groups.

Table 10 – Demographics and clinical characteristics of Parkinson's disease patients at follow–up

| | PD non–LIDs | PD LIDs |
|---|---|---|
| No. of PD patients | 7 | 8 |
| [b]Age | 65.64±7.57 | 59.95±10.56 [ns] |
| [b]$DD_{diagn}$ | 6.41±2.52 | 8.47±3.99 [ns] |
| [c]H&Y stage | 2.00±0.46 | 2.63±0.33** |
| [b]AIMS scale score | - | 9.75±3.15 |
| [b]Daily $LED_{Total}$ | 450.14±138.36 | 943.69±263.83** |
| [b]Daily $LED_{Ldopa}$ | 347.29±107.14 | 729.19±203.71*** |
| [b]Daily $LED_{Dag}$ | 102.86±31.27 | 214.50±60.22 [ns] |

Data represent mean values ± 1 SD; PD: Parkinson's disease; H&Y: Hoehn & Yahr staging scale in "off" medication state; AIMS: abnormal involuntary movements; Age and $DD_{diagn}$ are calculated in years. Daily $LED_{Total}$, $LED_{Ldopa}$, and $LED_{Dag}$ are calculated in mg. [b]Comparison of means was made with t–test for independent samples; [c]Comparison of Hoehn & Yahr scores between LIDs and non–LIDs groups was performed with Mann-Whitney U test; ns – no statistically significant difference between PD non–LIDs and PD LIDs groups; **denotes statistical significance p<0.01 between PD non–LIDs and PD LIDs groups; ***denotes statistical significance p<0.001 between PD non–LIDs and PD LIDs groups.

## 4.4.2 Imaging data

At follow–up, Parkinson's disease patients had lower mean putaminal ^{123}I–Ioflupane specific to non–specific binding (1.31 ± 0.45) as compared to baseline (1.94 ± 0.59) (p<0.001) and lower ^{123}I–Ioflupane specific to non–specific binding values (2.01 ± 0.43) versus (3.06 ± 0.67), respectively, in the caudate (p<0.001) – see Figures 16, 17.
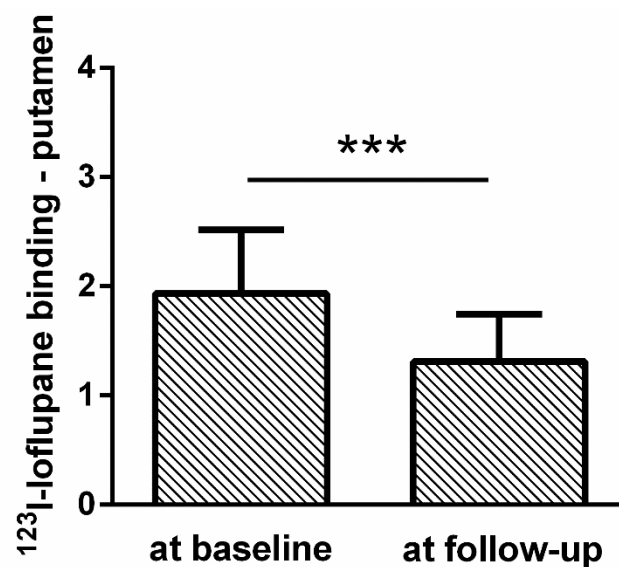


Figure 16 – ^{123}I–Ioflupane specific to non–specific binding in the putamen

[123]I–Ioflupane specific to non–specific binding in the putamen shown in 15 Parkinson's disease patients at baseline and at follow–up. Bars represent mean values + 1 SD. Mean values are calculated as an average for both hemispheres. Comparison of means was made with paired t–test for related samples; ***denotes p<0.001 statistical significance between baseline and follow–up.
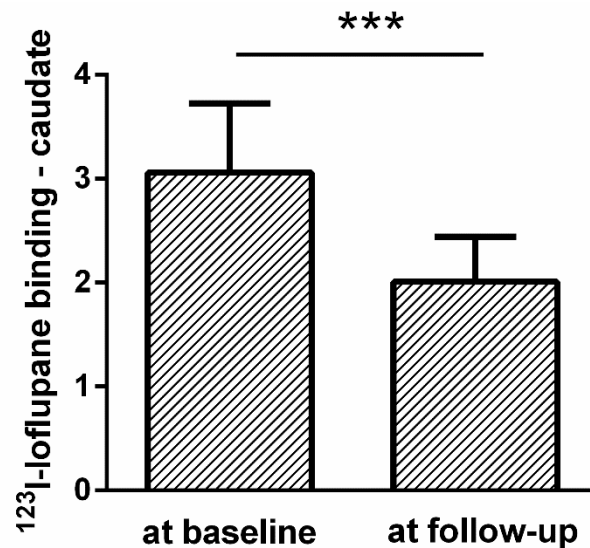
Figure 17 – ^{123}I–Ioflupane specific to non–specific binding in the caudate

[123]I–Ioflupane specific to non–specific binding in the caudate shown in 15 Parkinson's disease patients at baseline and at follow–up. Bars represent mean values + 1 SD. Mean values are calculated as an average for both hemispheres. Comparison of means was made with paired t–test for related samples; ***denotes $p < 0.001$ statistical significance between baseline and follow–up.

At follow–up, putaminal ^{123}I–Ioflupane specific to non–specific binding values were significantly reduced in the dyskinetic group ($p < 0.01$) and in the non–dyskinetic group ($p < 0.05$) as compared to baseline (Table 11–A). For the caudate, ^{123}I–Ioflupane specific to non–specific binding values were significantly reduced in the dyskinetic group ($p < 0.001$) and in the non–dyskinetic group ($p < 0.05$) as compared to baseline (Table 11–A).

At baseline, the mean ^{123}I–Ioflupane specific to non–specific binding value in the putamen was not statistically different in the dyskinetic group ($1.87 \pm 0.41$) as compared to the mean of the non–dyskinetic group ($2.01 \pm 0.73$). At follow–up, putaminal ^{123}I–Ioflupane specific to non–specific binding values were significantly

lower (p<0.05) in the dyskinetic group (1.12 ± 0.32) as compared to the Parkinson's disease patients without LIDs (1.54 ± 0.46) (p<0.05). In the between–subgroup comparison, no statistically significant difference was found for the caudate (Table 11–B, Figures 18–20).

Table 11 –Mean $^{123}$I–Ioflupane specific to non–specific binding values at baseline and at follow–up

A. Comparison of baseline and follow-up for each subgroup

|  | BASELINE | FOLLOW–UP | BASELINE | FOLLOW–UP |
|---|---|---|---|---|
|  | PD non–LIDs | | PD LIDs | |
| No. of PD patients | 7 | 7 | 8 | 8 |
|  | $^{123}$I–Ioflupane specific to non–specific binding (DAT) | | | |
| Caudate | 3.02±0.72 | 2.20±0.35* | 3.10±0.59 | 1.84±0.45*** |
| Putamen | 2.01±0.73 | 1.54±0.46* | 1.87±0.41 | 1.12±0.32** |

B. Between–subgroup comparison at baseline and at follow–up

|  | BASELINE | | FOLLOW–UP | |
|---|---|---|---|---|
|  | PD non–LIDs | PD LIDs | PD non–LIDs | PD LIDs |
| No. of PD patients | 7 | 8 | 7 | 8 |
|  | $^{123}$I–Ioflupane specific to non–specific binding (DAT) | | | |
| Caudate | 3.02±0.72 | 3.10±0.59 ns | 2.20±0.35 | 1.84±0.45 ns |
| Putamen | 2.01±0.73 | 1.87±0.41 ns | 1.54±0.46 | 1.12±0.32* |

Data represent mean ± 1 SD. Mean values are calculated as an average for both hemispheres.

**A.** Comparison of means was made with paired t–test for related samples; *denotes statistical significance p<0.05 between baseline and follow–up; **denotes statistical significance p<0.01 between baseline and follow–up; ***denotes statistical significance p<0.001 between baseline and follow–up

**B.** Comparison of means was made with t–test for independent samples; ns – no statistically significant difference between PD non–LIDs and PD LIDs groups; *denotes statistical significance p<0.05 between the PD non–LIDs and the PD–LIDs group at follow–up
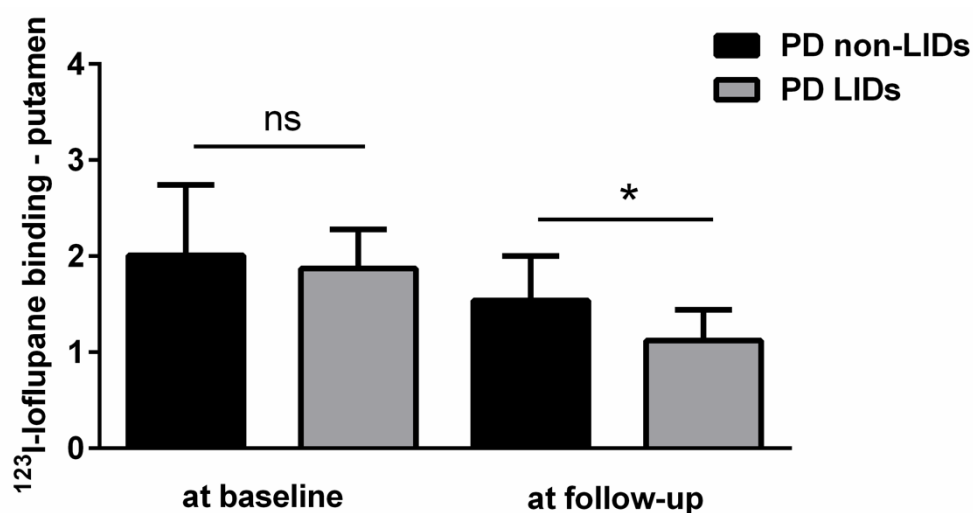
Figure 18 – ^{123}I–Ioflupane specific to non–specific binding in the putamen

[123]I–Ioflupane specific to non–specific binding in the putamen shown in 7 Parkinson's disease (PD) patients without LIDs (PD non–LIDs) and 8 PD patients with LIDs at baseline (left two bars) and at follow–up (right two bars). Bars represent mean values + 1 SD. Mean values are calculated as an average for both hemispheres. Comparison of means was made with t–test for independent samples; ns – no statistically significant difference between PD non–LIDs and PD LIDs groups at baseline; *denotes $p<0.05$ statistical significance between PD non–LIDs and PD LIDs groups at follow–up.
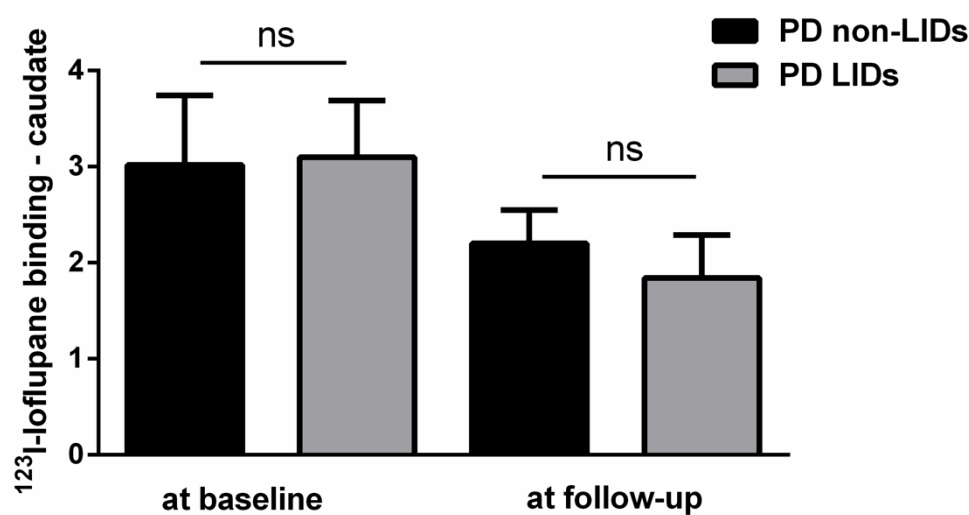


Figure 19 – ^{123}I–Ioflupane specific to non–specific binding in the caudate

[123]I–Ioflupane specific to non–specific binding in the caudate shown in 7 Parkinson's disease (PD) patients without LIDs (PD non–LIDs) and 8 PD patients with LIDs at baseline (left two bars) and at follow–up (right two bars). Bars represent mean values + 1 SD. Mean values are calculated as an average for both hemispheres. Comparison of means was made with t–test for independent samples; ns – no statistically significant difference between PD non–LIDs and PD LIDs groups.

PD patient who did not have LIDs at follow– up

PD patient who had LIDs at follow–up
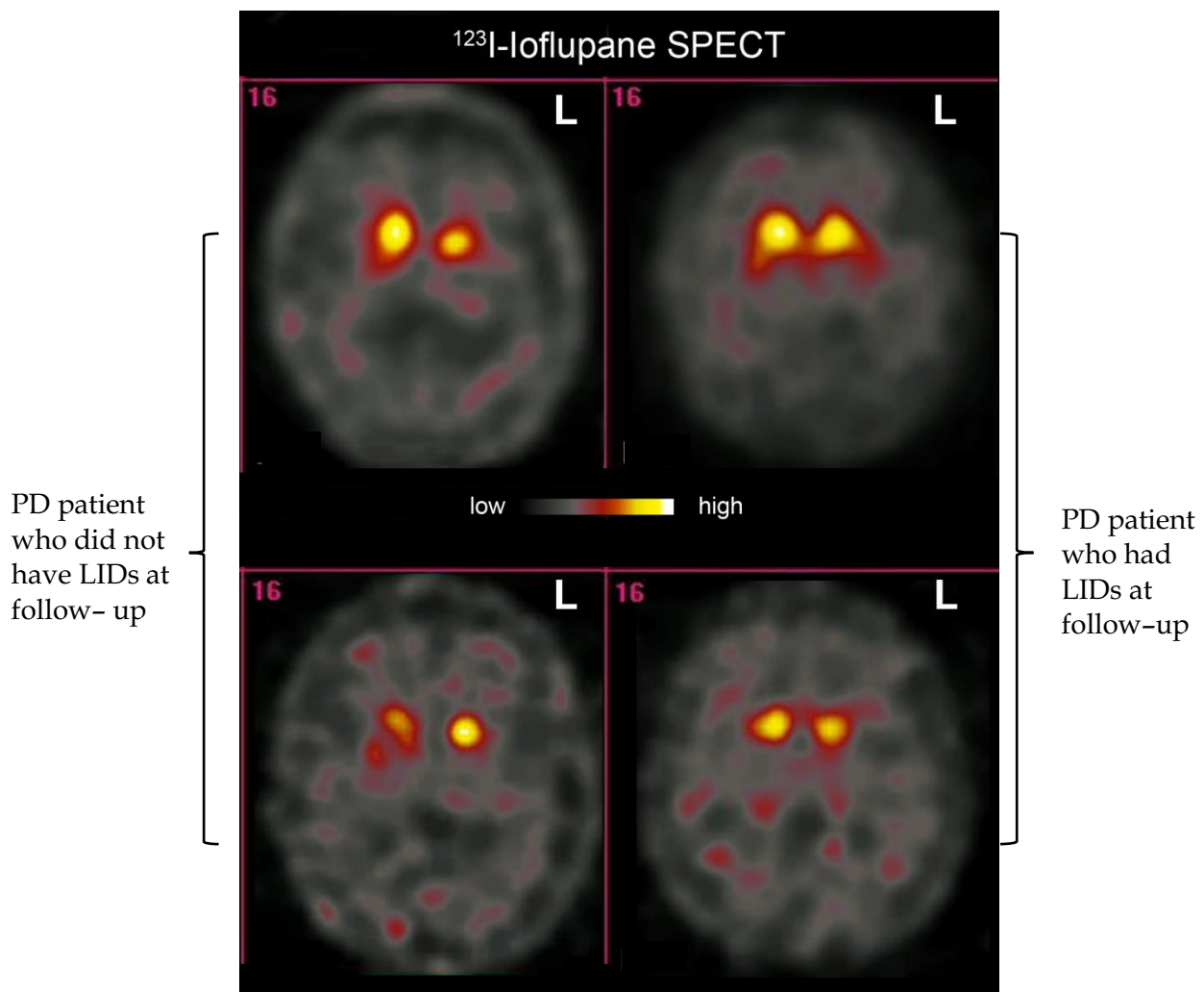
Figure 20 – Representative images (in the axial plane) of ^{123}I–Ioflupane specific to non–specific binding (DAT) in the striatum of two Parkinson's disease patients at baseline (upper row) and at follow–up (lower row)

At baseline, both patients were drug–naïve. At follow–up, both patients were treated with levodopa for at least two years. At that time, patient on the left had not developed LIDs, while patient on the right had become dyskinetic; L: left; colour scale represents ^{123}I–Ioflupane specific to non–specific binding (from high to low).

## 4.5 Summary of findings

At baseline, both groups of patients who later developed LIDs and those who did not develop LIDs were matched for age, disease duration and Hoehn & Yahr scores. There was no between–group statistically significant difference in the baseline ^{123}I–Ioflupane

specific to non–specific binding values in both the caudate and the putamen. At follow–up, the Parkinson's disease patients with LIDs showed DAT decline of greater extent in the putamen as compared to the non–LIDs group. Parkinson's patients with LIDs also had higher Hoehn & Yahr scores, notwithstanding the two groups being still matched for age and disease duration. Taken together this data suggest, that the development of LIDs may be dependent on the magnitude of DAT decline in the putamen over time. Patients with similar disease duration but faster dopaminergic decline are possibly susceptible to develop LIDs earlier.

# Chapter 5

# Striatal SERT–to–DAT binding ratios in Parkinson's disease: relevance to LIDs

## 5.1 Introduction

As Parkinson's disease progresses, dopaminergic terminals in the striatum are believed to lose the capacity to maintain a stable dopamine release in the synapse (Leenders et al., 1986). In *advanced* Parkinson's disease, the same amount of exogenous levodopa may induce different dopamine release in the synapse as compared to early diagnosed patients (Tedroff et al., 1996). The occurrence of LIDs has been linked with dramatic swings of dopamine levels in the synapse (de la Fuente–Fernández et al., 2004; Pavese et al., 2006). Hence, the occurrence of LIDs seems to be dependent on the rate of dopamine release in the synapse.

The serotonergic terminals have the capacity to uptake exogenous levodopa, convert it to dopamine, store it in synaptic vesicles and release into the synapse in an activity–dependant manner (Ng et al., 1971; Tanaka et al., 1999; Maeda et al., 2005; Kannari et al., 2006). Physiologically, the dopamine neurotransmission can terminate via the active reuptake of dopamine back into the neuronal body via the DAT (reviewed by Piccini. 2003b). However, the serotonergic terminals lack auto–regulatory feedback mechanisms as they do not express the DAT.

Chemical and pharmacological blockade of striatal serotonergic function has been shown to significantly reduce the AIMS in the animal model of Parkinson's disease (Carta et al., 2007; Bézard et al., 2013; Muñoz et al., 2008; Conti et al., 2014). In humans, striatal serotonergic terminals are proposed to be affected by Parkinson's in the advanced stages (Politis et al., 2010) while, both buspirone (Politis et al., 2014) and eltoprazine (Svenningsson et al., 2015), which are serotonin receptor partial agonists

have shown anti–dyskinetic effects when administered prior to levodopa, without counteracting levodopa's main effects.

DAT and SERT availabilities *in vivo* reflect the level of integrity of the dopaminergic and serotonergic terminals, respectively. ^{123}I–Ioflupane and ^{11}C–DASB are specific markers of DAT and SERT availability, respectively. Hence, functional imaging in humans through ^{123}I–Ioflupane SPECT and ^{11}C–DASB PET could visualise striatal DAT and SERT availabilities *in vivo* and reflect whether there is a relationship between the two relevant to dyskinesias.

## 5.2 Aim and hypothesis

This study intended to estimate the role of presynaptic terminal binding ratios in Parkinson's disease patients in relation to the presence of LIDs. I hypothesised that in Parkinson's, there is an imbalanced SERT–to–DAT binding ratio in the striatum that is associated to LIDs.

## 5.3 Methods

### 5.3.1 Participants

36 patients with idiopathic Parkinson's disease were screened for enrolment in the study, of which six failed at one of the exclusion criteria and two declined from participation in the study. 28 patients with idiopathic Parkinson's disease participated in the study. At the time of scanning, 17 patients had a history of LIDs while 11 did not experience LIDs. Twelve healthy volunteers were also included as controls.

## 5.3.2 Clinical assessments

Parkinson's disease patients were recruited from the Movement Disorders Clinics of the Imperial College Healthcare NHS Trust, London, UK. All participants of this study, including the controls' group, were assessed for depression using the HAM–D scale and for cognitive impairment using the MMSE. None of the participants of this study had a history of depression or any other neurological or psychiatric disorder. Clinical evaluation of motor and non–motor symptoms' severity was performed using the UPDRS (Goetz et al., 2007). In particular, Parkinson's disease motor symptoms' severity was performed using the III part of the UPDRS form and the Hoehn & Yahr staging scale (Hoehn and Yahr. 1967).

At screening, Parkinson's disease patients were on levodopa treatment for at least two years. Patients with a history of dementia and/or depression were excluded from this study. Clinical data were acquired by detailed medical history including medication history cross checked with patients' medical notes and clinical letters to their general practitioners. Parkinson's disease patients were assessed in an outpatient clinical setting for their motor and non–motor symptoms including the UPDRS and the Hoehn & Yahr staging scale. Presence of LIDs was assessed on separate day within 1 hour after the patients had taken their usual levodopa dose (range of single dose: 100–200mg). LIDs were scored using the AIMS scale, for every 15 minutes for the next 120 minutes. I also calculated the time from clinical diagnosis to initiation of dopaminergic medication for each individual.

All normal controls were assessed using the HAM–D and MMSE scales and exclusion criteria for depression and dementia were applied as described above. None of the normal controls had a history of depression or any other neurological or psychiatric disorder. See also sections, 2.2 and 2.3.

## 5.3.3 Imaging procedures

All subjects had brain SPECT imaging with ^{123}I–Ioflupane and brain PET imaging with ^{11}C–DASB. All subjects also had a 1.5 T1–weighted MRI scan for coregistration to the PET imaging data. See details in *Chapter 2*, Sections 2.6, 2.7, 2.8, 2.8.1, 2.8.2 and 2.8.3.

## 5.3.4 ^{11}C–DASB PET imaging data analysis

See details in *Chapter 2*, Sections 2.9 and 2.9.3.

## 5.3.5 ^{123}I–Ioflupane SPECT imaging data analysis

See details in *Chapter 2*, Sections 2.9 and 2.9.4.

## 5.3.6 SERT–to–DAT binding ratios

See details in *Chapter 2*, Section 2.9.6.

## 5.3.7 Statistical analyses

For multiple comparisons of values that were normally distributed, one–way ANOVA was used to compare means and *post hoc* Bonferroni correction was applied.

Comparisons of means between two groups (either controls to PD group or LIDs to non–LIDs) were performed with t–test for independent samples. For multiple comparisons of values that did not have a normal distribution, the non–parametric Kruskall–Wallis test was used; *post hoc* checked with Dunn's test. Comparisons between two groups were performed with Mann–Whitney U test for independent samples. See also Section 2.10 and legends of Tables 12, 13 and Figures 21–26 and 28 below.

## 5.4 Results

## 5.4.1 Clinical data

The demographics and clinical characteristics of Parkinson's disease patients and normal controls are in Table 12. The group of patients with LIDs were younger (61.69±8.89) as compared to the group of patients without LIDs (69.32±4.67) ($p<0.05$). The mean $DD_{diagn}$ was significantly higher ($p<0.05$) in the LIDs group (9.56±5.48) as compared to the group of Parkinson's patients without LIDs (5.82±4.88). The mean duration on dopaminergic medication was significantly higher ($p<0.05$) for the LIDs group (8.40±5.07) as compared to the non–LIDs group (4.41±2.07). The mean $LED_{Total}$ for the PD LIDs group was significantly different to those from the PD non–LIDs group ($p<0.05$).

Table 12 – Demographics and clinical characteristics of Parkinson's disease patients and controls

| | normal controls | PD patients | | |
|---|---|---|---|---|
| | | all | PD non–LIDs | PD LIDs |
| No. of participants | 12 | 28 | 11 | 17 |
| [a]Sex | 7M:5F | 19M:9F [ns] | 10M:1F | 9M:8F [ns] |
| [b]Age | 61.41±8.64 | 64.87±8.21 [ns] | 69.32±4.67 | 61.69±8.89* |
| [b]MMSE score | 29.70±0.67 | 28.28±1.22 [ns] | 28.00±1.26 | 28.44±1.20 [ns] |
| [b]HAM–D score | 1.80±1.62 | 4.28±1.25 [ns] | 4.27±0.65 | 4.28±1.53 [ns] |
| [b]DD$_{diagn}$ | - | 7.89±5.01 | 5.82±4.9 | 9.56±5.48* |
| [c]H&Y stage | - | 2.34±0.57 | 2.27±0.47 | 2.39±0.63 [ns] |
| [b]UPDRS–III | - | 27.59±8.32 | 26.70±7.25 | 28.11±9.07 [ns] |
| [b]UPDRS total | - | 45.03±10.89 | 40.55±10.30 | 47.78±10.59 [ns] |
| AIMS scale score | - | - | - | 8.06±4.26 |
| [b]Duration on DA medication | - | 6.69±4.68 | 4.41±2.07 | 8.40±5.07* |
| [b]Time from diagnosis to initiation of DA medication | - | - | 1.45±1.05 | 1.03±1.27 [ns] |
| [b]Daily LED$_{Total}$ | - | - | 537.59±199.87 | 826.59±350.70* |
| [b]Daily LED$_{Ldopa}$ | - | - | 376.68±167.68 | 650.82±369.69 [ns] |
| [b]Daily LED$_{Dag}$ | - | - | 160.91±193.87 | 175.76±207.02 [ns] |

Data represent mean values ± 1 SD; PD: Parkinson's disease; MMSE: Mini mental state examination; HAM–D: Hamilton rating scale for depression; H&Y: Hoehn & Yahr staging scale in "off" medication state; UPDRS–III: Unified Parkinson's disease Rating Scale–score of part III in "off" medication state; UPDRS total: Unified Parkinson's disease Rating Scale–total score in "off" medication state; AIMS: abnormal involuntary movements; DA: dopaminergic; Age, DD$_{diagn}$, duration on DA medication and time from diagnosis to initiation of DA medication are calculated in years. Daily LED$_{Total}$, LED$_{Ldopa}$, and LED$_{Dag}$ are calculated in mg. Multiple comparisons were conducted with one–way ANOVA followed by *post hoc* Bonferroni correction; [a]Comparison for differences in sex was performed with chi–squared ($\chi^2$) test; [b]Comparison of means was made with t–test for independent samples; [c]Comparison of Hoehn & Yahr scores between LIDs and non–LIDs groups was performed with Mann–Whitney U test; ns – no statistically significant difference between PD patients and controls or PD non–LIDs and PD LIDs groups; *denotes statistical significance p<0.05 between PD non–LIDs and PD LIDs groups

## 5.4.2 Imaging data

Parkinson's disease patients showed reduced $^{11}$C–DASB $BP_{ND}$ (p<0.01) in the putamen as compared to normal controls. Parkinson's disease patients without LIDs showed 37% loss of $^{11}$C–DASB $BP_{ND}$, while the Parkinson's disease patients with LIDs showed 31% loss as compared to normal controls (between–group comparison for the putamen; p>0.05). No statistically significant difference was found for the caudate (between–group comparison for the caudate; p>0.05).
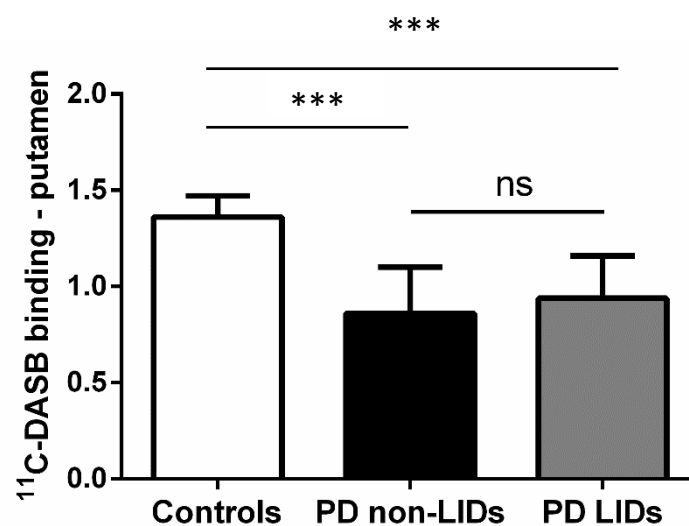


Figure 21 – $^{11}$C–DASB $BP_{ND}$ in the putamen

$^{11}$C–DASB $BP_{ND}$ in the putamen shown in 12 normal controls (white bar), 17 Parkinson's disease (PD) patients without LIDs (non–LIDs) (black bar) and 11 PD patients with LIDs (grey bar). Bars represent mean values + 1 SD. Mean values are calculated as an average for both hemispheres. Multiple comparison was conducted with one–way ANOVA followed by *post hoc* Bonferroni correction. Comparison of means was made with t–test for independent samples; ns – no statistically significant difference between PD non–LIDs and PD LIDs groups; *** denotes statistical significance p<0.001 between each PD group and the normal controls.

Figure 22 – $^{11}$C–DASB BP$_{ND}$ in the caudate

$^{11}$C–DASB BP$_{ND}$ in the caudate shown in 12 normal controls (white bar), 17 Parkinson's disease (PD) patients without LIDs (non–LIDs) (black bar) and 11 PD patients with LIDs (grey bar). Bars represent mean values + 1 SD. Mean values are calculated as an average for both hemispheres. Multiple comparison was conducted with one–way ANOVA followed by *post hoc* Bonferroni correction. Comparison of means was made with t–test for independent samples; ns – no statistically significant difference between PD non–LIDs and PD LIDs groups; *** denotes statistical significance p<0.001 between each PD group and the normal controls.

Parkinson's disease patients showed reduced $^{123}$I–Ioflupane specific to non–specific binding values (p<0.001) as compared to controls in the caudate and the putamen. In comparison to controls, Parkinson's patients without LIDs showed 51% loss of $^{123}$I–Ioflupane specific to non–specific binding in the putamen, while patients with LIDs showed 62% loss (between–group difference for the putamen p>0.05). No statistically significant difference was found between groups for the caudate p>0.05).

All Parkinson's disease patients had increased $^{11}$C–DASB BP$_{ND}$ to $^{123}$I–Ioflupane binding ratio as compared to normal controls (p<0.001). Parkinson's patients with LIDs had $^{11}$C–DASB BP$_{ND}$ to $^{123}$I–Ioflupane binding ratios increased on average by

103.4% as compared to normal controls, while in the group of patients without LIDs the mean ratio was increased by 75.8%, as compared to controls. Between–group difference in the binding ratio for the putamen was statistically significant (p<0.001). No statistically significant difference was found in the caudate for the ^{11}C–DASB BP$_{ND}$ to ^{123}I–Ioflupane binding ratios.
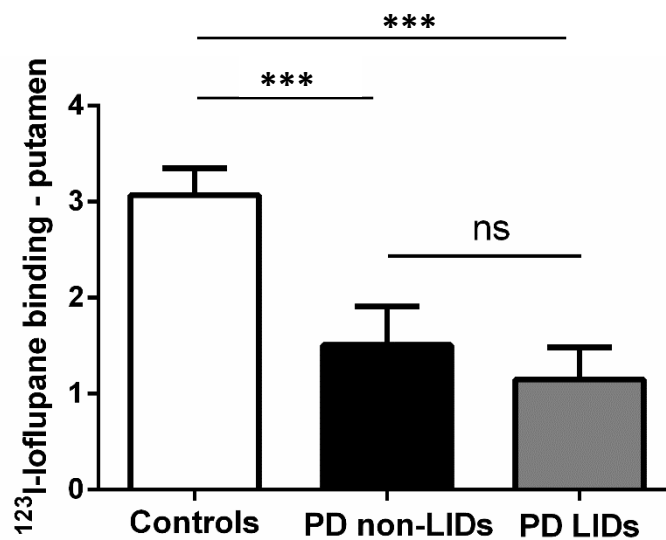


Figure 23 – ^{123}I–Ioflupane specific to non–specific binding in the putamen

[123]I–Ioflupane specific to non–specific binding in the putamen shown in 12 normal controls (white bar), 17 Parkinson's disease (PD) patients without LIDs (non–LIDs) (black bar) and 11 PD patients with LIDs (grey bar). Bars represent mean values + 1 SD. Mean values are calculated as an average for both hemispheres. Multiple comparison was conducted with one–way ANOVA followed by *post hoc* Bonferroni correction. Comparison of means was made with t–test for independent samples; ns – no statistically significant difference between PD non–LIDs and PD LIDs groups; *** denotes statistical significance p<0.001 between each PD group and the normal controls.

Figure 24 – ^{123}I–Ioflupane specific to non–specific binding in the caudate

[123]I–Ioflupane specific to non–specific binding in the caudate shown in 12 normal controls (white bar), 17 Parkinson's disease (PD) patients without LIDs (non–LIDs) (black bar) and 11 PD patients with LIDs (grey bar). Bars represent mean values + 1 SD. Mean values are calculated as an average for both hemispheres. Multiple comparison was conducted with one–way ANOVA followed by *post hoc* Bonferroni correction. Comparison of means was made with t–test for independent samples; ns – no statistically significant difference between PD non–LIDs and PD LIDs groups; *** denotes statistical significance between each PD group and the normal controls.

Table 13 – Mean values of ^{11}C–DASB $BP_{ND,}$ ^{123}I–Ioflupane specific to non–specific binding, and the SERT–to–DAT binding ratios

| | normal controls | PD patients | | |
|---|---|---|---|---|
| | | all | PD non–LIDs | PD LIDs |
| No. of participants | 12 | 28 | 11 | 17 |
| ^{11}C–DASB $BP_{ND}$ (SERT) | | | | |
| [a]Caudate | 1.31±0.06 | 0.58±0.20** | 0.62±0.22 | 0.56±0.18 ns |
| [a]Putamen | 1.36±0.11 | 0.90±0.25* | 0.86±0.24 | 0.94±0.22 ns |
| ^{123}I–Ioflupane specific to non–specific binding (DAT) | | | | |
| [a]Caudate | 3.42±0.44 | 1.98±0.52** | 2.10±0.49 | 1.90±0.53 ns |
| [a]Putamen | 3.07±0.28 | 1.26±0.42** | 1.51±0.40 | 1.15±0.33 ns |
| SERT–to–DAT binding ratios | | | | |
| [b]Caudate | 0.38±0.09 | 0.30±0.11 ns | 0.30±0.10 | 0.31±0.11ns |
| [b]Putamen | 0.44±0.21 | 0.85±0.39*** | 0.78±0.28 | 0.90±0.45*** |

Data represent mean ± 1 SD; PD: Parkinson's disease; Mean values are calculated as an average for both hemispheres. Multiple comparison was conducted with one–way ANOVA followed by *post hoc* Bonferroni correction (for $BP_{ND}$ values) or with the non–parametric Kruskall–Wallis test was used; *post hoc* checked with Dunn's test (for binding ratios). [a]Comparison of means was made with t–test for independent samples; [b]Comparison was made with Mann–Whitney U test for independent samples; ns – no statistically significant difference between PD non–LIDs and PD LIDs groups or PD patients and the normal controls' group; *denotes statistical significance $p<0.05$ between the PD patients and the normal controls' group; **denotes statistical significance $p<0.01$ between the PD patients and the normal controls' group; ***denotes statistical significance $p<0.001$ between PD non–LIDs and PD LIDs groups or PD patients and the normal controls' group.
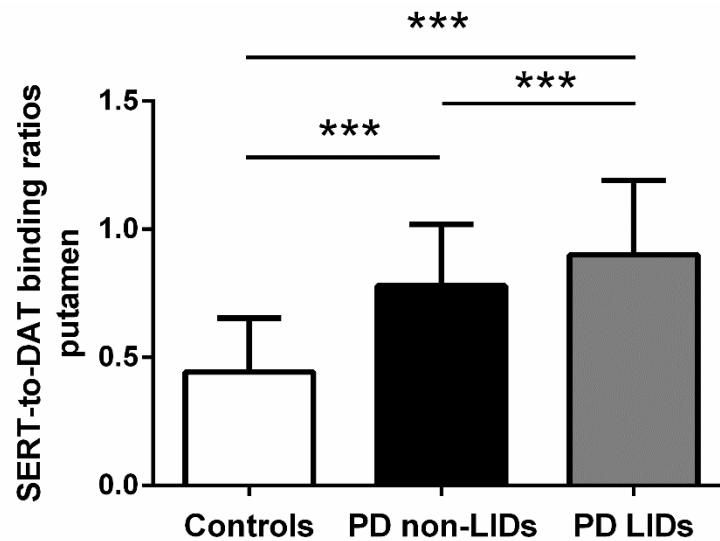


Figure 25 – SERT–to–DAT binding ratios in the putamen

SERT–to–DAT binding ratios in the putamen shown in 12 normal controls (white bar), 17 Parkinson's disease (PD) patients without LIDs (non–LIDs) (black bar) and 11 PD patients with LIDs (grey bar). Bars represent mean values +1 SD. Mean values are calculated as an average for both hemispheres. Multiple comparison was conducted with the Kruskall–Wallis test *post hoc* checked with Dunn's test. Between group comparison was made with Mann–Whitney U test for independent samples; ***denotes statistical significance $p<0.001$ between PD non–LIDs and PD LIDs groups or between each PD group and the normal controls.
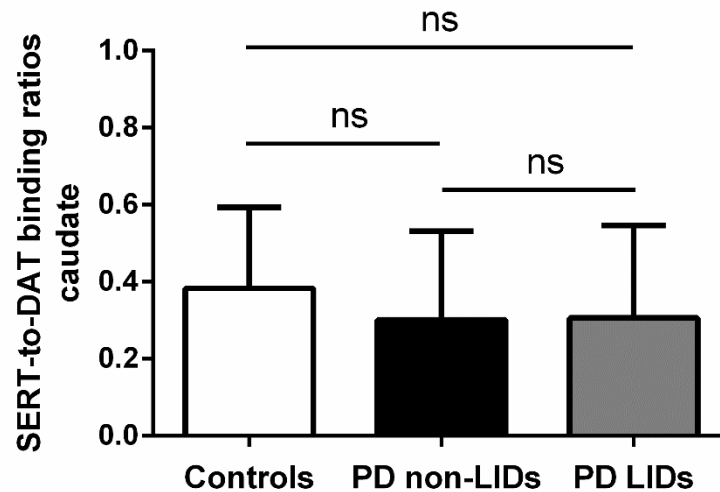
Figure 26 –SERT–to–DAT binding ratios in the caudate

SERT–to–DAT binding ratios in the caudate shown in 12 normal controls (white bar), 17 Parkinson's disease patients (PD) without LIDs (non–LIDs) (black bar) and 11 PD patients with LIDs (grey bar). Bars represent mean values + 1 SD. Mean values are calculated as an average for both hemispheres. Multiple comparison was conducted with the Kruskall–Wallis test *post hoc* checked with Dunn's test. Between–group comparison was made with Mann–Whitney U test for independent samples; ns – no statistically significant difference between PD non–LIDs and PD LIDs groups or PD patients and the normal controls' group.

## 5.4.3 Correlations

Higher putaminal $^{11}$C–DASB BP$_{ND}$ to $^{123}$I–Ioflupane binding ratios significantly correlated with longer disease duration from diagnosis for all Parkinson's patients ($r=0.52$; $p<0.01$) – see Figure 27.

No correlation was found between putaminal $^{11}$C–DASB BP$_{ND}$ and either age, UPDRS, AIMS scale scores, the mean LED$_{Total}$, the mean LED$_{Ldopa}$, or the times from diagnosis to initiation of dopaminergic medication. No correlation was found between putaminal $^{123}$I–Ioflupane specific to non–specific binding values and either age,

UPDRS, AIMS scale scores, the mean $LED_{Total}$, the mean $LED_{Ldopa}$, or the times from diagnosis to initiation of dopaminergic medication. No correlation was found between putaminal ^{11}C–DASB $BP_{ND}$ to ^{123}I–Ioflupane binding ratios and either age, UPDRS, AIMS scale scores, the mean $LED_{Total}$, the mean $LED_{Ldopa}$, or the times from diagnosis to initiation of dopaminergic medication.
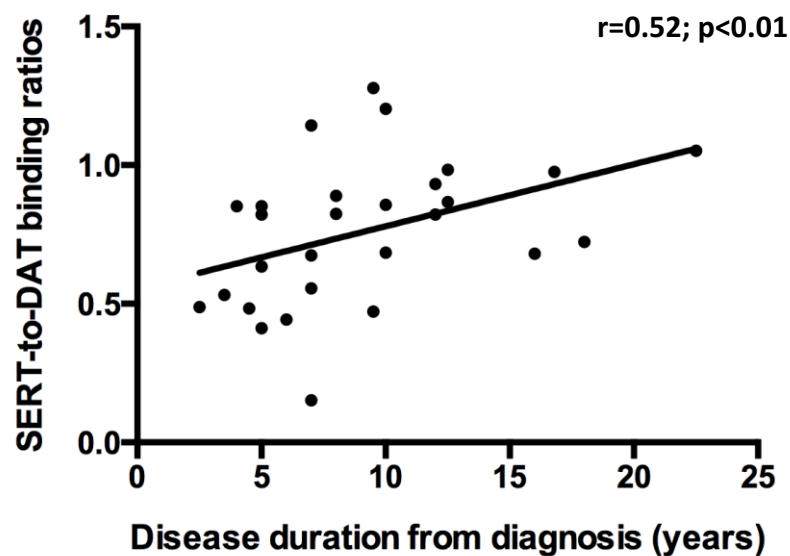


Figure 27 – Correlation of SERT–to–DAT binding ratios in the putamen and disease duration in 28 Parkinson's disease patients

Statistical analysis was performed with one–tailed Spearman correlation between disease duration from diagnosis (in years) and SERT–to–DAT binding ratios in the putamen of 28 Parkinson's patients; r=0.52 p<0.01. Each point in the graph represents one Parkinson's disease patient.
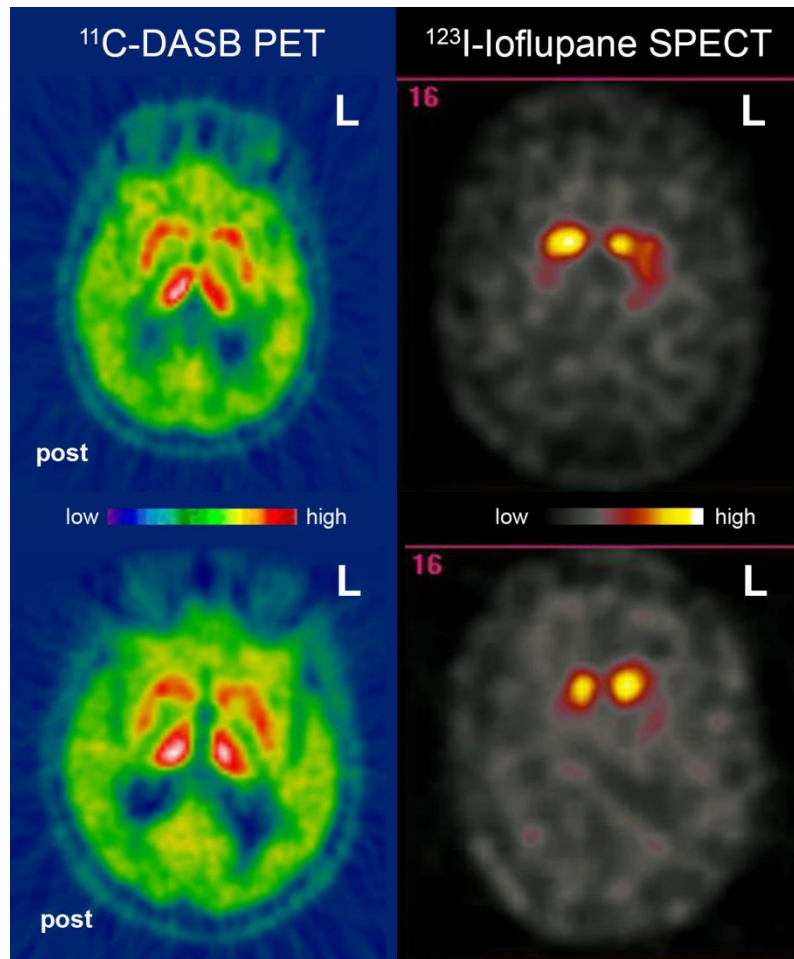
Figure 28 – Representative images (in the axial plane) of $^{11}$C–DASB binding (SERT) and $^{123}$I–Ioflupane specific to non–specific binding (DAT) in the striatum in two Parkinson's disease patients; without LIDs (upper row) and with LIDs (lower row)

L: left; post: posterior; colour scales represent $^{11}$C–DASB and $^{123}$I–Ioflupane specific to non–specific binding (from high to low)

## 5.5 Summary of findings

In this study, I investigated the role of striatal SERT–to–DAT binding ratios in a cohort of Parkinson's disease patients and a group of age–matched normal controls. I found that Parkinson's disease patients have significantly higher SERT–to–DAT binding ratios in the putamen (p<0.001) as compared to controls.

I then investigated whether the striatal SERT–to–DAT binding ratios are related with the presence of LIDs within the Parkinson's disease group. I found that Parkinson's disease patients with LIDs have increased SERT–to–DAT binding ratios in the putamen (p<0.001) as compared to non–dyskinetic patients. The DAT–specific binding in the putamen was lower in the group of patients with LIDs, however, differences did not reach significance. I then investigated whether the SERT–to–DAT binding ratios are related to longer disease duration and I found a statistically significant correlation between the putaminal SERT–to–DAT binding ratios and the disease duration in all Parkinson's patients (p<0.01). The findings from this study supports the hypothesis that an imbalance of the putaminal SERT–to–DAT binding ratio is possibly related to the occurrence of LIDs, once the dopaminergic innervation in the striatum is critically low. Putaminal SERT–to–DAT binding ratio is increased in advanced Parkinson's and patients are more likely to experience LIDs.

# Chapter 6

# Striatal SERT–to–DAT binding ratios in Parkinson's disease in relation to LIDs: a longitudinal study

## 6.1 Introduction

Presynaptic mechanisms of striatal dopaminergic neurotransmission are believed to be related to the development of LIDs in addition to the role of striatal serotonergic terminals. As Parkinson's disease progresses and DAT availabilities in the striatum decline further, patients have more severe disease and they are at high risk for developing LIDs. SERT availabilities in the striatum have been proposed to decline unevenly across different stages of Parkinson's disease (Politis et al., 2010). In fact, it has been proposed that the serotonergic degeneration in the striatum follows the dopaminergic one. Hence, the interaction of serotonergic and dopaminergic terminals in the striatum may become critical for the development of LIDs only in later stages of the disease.

## 6.2 Aims and hypotheses

Using PET, I conducted a cross–sectional study to a different cohort of Parkinson's patients to validate the role of striatal SERT–to–DAT binding ratio in Parkinson's patients in relation to LIDs. Further to this, I assessed the changes in striatal SERT, DAT availability and SERT–to–DAT binding ratios in Parkinson's patients over time *and* in relation to the development of LIDs (longitudinal study). I hypothesised that (a) dyskinetic patients have higher striatal SERT–to–DAT binding ratios than non–dyskinetic patients, (b) SERT decreases will be less pronounced than the decreases in the DAT, and (c) as Parkinson's disease progresses, the SERT–to–DAT binding ratio increases and Parkinson's disease patients experience dyskinesia.

## 6.3 Methods

### 6.3.1 Participants

*Cross–sectional study*

31 patients with idiopathic Parkinson's disease were screened for enrolment in the study, of which three failed at one of the exclusion criteria. 28 patients with idiopathic Parkinson's disease who were treated with dopaminergic medicines were included in the study. At the time of scanning, seven patients had LIDs while 21 did not experience LIDs.

*Longitudinal study*

Twelve patients of the 21 one who did not have LIDs were included in the longitudinal study and had repeated $^{11}$C–DASB and $^{11}$C–PE2I PET after 17 months (±11 weeks).

### 6.3.2 Clinical assessments

Parkinson's disease patients were recruited from Movement Disorders Specialists' Clinics (Transeuro Consortium) and online advertisements and had been regularly followed up by Movement Disorders Specialists. All participants of this study were assessed for depression using the BDI and for cognitive impairment using the MMSE. None of the participants of this study had a history of depression or any other neurological or psychiatric disorder. Clinical evaluation of motor and non–motor symptoms' severity was performed using the UPDRS (Goetz et al., 2007). In particular, Parkinson's disease motor symptoms' severity was performed using the III part of the UPDRS form and the Hoehn & Yahr staging scale (Hoehn and Yahr. 1967). Presence

of LIDs was assessed on separate day within 1 hour after the patients had taken their usual levodopa dose (range of single dose: 100–200mg) using the IV part of the UPDRS scale, the Rush dyskinesia rating scale and the AIMS scale. LIDs scores were rated using the AIMS scale within 1 hour after the patients had taken their usual levodopa dose (range of single dose: 100–200mg) for every 15 minutes for the next 120 minutes. I also calculated the time from clinical diagnosis to initiation of dopaminergic medication for each individual. See also Sections 2.2 and 2.3.

### 6.3.3 Imaging procedures

All subjects had brain PET imaging with ^{11}C–PE2I and brain PET imaging with ^{11}C–DASB. All subjects also had a 3 Tesla T1–weighted MRI scan for coregistration to the PET imaging data. See details in *Chapter 2*, Sections 2.6, 2.7, 2.8, 2.8.1 and 2.8.3.

### 6.3.4 PET imaging data analysis

See details in *Chapter 2*, Sections 2.9 and 2.9.5.

### 6.3.5 Calculation of SERT–to–DAT binding ratios

See details in *Chapter 2*, Section 2.9.6.

### 6.3.6 Statistical analyses

For values that were normally distributed, comparisons between LIDs and non–LIDs groups were performed with t–test for independent samples and paired t–tests for related samples. For values that did not have a normal distribution, comparisons between LIDs and non–LIDs groups were performed with Mann–Whitney U test for

independent samples and Wilcoxon signed–rank test for related samples. See also Section 2.10 and legends of Tables 14–17 and Figures 29–35, and 37 below.

## 6.4 Results

*Cross–sectional study*

## 6.4.1 Clinical and Imaging data

The demographics and clinical characteristics of Parkinson's disease patients are in Table 14. The mean $DD_{diagn}$ was significantly higher ($p<0.01$) in the LIDs group (7.51 ± 1.57) as compared to the group of Parkinson's patients without LIDs (4.94 ± 1.52). The mean $LED_{Total}$ and $LED_{Ldopa}$ for the LIDs group was higher as compared to the non–LIDs group ($p<0.05$). The UPDRS–III scores in "off" medication state were higher in the LIDs group as compared to the non–LIDs group; ($p<0.05$).

The mean $^{11}C$–DASB $BP_{ND}$ values in the putamen (1.27 ± 0.23) and caudate (0.54±0.15) of Parkinson's patients with LIDs were not statistically different to the mean $^{11}C$–DASB $BP_{ND}$ in the putamen (1.26 ± 0.18) and caudate (0.61±0.15) of the patients without LIDs. The mean $^{11}C$–PE2I $BP_{ND}$ in the putamen of Parkinson's disease patients with LIDs 1.32±0.32 were significantly lower as compared to the mean $^{11}C$–PE2I $BP_{ND}$ values of the patients without LIDs (1.64±0.51; $p<0.05$). Parkinson's patients with LIDs had significantly higher $^{11}C$–DASB to $^{11}C$–PE2I $BP_{ND}$ ratio values in the putamen as compared to the group of patients without LIDs ($p<0.01$) – see Figures below and Table 15.

Table 14 – Demographics and clinical characteristics of Parkinson's disease patients

| | PD patients | | |
|---|---|---|---|
| | all | PD non–LIDs | PD LIDs |
| No. of PD patients | 28 | 21 | 7 |
| [a]Sex | 23M:6F | 17M:4F | 5M:2F ns |
| [b]Age | 55.43±7.13 | 55.56±6.87 | 53.32±8.43 ns |
| MMSE score | 29.70±0.59 | - | - |
| BDI score | 4.47±3.78 | - | - |
| [b]$DD_{diagn}$ | 5.79±2.23 | 4.94±1.52 | 7.51±1.57** |
| [c]H&Y stage | 1.97±0.18 | 1.95±0.22 | 2.00±0.00 ns |
| [b]UPDRS–III | 34.27±10.56 | 28.38±9.49 | 37.28±11.53* |
| [b]UPDRS total | 45.60±15.48 | 42.62±15.35 | 53.86±16.10 ns |
| AIMS scale score | - | - | 2.75±2.05 |
| [b]Duration on DA medication | 2.12±1.76 | 1.59±1.03 | 4.12±3.00 ns |
| [b]Time from diagnosis to initiation of DA medication | 3.81±1.97 | 3.43±1.42 | 5.30±2.17 ns |
| [b]Daily $LED_{Total}$ | 744.97±443.87 | 607.24±347.21 | 1115.33±547.39* |
| [b]Daily $LED_{Ldopa}$ | 427.27±438.13 | 300.57±318.55 | 815.19±595.19* |
| [b]Daily $LED_{Dag}$ | 232.7±142.39 | 225.71±126.50 | 214.43±192.27 ns |

Data represent mean values ± 1 SD; PD: Parkinson's disease; MMSE: Mini mental state examination; BDI: Beck's depression inventory; H&Y: Hoehn & Yahr staging scale in "off" medication state; UPDRS–III: Unified Parkinson's disease Rating Scale–score of part III in "off" medication state; UPDRS total: Unified Parkinson's disease Rating Scale–total score in "off" medication state; AIMS: abnormal involuntary movements; DA: dopaminergic; Age, $DD_{diagn}$, duration on DA medication and time from diagnosis to initiation of DA medication are calculated in years. Daily $LED_{Total}$, $LED_{Ldopa}$, and $LED_{Dag}$ are calculated in mg. [a]Comparison for differences in sex was performed with chi–squared ($\chi^2$) test; [b]Comparison of means between PD non–LIDs and PD LIDs groups was made with t–test for independent samples; [c]Comparison between LIDs and non–LIDs groups was performed with Mann–Whitney U test; ns – no statistically significant difference between PD non–LIDs and PD LIDs groups; *denotes statistical significance $p<0.05$ between PD non–LIDs and PD LIDs groups; **denotes statistical significance $p<0.01$ between PD non–LIDs and PD LIDs groups

Table 15 – Mean $^{11}C$–DASB $BP_{ND}$, $^{11}C$–PE2I $BP_{ND}$ and the SERT–to–DAT binding ratios.

| | PD non–LIDs | PD LIDs |
|---|---|---|
| No. of PD patients | 21 | 7 |
| $^{11}C$–DASB $BP_{ND}$ (SERT) | | |
| [a]Caudate | 0.61±0.15 | 0.54±0.15 ns |
| [a]Putamen | 1.26±0.18 | 1.27±0.23 ns |
| $^{11}C$–PE2I $BP_{ND}$ (DAT) | | |
| [a]Caudate | 2.57±0.88 | 2.10±0.75 ns |
| [a]Putamen | 1.64±0.51 | 1.32±0.32* |
| SERT–to–DAT binding ratios | | |
| [b]Caudate | 0.26±0.09 | 0.27±0.08ns |
| [b]Putamen | 0.82±0.21 | 0.99±0.13** |

Data represent mean ± 1 SD; PD: Parkinson's disease; Mean values are calculated as an average for both hemispheres; [a]Comparison of means was made with t–test for independent samples between PD non–LIDs and PD LIDs groups; [b]Comparison between groups was made with Mann–Whitney U test for independent samples between PD non–LIDs and PD LIDs groups; ns – no statistically significant difference between PD non–LIDs and PD LIDs groups; *denotes statistical significance $p<0.05$ between PD non–LIDs and PD LIDs groups **denotes statistical significance $p<0.01$ between PD non–LIDs and PD LIDs groups.
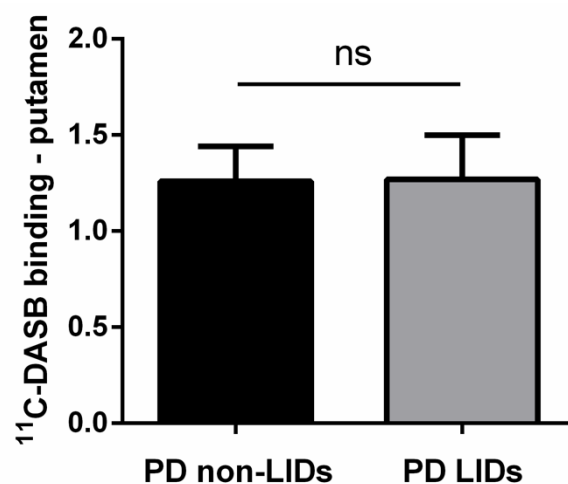


Figure 29 – $^{11}C$–DASB $BP_{ND}$ in the putamen

$^{11}C$–DASB $BP_{ND}$ in the putamen shown in 21 Parkinson's disease (PD) patients without LIDs (non–LIDs) (black bar) and 7 PD patients with LIDs (grey bar). Bars represent mean values + 1 SD. Mean values are calculated as an average for both hemispheres. Comparison of means was made with t–test for independent samples; ns – no statistically significant difference between PD non–LIDs and PD LIDs groups.
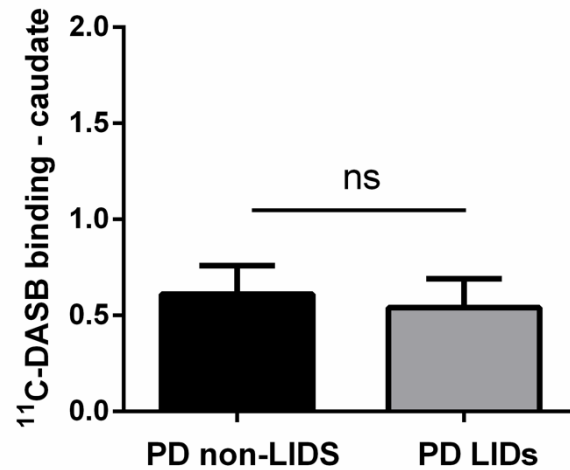
Figure 30– $^{11}$C–DASB BP$_{ND}$ in the caudate

$^{11}$C–DASB BP$_{ND}$ in the caudate shown in 21 Parkinson's disease (PD) patients without LIDs (non–LIDs) (black bar) and 7 PD patients with LIDs (grey bar). Bars represent mean values + 1 SD. Mean values are calculated as an average for both hemispheres. Comparison of means was made with t–test for independent samples; ns – no statistically significant difference between PD non–LIDs and PD LIDs groups.
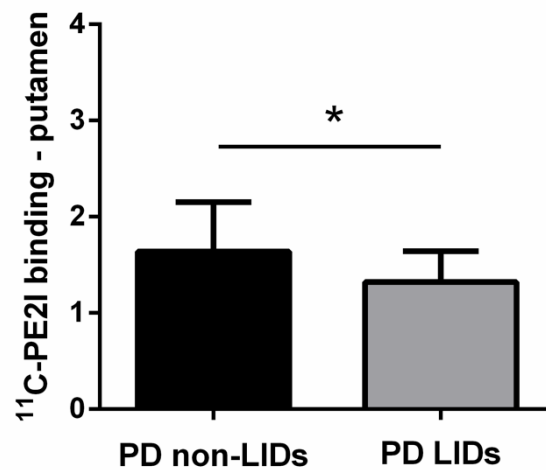


Figure 31 – $^{11}$C–PE2I BP$_{ND}$ in the putamen

$^{11}$C–PE2I BP$_{ND}$ in the putamen shown in 21 Parkinson's disease (PD) patients without LIDs (non–LIDs) (black bar) and 7 PD patients with LIDs (grey bar). Bars represent mean values + 1 SD. Mean values are calculated as an average for both hemispheres. Comparison of means was made with t–test for independent samples; *denotes statistical significance p<0.05 between PD non–LIDs and PD LIDs groups.
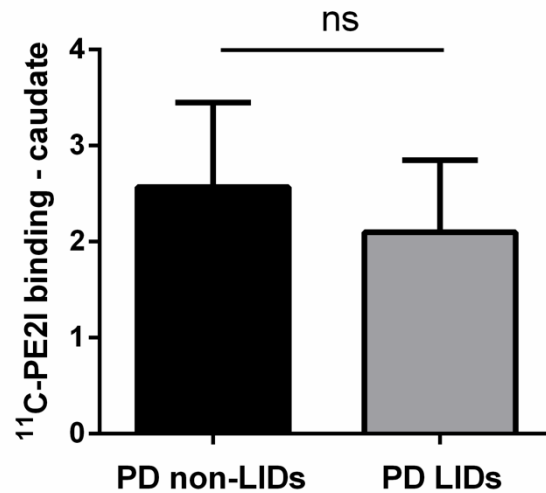
Figure 32 – $^{11}$C–PE2I BP$_{ND}$ in the caudate

$^{11}$C–PE2I BP$_{ND}$ in the caudate shown in 21 Parkinson's disease (PD) patients without LIDs (non–LIDs) (black bar) and 7 PD patients with LIDs (grey bar). Bars represent mean values + 1 SD. Mean values are calculated as an average for both hemispheres. Comparison of means was made with t–test for independent samples; ns – no statistically significant difference between PD non–LIDs and PD LIDs groups.
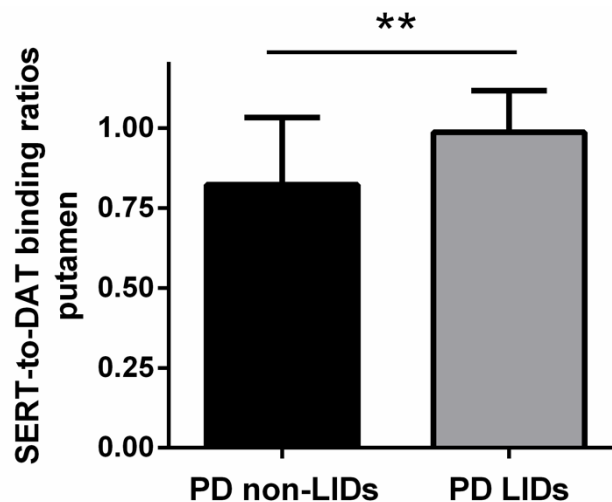


Figure 33 – SERT–to–DAT binding ratios in the putamen

SERT–to–DAT binding ratios in the putamen shown in 21 Parkinson's disease (PD) patients without LIDs (non–LIDs) (black bar) and 7 PD patients with LIDs (grey bar). Bars represent mean values + 1 SD. Mean values are calculated as an average for both hemispheres. Comparison between groups was made with Mann–Whitney U test for independent samples; **denotes statistical significance $p < 0.01$ between PD non–LIDs and PD LIDs groups.
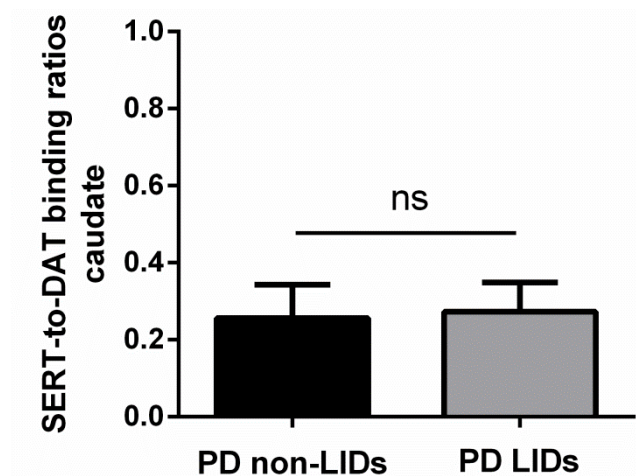
Figure 34 – SERT–to–DAT binding ratios in the caudate

SERT–to–DAT binding ratios in the caudate shown in 21 Parkinson's disease (PD) patients without LIDs (non–LIDs) (black bar) and 7 PD patients with LIDs (grey bar). Bars represent mean values + 1 SD. Mean values are calculated as an average for both hemispheres. Comparison between groups was made with Mann–Whitney U test for independent samples; ns – no statistically significant difference between PD non–LIDs and PD LIDs groups.

## 6.4.2 Correlations

Higher putaminal ^{11}C–DASB to ^{11}C–PE2I $BP_{ND}$ ratios correlated with longer disease duration from diagnosis for all Parkinson's patients (r=0.42; two–tailed, p<0.05) – see Figure 35. ^{11}C–PE2I $BP_{ND}$ in the putamen inversely correlated with UPDRS–III scores (r = –0.38; p<0.05) and total UPDRS scores (r = –0.38; p<0.05) for all Parkinson's disease patients.
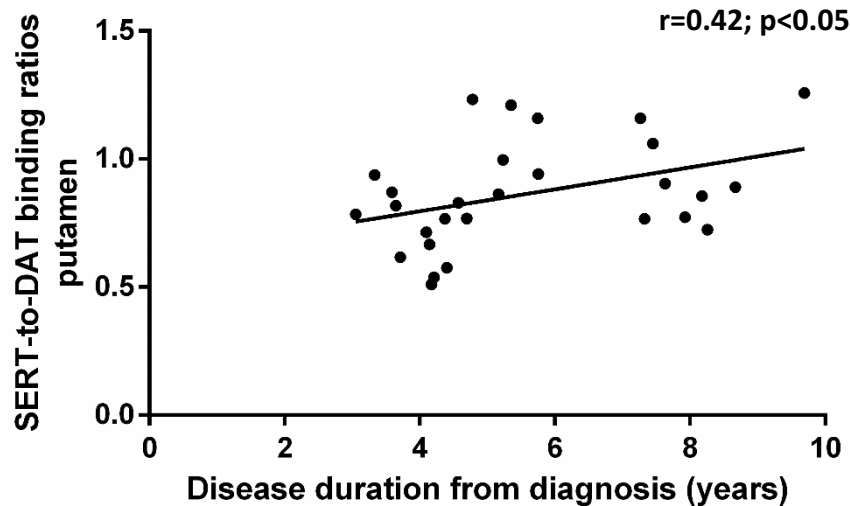
Figure 35 – Correlation of SERT–to–DAT binding ratios in the putamen and disease duration in 28 Parkinson's disease patients

Statistical analysis was performed with two–tailed Spearman correlation between disease duration from diagnosis (in years) and SERT–to–DAT binding ratios in the putamen of 28 Parkinson's patients; r=0.42 p<0.05. Each point in the graph represents one Parkinson's disease patient.

No correlation was found between $^{11}$C–PE2I $BP_{ND}$ in the caudate and the UPDRS–III and total UPDRS scores. No correlation was found between $^{11}$C–DASB $BP_{ND}$ and the UPDRS scores. No correlation was found between putaminal $^{11}$C–PE2I $BP_{ND}$ and either age, the mean $LED_{Total}$, the mean $LED_{Ldopa}$, or the times from diagnosis to initiation of dopaminergic medication. No correlation was found between putaminal $^{11}$C–DASB $BP_{ND}$ and either age, UPDRS, the mean $LED_{Total}$, the mean $LED_{Ldopa}$, or the times from diagnosis to initiation of dopaminergic medication. No correlation was found between putaminal $^{11}$C–DASB to $^{11}$C–PE2I $BP_{ND}$ ratios and either age, UPDRS, the mean $LED_{Total}$, the mean $LED_{Ldopa}$, or the times from diagnosis to initiation of dopaminergic medication.
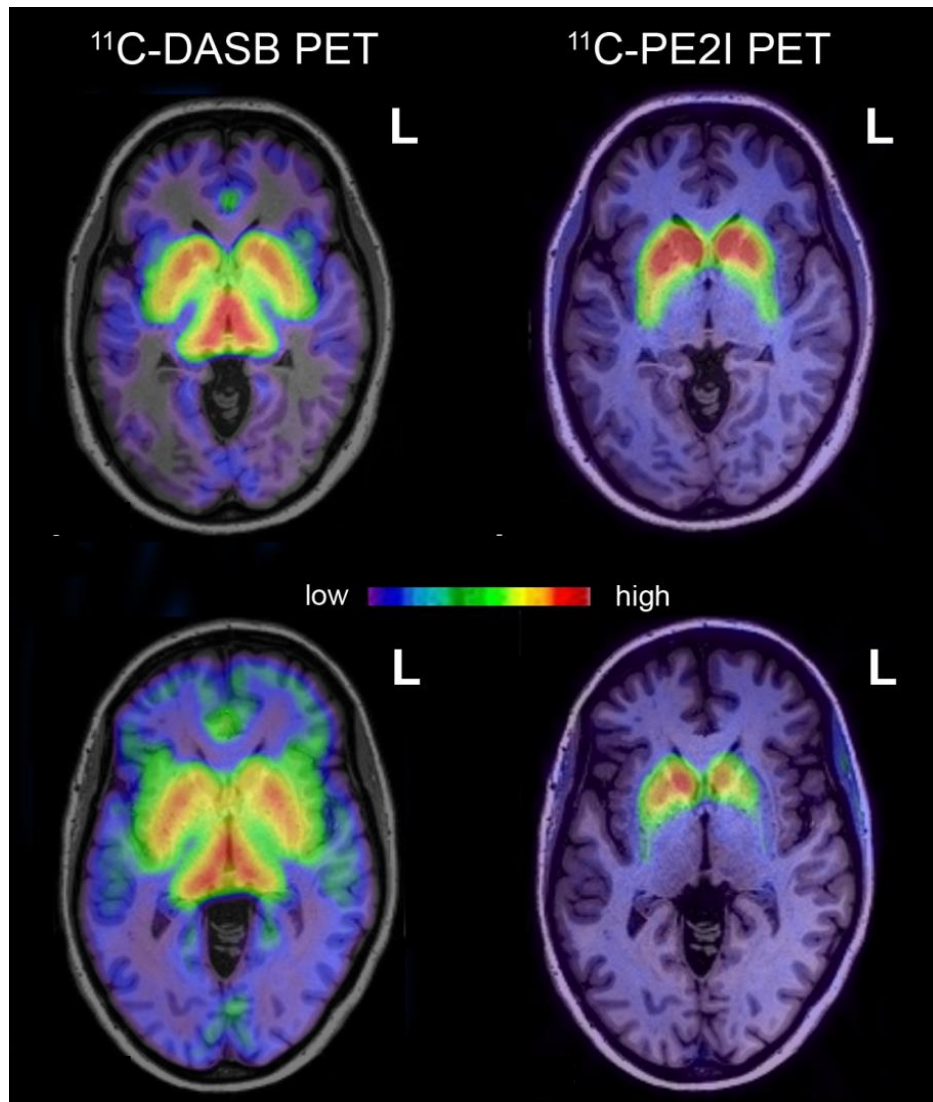
Figure 36 – Representative PET images (in the axial plane) of ^{11}C–DASB binding (SERT) and ^{11}C–PE2I binding (DAT) in the striatum in two Parkinson's disease patients; patient without LIDs is shown in the upper row; patient with LIDs in the lower row

L: left; colour scales represent ^{11}C–DASB and ^{11}C–PE2I binding (from low to high).

*Longitudinal study*
6.4.3 Clinical and Imaging data

12 patients of the 21 who did not have LIDs were included in the longitudinal study and had repeated ^{11}C–DASB and ^{11}C–PE2I PET after 17 months (±11 weeks). The demographics and clinical characteristics of these 12 patients are summarised in Table

16 below. The 12 Parkinson's disease patients had lower $^{11}$C–DASB BP$_{ND}$ values in the putamen (1.23 ± 0.19) as compared to baseline (1.28 ± 0.14; p>0.05) and in the caudate (0.51 ± 0.15) versus (0.62 ± 0.13) (p<0.01). All 12 Parkinson's disease patients had lower putaminal $^{11}$C–PE2I BP$_{ND}$ values in the putamen (1.39 ± 0.41) as compared to baseline (1.63 ± 0.41) (p<0.001) and in the caudate (2.35 ± 0.75) versus (2.69 ± 0.87) (p<0.01). Furthermore, percentage changes in individual putaminal $^{11}$C–PE2I BP$_{ND}$ were greater on average (14.52% ± 10.20) than percentage changes in individual putaminal $^{11}$C–DASB BP$_{ND}$ values (4.32 ± 3.43; p<0.05). The SERT–to–DAT binding ratios increased significantly (p<0.01) in all 12 patients (on average by 12.76% ± 10.99) over this time.

At follow–up, three Parkinson's disease patients became dyskinetic while nine were still classified as non–dyskinetic. The $^{11}$C–DASB to $^{11}$C–PE2I BP$_{ND}$ ratios of these three patients for the putamen were 0.98, 0.88 and 1.29, respectively. Their putaminal $^{11}$C–DASB BP$_{ND}$ values had decreased by 0.31%, 0.87% and 0.08%, respectively and their putaminal $^{11}$C–PE2I BP$_{ND}$ had decreased by 21.79%, 12.73% and 2.02%, respectively. Their DD$_{diagn}$ were 8.96, 9.39 and 5.93 years, respectively.

As only three patients became dyskinetic by the follow–up PET time point, appropriate statistical comparisons between the PD LIDs (N = 3) versus the PD non–LIDs group (N = 9) were not deemed appropriate.

Table 16 –Demographics and clinical characteristics of Parkinson's disease patients

| | BASELINE | FOLLOW–UP |
|---|---|---|
| No. of PD patients | 12 | |
| Sex | 10M:2F | |
| [a]Age | 57.34±6.94 | 58.75±6.85 |
| [a]$DD_{diagn}$ | 5.35±1.75 | 6.75±1.79 |
| [b]H&Y stage | 1.92±0.28 | 2.08±0.28 ns |
| [a]UPDRS–III | 32.17±10.59 | 36.92±8.12* |
| [a]UPDRS total | 46.75±15.40 | 52.83±13.34* |
| [a]Daily $LED_{Total}$ | 680.60±349.76 | 826.31±352.99 ns |
| [a]Daily $LED_{Ldopa}$ | 346.85±344.69 | 496.81±346.08* |
| [a]Daily $LED_{Dag}$ | 254.58±126.28 | 237.83±92.48* |

Data represent mean values ± 1 SD; PD: Parkinson's disease; H&Y: Hoehn & Yahr staging scale in "off" medication state; UPDRS–III and UPDRS total are Unified Parkinson's disease Rating Scale scores (part III and total scores) in "off" medication state; Age and $DD_{diagn}$ are calculated in years. Daily $LED_{Total}$, $LED_{Ldopa}$, and $LED_{Dag}$ are calculated in mg. [a]Comparison of means was made with paired t–test for related samples; [b]Comparison of Hoehn & Yahr scores between baseline and follow–up was performed with Wilcoxon signed–rank test for related samples; ns – no statistically significant difference between baseline and follow–up; *denotes statistical significance p<0.05 between baseline and follow–up

Table 17 – Mean ^{11}C–DASB $BP_{ND}$, ^{11}C–PE2I $BP_{ND}$ and the SERT–to–DAT binding ratios at baseline and at follow–up

| | BASELINE | FOLLOW–UP |
|---|---|---|
| No. of PD patients | 12 | |
| ^{11}C–DASB $BP_{ND}$ (SERT) | | |
| [a]Caudate | 0.62±0.13 | 0.51±0.15** |
| [a]Putamen | 1.28±0.14 | 1.23±0.19 ns (↓ 4.32%) |
| ^{11}C–PE2I $BP_{ND}$ (DAT) | | |
| [a]Caudate | 2.69±0.87 | 2.35±0.75** |
| [a]Putamen | 1.63±0.41 | 1.39±0.41*** (↓ 14.52%) |
| SERT–to–DAT binding ratios | | |
| [b]Caudate | 0.25±0.09 | 0.22±0.04 ns |
| [b]Putamen | 0.83±0.19 | 0.93±0.19** (↑ 12.76%) |

Data represent mean ± 1 SD; PD: Parkinson's disease; Mean values are calculated as an average for both hemispheres; [a]Comparison of means was made with paired t–test for related samples between baseline and follow–up; [b]Comparison between baseline and follow–up was made with Wilcoxon signed–rank test for related samples; ns – no statistically significant difference between baseline and follow–up; **denotes statistical significance p<0.01 between baseline and follow–up; ***denotes statistical significance p<0.001 between baseline and follow–up. % refer to percentage changes over time in putaminal values.
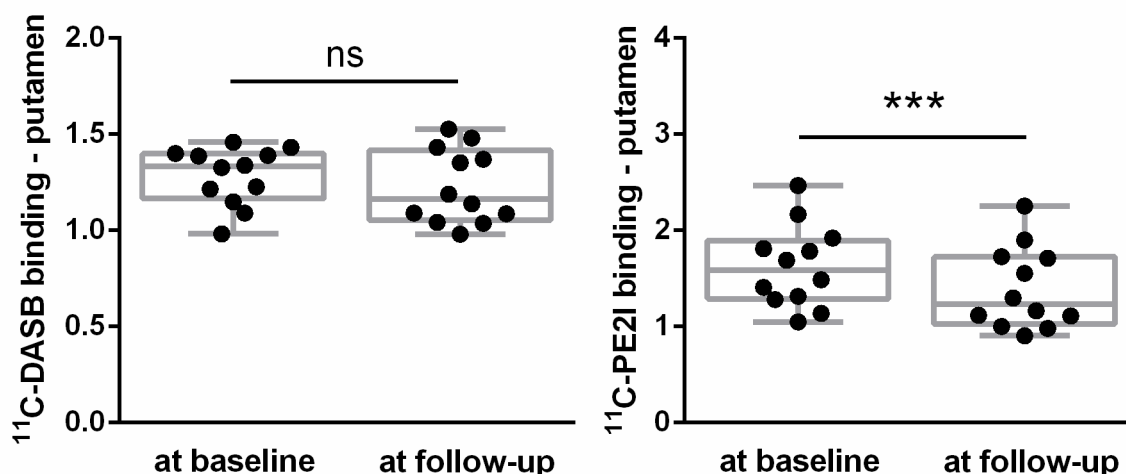
Figure 37 – Scatter plots showing putaminal $^{11}$C–DASB BP$_{ND}$ (left graph) and $^{11}$C–PE2I BP$_{ND}$ (right graph) values (y–axis) of Parkinson's disease patients at baseline and at follow–up

Each black point represents individual BP$_{ND}$ values. Each box represents (from the bottom to the top in the x–axis) quartile 1, median, quartile 3; whiskers represent the minimum and maximum BP$_{ND}$ values; Comparison of means was made with paired t–test for related samples between baseline and follow–up; ns – no statistically significant difference between baseline and follow–up; ***denotes statistical significance p<0.001 between baseline and follow–up.

## 6.5 Summary of findings

*Cross–sectional study*

The Parkinson's disease patients with LIDs had higher SERT–to–DAT binding ratios in the putamen as compared to non–dyskinetic patients in this cohort. Between–group comparison showed higher putaminal $^{11}$C–PEI BP$_{ND}$ in the dyskinetic group, while between–group differences in the putaminal $^{11}$C–DASB BP$_{ND}$ were not statistically significant. Lower putaminal $^{11}$C–PEI BP$_{ND}$ values correlated with higher UPDRS–III and UPDRS total scores. Higher SERT–to–DAT binding ratios in the putamen correlated with longer disease duration for all Parkinson's disease patients.

*Longitudinal study*

The $^{11}$C–PE2I BP$_{ND}$ values in the putamen were significantly lower at follow–up as compared to baseline (p<0.001). The putaminal $^{11}$C–DASB BP$_{ND}$ values had on average reduced only by 4.32% at follow–up; this difference was not statistically significant. The $^{11}$C–DASB to $^{11}$C–PE2I BP$_{ND}$ ratios in the putamen were higher at follow–up as compared to baseline for all Parkinson's disease patients (p<0.01). Furthermore, three Parkinson's disease patients became dyskinetic at follow–up time; their $^{11}$C–DASB to $^{11}$C–PE2I BP$_{ND}$ ratios for the putamen were 0.978, 0.878, and 1.282 respectively. These three patients had minimal reductions in putaminal $^{11}$C–DASB BP$_{ND}$ as compared to the rest of the patients who did not became dyskinetic. Their $^{11}$C–PE2I BP$_{ND}$ putaminal reductions were variable and comparable to the reductions seen in putaminal $^{11}$C–PE2I BP$_{ND}$ values in the rest of the group.

Although both putaminal SERT and DAT availabilities decrease as Parkinson's disease progresses, reductions observed in DAT binding were greater than in SERT. This imbalance in the rate of SERT and DAT decline reflects the increase of the SERT–to–DAT binding ratio over time. These findings suggest that there may be a threshold of SERT–over–DAT terminal availability in the putamen, above which Parkinson's patients are likely to become dyskinetic; however, appropriate comparisons will need statistical tests in a larger sample size.

# ☞ Chapter 7

# Discussion on findings, limitations, clinical relevance and future plans

## 7.1 Discussion on findings

The studies described in this thesis intended to explore the relationship between dopaminergic and serotonergic striatal terminals relevant to the development of Parkinson's dyskinesias. I have shown that at the time of diagnosis, the magnitude of striatal dopaminergic depletion in early Parkinson's alone does not predict the appearance of future LIDs. I have shown that in Parkinson's patients of later stages, there is an imbalance of the serotonergic-over-dopaminergic striatal terminals that is related to disease duration and this could be a factor for the appearance of LIDs. I have demonstrated that as Parkinson's continues to progress, putaminal serotonergic terminals remain relatively unchanged in comparison to the dopaminergic ones and that the aforementioned imbalance increases over time. Taken together, these data suggested a combined role of serotonergic and dopaminergic terminals in the development of LIDs.

To my knowledge, there has been one previous imaging study using a high affinity DAT–specific radioligand investigated whether the magnitude of DAT decline in the striatum can predict the development of LIDs (Hong et al., 2014). The researchers analysed $^{18}$F–FP–CIT PET data alongside with clinical data from a large cohort of *de novo* Parkinson's patients and showed that lower putaminal DAT availability at diagnosis is a risk factor for the development of LIDs. Nonetheless, according to the findings of my study, patients who later developed LIDs had already more severe disease (significantly higher UPDRS scores) at the time of scanning. It could be argued whether the differences in striatal DAT availability observed in *de novo* disease reflect

different levels of severity and not a predictive value of DAT–specific imaging relevant to dyskinesias. In the study of *Chapter 3* (that intended to estimate the role of striatal DAT availability, as a prognostic marker for the appearance of LIDs), *de novo* Parkinson's patients had variable striatal ^{123}I–Ioflupane specific to non–specific binding but were matched for age and disease severity at the time of scanning. The Parkinson's patients who later became dyskinetic had progressed more (significantly higher Hoehn & Yahr scores) than those who did not develop LIDs by that time. In addition, the patients who later developed LIDs were taking significantly higher amounts of levodopa as compared to the non–dyskinetic group (p<0.001) and were still matched for age. By matching patients for age and disease severity, the findings of the study of *Chapter 3* support that the development of LIDs relatively early (within five years from diagnosis of Parkinson's) cannot be predicted by DAT–specific imaging around the time of diagnosis and proposed that the development of LIDs may be related to other factors which are not related to striatal DAT availability at the time of diagnosis.

In the study of *Chapter 4* (that intended to explore whether striatal DAT availability changes over time are related to the appearance of LIDs), Parkinson's patients with similar disease duration but faster dopaminergic decline were found susceptible to develop LIDs earlier than those who progressed slower over the same amount of time. Imaging studies in controls have shown that the density of striatal DAT declines progressively and that this decline is age–related (Ishibashi et al., 2009) and similar for the caudate and the putamen (Shingai et al., 2014). Imaging studies in striatal DAT

losses in Parkinson's have suggested that the observed decline is greater in Parkinson's as compared to controls and that there is marked variability in the putaminal losses among Parkinson's patients (Marek et al., 2001). A longitudinal study designed to assess the decline rate (relative annual rate) of striatal β–CIT binding in Parkinson's, found that the rate of decline is indifferent between patients who develop dyskinesias or motor fluctuations to Parkinson's patients free of motor complications (Pirker et al., 2003). Nonetheless, the patients of the above cohort had variable Hoehn & Yahr stages at the time of baseline DAT–specific SPECT imaging (Pirker et al., 2003). In the longitudinal studies of this thesis (*Chapters 4* and *6*), Parkinson's patients had variable reductions in DAT–specific to non–specific binding over time but were matched for Hoehn & Yahr staging at the time of baseline scanning. These finding suggests that striatal dopaminergic decline (as reflected by DAT–specific imaging) is not uniform for all Parkinson's patients. In the study of *Chapter 4*, patients who later developed LIDs showed greater reductions (indicative of a faster decline) in the putamen in comparison to the non–dyskinetic patients (the latter group had smaller reductions over the same amount of time). It could be argued whether the observed differences in striatal DAT–specific to non–specific binding over time are related to toxic effects of chronic levodopa treatment or due to a down–regulation of the striatal DAT in response to chronic exposure to levodopa (Troiano et al., 2009). Nonetheless, studies looking into the chronic effects of levodopa and dopamine receptor agonists on striatal DAT density (Parkinson Study Group. 2002; Fahn et al., 2004) have been inconclusive (reviewed by Brooks. 2016).

As Parkinson's progresses, reductions in striatal DAT density have been proposed to support presynaptic mechanisms as responsible for the development of LIDs (reviewed by Cenci. 2014). Parkinson's patients in advanced stages are believed to lose their ability to maintain a stable rate of dopamine release in the striatum. PET studies with ^{11}C–raclopride, which reflects postsynaptic dopamine D2 receptors distribution, are able to estimate *in vivo* dopamine release in the striatum (Piccini et al., 1999). ^{11}C–raclopride has high affinity for the postsynaptic dopamine D2 receptors and are therefore subject to competitive displacement by endogenous levodopa (Volkow et al., 1994; Piccini et al., 2003a). Thus, the acute administration of levodopa is expected to increase the dopamine release in the synapse of dopaminergic terminals. Tedroff and colleagues by using this method have shown that the same dose of exogenous levodopa can induce higher levels of synaptic dopamine in advanced Parkinson's patients in comparison to patients who are in earlier stages of the disease (Tedroff et al., 1996).

Furthermore, standard doses of levodopa have been shown to cause dramatic increases of dopamine in the synapse in dyskinetic patients as compared to Parkinson's patients without LIDs (de la Fuente–Fernández et al., 2004). Pavese and Piccini showed that standard levodopa doses can induce large decreases of ^{11}C–raclopride binding in the synapse which correlated with Parkinson's disease severity as well as with higher dyskinesias scores (Pavese et al., 2006). Wide fluctuations in the synaptic concentration of dopamine in patients with motor fluctuations have been also shown to precede clinically apparent LIDs (de la Fuente–Fernández et al., 2001) and

have been linked with longer disease duration and a younger age at onset (Sossi et al., 2006). It should be noted that in Parkinson's the firing neuronal rate in the basal ganglia is proposed to be not only reduced (as compared to controls) but also altered during LIDs (Papa et al., 1999; Levy et al., 2001; Li et al., 2015). In Parkinson's, physiological toning firing is proposed to alter to burst firing that leads to sudden release of high concentration of dopamine into the synapse.

Alongside the above dopaminergic mechanisms, serotonergic terminals have been proposed to contribute to LIDs. Serotonergic terminals can express AADC and the type–2 vesicular monoamine transporter, and convert exogenous levodopa into dopamine, however, they lack auto–regulatory feedback mechanisms and dopamine is proposed to be released in an uncontrolled manner (Ng et al., 1970; Tanaka et al., 1999; Maeda et al., 2005; Kannari et al., 2006) as a false neurotransmitter. Animal studies have provided further evidence supporting a "serotonergic hypothesis" for the development of LIDs. The chemical blockade of serotonin neurons as well as selective lesions in the serotonin terminals can lead into a dramatic reduction of the induced involuntary movements without counteracting levodopa's main effects (Carta et al., 2007; Bézard et al., 2013; Nevalainen et al., 2014; Conti et al., 2014). In addition, serotonin receptor agonists have been shown to have anti–dyskinetic effects in both rodent and non–human primate models of dyskinesias (Muñoz et al., 2008; Bézard et al., 2013). In humans, a recent clinical and PET imaging study showed that buspirone, a 5–HT1a partial agonist, alleviated dyskinesias scores when administered prior to levodopa; while in the PET arm of the study buspirone was shown to

normalise in the striatum the levodopa–induced increases of synaptic dopamine (Politis et al., 2014). The authors of this study used PET imaging with ^{11}C–DASB and ^{11}C–raclopride to assess the degree of serotonin innervation and the amount of dopamine release in the striatum, respectively. Changes in ^{11}C–raclopride BPND values positively correlated with the striatal levels of ^{11}C–DASB BPND values, suggesting a relationship between peak levels of dopamine and the density of striatal serotonin innervation. Similarly, a recent Phase I/IIa clinical trial in Parkinson's disease patients (Svenningsson et al., 2015) confirmed anti–dyskinetic effects of the 5–HT1a/5–HT1b partial agonist, eltoprazine, following the promising results of the same drug in MPTP–treated macaques (Bézard et al., 2013).

The SERT–to–DAT binding ratio has been used here to study whether human serotonergic and dopaminergic striatal terminals are related to each other and together contribute to LIDs. The SERT–to–DAT binding ratio has been used as an index to reflect a possible imbalance between serotonergic and dopaminergic striatal terminals. Nevertheless, unlike its components (SERT, DAT specific to non–specific binding), the ratio should not be viewed as an *in vivo* marker, but as an index that is calculated from them.

A recent imaging study estimated midbrain–SERT to striatal–DAT binding ratio in early stage, drug–naïve Parkinson's disease patients. The authors of that study showed that imbalanced ratios (calculated from different brain regions) do not predict the development of LIDs in early stages of the disease, and hypothesised that

imbalance ratios may occur at later stages of Parkinson's disease (Suwijn et al., 2013).

I have shown that the SERT–to–DAT binding ratio in the putamen is significantly increased in Parkinson's patients as compared to age–matched normal controls. In the cross-sectional studies of *Chapters 5* and *6*, the ratio was used to compare the Parkinson's patients with LIDs to those who had not have a history of LIDs. The statistically significant difference in the putaminal ratio values between the two groups suggests that the observed imbalance in the putamen may be a factor relative to LIDs. The difference in the binding ratios between PD LIDs and PD non–LIDs patients is in line with a recently published PET imaging study from Lee and colleagues who assessed SERT–over–DAT function in the striatum of Parkinson's patients including a subgroup of drug–naïve patients (Lee JY et al., 2015). This study did not include a group of age–matched controls to compare the drug–naïve group to. The researchers showed that SERT–over–DAT binding ratios are increased in the putamen of dyskinetic patients as compared to non–dyskinetic patients and concluded that striatal serotonergic–over–dopaminergic terminals' imbalance may be a marker of disease progression and that disease progression that may be linked to the appearance of LIDs (Lee JY et al., 2015).

In the cross–sectional study of *Chapter 5*, putaminal SERT-to-DAT binding ratios in the Parkinson's group were increased in comparison to controls and also correlated positively with disease duration (the latter was a finding also in the cross–sectional study of *Chapter 6*). In addition, putaminal SERT-to-DAT binding ratios increased further over time (longitudinal study of *Chapter 6*). Taken together, the increases in the

Parkinson's binding ratios over time therefore suggest that the magnitude of the imbalance may be connected just to Parkinson's progression per se. To my knowledge, there is no other *in vivo* imaging study in Parkinson's nor in controls that has looked into the changes of the striatal serotonergic innervation over time. The longitudinal study of *Chapter 6* shows that the reductions in the putaminal SERT over time (as reflected by changes in ^{11}C–DASB $BP_{ND}$ values) were less pronounced as compared to those observed in the DAT (as reflected by changes in ^{11}C–PE2I $BP_{ND}$ values). Given that the underlying mechanisms of LIDs have been associated to longer disease duration rather than to the duration of levodopa treatment (Cilia et al., 2014), at follow-up, all Parkinson's patients would theoretically have more chances to develop LIDs as compared to the stage they were at, when they had the baseline scans.

Using ^{11}C–DASB PET, the results of the longitudinal study of *Chapter 6* show that the serotonergic terminals do not change significantly over time for the whole group of Parkinson's patients. This could be an observation that applies to many other terminals in the Parkinson's brain. However, the above finding is in line with current knowledge in the field. A cross–sectional PET study targeting the striatal SERT availability in Parkinson's, showed losses in putaminal SERT (as reflected by ^{11}C–DASB $BP_{ND}$) in established and advanced Parkinson's as compared to patients with early disease and to normal controls (Politis et al., 2010). In addition, striatal serotonergic markers have been detected in terminal stages of Parkinson's disease (Kish et al., 2008). The findings of this studies indicate that although there is serotonergic degeneration in the putamen, this seems to follow chronologically the

dopaminergic one. The slower striatal serotonergic decline in Parkinson's is relevant to the proposed mechanism, as the striatal serotonergic terminals are able to uptake levodopa and regionally release dopamine as a false neurotransmitter. The data of the longitudinal study of *Chapter 6* demonstrate that putaminal SERT density (as reflected by percentage changes in $^{11}C$–DASB $BP_{ND}$ values) declines to a slight extent than the putaminal DAT one (as reflected by percentage changes in $^{11}C$–PET $BP_{ND}$ values). This discrepancy may be just an observation of the fact that Parkinson's neuropathology affects primarily the dopaminergic terminals. Therefore, as Parkinson's progresses, the serotonergic terminals are regarded as relatively preserved in comparison to the depleted dopaminergic ones. As the serotonergic terminals do not have the dopamine autoreceptors, the uptake of levodopa and the release of dopamine as a false neurotransmitter by the serotonergic terminals does not occur in a physiological manner. Hence, with reduced DAT sites in the striatum and the presence of abnormal neuronal firing and aberrant role of the striatal serotonergic terminals, excessive amounts of levodopa may lead to dramatic swings of synaptic dopamine levels and the occurrence of peak dose LIDs.

In the longitudinal study of *Chapter 6*, I observed that, over time, the putaminal SERT–to–DAT binding ratio values significantly increased, however, not all Parkinson's patients became dyskinetic. In the longitudinal study of *Chapter 6*, over the same period of time, three Parkinson's patients had minimal decline (< 1%) in putaminal $^{11}C$–DASB $BP_{ND}$. Their reductions were comparable to the reductions seen in putaminal $^{11}C$–PE2I $BP_{ND}$ values in the rest of the group. These three patients all had

high putaminal $^{11}C$–DASB–to–$^{11}C$–PE2I binding ratios and had become dyskinetic by the follow–up scanning time. At follow–up, their putaminal binding ratios were within the range of the PD LIDs group of the cross–sectional cohort. As only three patients became dyskinetic by the follow–up PET time point, appropriate statistical comparisons between the PD LIDs (N = 3) versus the PD non–LIDs group (N = 9) were not deemed appropriate. As the components of the binding ratio change unevenly over time, the interpretation of individual ratio values has to be done in the context of disease progression and only as an index reflective of SERT–over–DAT imbalance. Therefore, with the current set of data, the individual putaminal ratio values of these three patients cannot be interpreted fully at the moment but once the longitudinal study of *Chapter 6* will be completed. The conduct of a study in a larger cohort comprised of two statistically comparable groups (PD LIDs versus PD non–LIDs) could provide a better understanding on the possible factors for the development of LIDs over time.

In conclusion, the studies described in this thesis propose that striatal serotonergic and dopaminergic terminals' changes over time are a contributing factor for the development of LIDs. The findings of the above studies provide useful insight in the pathophysiology of LIDs with direct implications for further research in the therapeutics of Parkinson's dyskinesia.

A possible mechanism for the striatal serotonergic and dopaminergic terminals' changes over time can be sketched as follows. In early Parkinson's disease, putamen

and caudate nuclei are affected by Parkinson's pathology and endogenous levodopa is believed to be no more sufficient. Motor symptoms are present at this stage (typically mild and unilateral) and pharmacotherapy guidelines point towards dopamine replacement therapies. Levodopa is now introduced as treatment and the partly depleted striatum encounters exogenous amounts of levodopa for the first time. Exogenous levodopa is added on to endogenous so that the total intrastriatal levodopa can be converted into dopamine. Dopamine synthesis, storage, release and reuptake are believed to be conducted by the remaining dopaminergic neurons, which are assumed to be adequately functional.

However, striatal serotonergic neurons are also able to convert *in vivo* levodopa to dopamine (Ng et al., 1970; Ng et al., 1971; Tanaka et al., 1999; Maeda et al., 2005; Kannari et al., 2006). I propose that in Parkinson's, exogenous levodopa is converted into dopamine partly by dopaminergic and partly by serotonergic terminals and that this release is fairly dependent on the integrity of both dopaminergic and serotonergic striatal terminals. Evidence from studies in the long term effects of levodopa therapy, propose that in advanced disease, the remaining striatal neurons are not able to handle exogenous levodopa as they used to (Nutt and Holford. 1996). As Parkinson's disease continues to progress, even higher levodopa doses are being administered. I support the notion that in front of exogenous levodopa, striatal serotonergic terminals respond by releasing dopamine and I hypothesise that this 5–HT mediated release starts in the early stages of the disease. I propose that it continues for as long as excessive amounts of levodopa are being administered and serotonergic terminals are preserved, and that

it becomes problematic only in the late stages. I hypothesise that in early Parkinson's, the striatal serotonergic terminals promote the dopamine transmission as much as possible and temporarily have a beneficial role.

As disease progresses and the density of DAT in the striatum continues to decline and neuronal firing is already quite problematic, Parkinson's patients typically have more severe motor disease and take higher amounts of levodopa. At the same time, Parkinson's patients are at risk for experiencing motor fluctuations after each dose of exogenous levodopa. Imaging studies have shown that patients with motor fluctuations have excessive swings of synaptic dopamine levels as compared to patients with stable response to levodopa. At these stages, it may be the 5–HT mediated dopamine release alongside altered neuronal firing that lead to excessive swings of synaptic dopamine levels. The main reason to that may be that Parkinson's patients do not have enough putaminal DAT sites at this stage, to adequately control the excessive swings of synaptic dopamine. Long acting preparations of levodopa have been effective in improving motor fluctuations as compared to standard release levodopa. This effect may be achieved possibly by controlling the intrastriatal levodopa delivery rate and the rate of dopamine reuptake, respectively.

In the advanced stages of the disease, the striatum is almost depleted, while the remaining terminals handle even greater amounts of exogenous levodopa. The number of the remaining serotonergic terminals becomes now comparable to the remaining dopaminergic ones (reflected by greater SERT–over–DAT imbalance);

however, the striatum viewed as a system, is now completely unable to control the reuptake of excessive synaptic dopamine (significantly lower DAT). At this point, striatal DAT availabilities are critically low to reuptake the amounts of released dopamine. If serotonergic terminals' decline has not been great over time while the dopaminergic one has been pronounced, high doses of exogenous levodopa should be almost fully converted to dopamine and poorly reuptaken, thus resulting to a case of excessive swings of synaptic dopamine. These excessive swings of dopamine should not be now controlled adequately by the remaining DAT sites. This would lead to dramatic swings in postsynaptic dopamine receptor stimulation and possibly to the appearance of LIDs, for as long as patients are in an "on" medication state. The above point could be further supported by the fact that the duration of peak dose LIDs is dependent on the administered dose of levodopa.

On the other hand, if the serotonergic terminals' decline has been great over time while the dopaminergic one has been pronounced, high doses of exogenous levodopa should be only partly converted to dopamine and poorly reuptaken, thus resulting to moderate swings of the synaptic dopamine levels. Here, the amount of released dopamine should not suffice to stimulate the few remaining postsynaptic dopamine receptors as in earlier stages of the disease. Theoretically, at this stage and under these assumptions, smaller amounts of exogenous levodopa, should provide similar clinical benefit with larger amounts of levodopa. In fact, in terminal stages of Parkinson's, that the striatum is inevitably depleted from dopaminergic terminals, levodopa is unable to improve motor symptoms, let alone to induce any dyskinesias. The above notion

could be indirectly supported by the studies that propose upregulation of putaminal AADC in early Parkinson's, which however is not extended in advanced disease (Ekesbo et al., 1999; Rakshi et al., 1999).

Finally, it should be noted that the cross–sectional study of *Chapter 6* confirmed that lower putaminal $^{11}$C–PE2I BP$_{ND}$ values reflect more severe disease (higher UPDRS–III and UPDRS total scores), similarly to several imaging studies in Parkinson's that have utilised Fdopa and Ioflupane. Though not studied here (direct comparison of $^{11}$C–PE2I PET to $^{123}$I–Ioflupane SPECT in the same group of subjects), the above point adds evidence on the validity $^{11}$C–PE2I as a powerful radioligand for monitoring Parkinson's progression and the effect of novel pharmaceutical compounds and restorative therapies. Similarly, the SPECT studies of this thesis, encourage the conduct of $^{123}$I–Ioflupane SPECT imaging for research purposes that extend its validated diagnostic use to that of a monitoring biomarker.

## 7.2 Limitations

The studies presented in this thesis have several limitations relevant to the study design, patient selection and methodology. For instance, although the patients of the longitudinal studies of *Chapters 4* and *6*, were matched for DD$_{diagn}$ and severity, the patients of the cross–sectional studies 5 and 6 were not matched appropriately. It could be argued that comparing groups of Parkinson's disease patients with and without LIDs might not be a very effective way to look for changes in the SERT–to–DAT binding ratios relative to dyskinesias. As these patients with similar clinical

characteristics are difficult to identify in a Movement Disorders Clinics, the main objective of the cross–sectional studies described in this thesis was to look for differences in a diverse group of Parkinson's patients treated with levodopa relative to LIDs. That said, all Parkinson's patients of the cross–sectional studies were not *a priori* selected as either PD LIDs or PD non–LIDs. In the studies described in this thesis, the main inclusion criterion for the participants with Parkinson's was to be treated with levodopa i.e. to be *at risk* for having/developing (or not) LIDs. Each Parkinson's patient of the studies of this thesis was therefore first assessed in "on" medication state for having (or not) dyskinesias and was *then* categorised in one of the two groups (PD LIDs; PD non–LIDs). Hence, the differences in the clinical characteristics between the two groups in the cross–sectional studies of *Chapters 5* and *6* stand as results of statistical comparisons that were part of the study design. It would be most interesting to be able to identify and enrol in these studies Parkinson's patients matched for $DD_{diagn}$ and severity; however, this would potentially hamper the recruitment period and make the conduct of such a study infeasible.

Furthermore, the studies presented here do not comment on the severity of LIDs relative to the administered levodopa doses and the imaging data. The severity of LIDs for each individual is highly variable throughout a 24 hour day, as they are fairly dependent to the administered levodopa doses and subject to intrapatient variability. The AIMS scale is the only well–validated clinical rating scale for assessing the *severity* of dyskinesias. Nonetheless, participants with Parkinson's disease in the studies of this thesis were not taking standardised levodopa doses each time an AIMS

assessment was performed. Hence, individual AIMs scale scores have not been recorded following usual levodopa doses of each participant. Individual AIMS scores were therefore used just to determine if an individual Parkinson's patient is to be categorised as dyskinetic or non–dyskinetic. This point should be indeed viewed as a limitation of the study design.

The time from diagnosis to PET/SPECT imaging and the time from the onset of LIDs to PET/SPECT imaging vary among individuals in the studies of this thesis. This variability of timing of dyskinesias relative to imaging is a limitation of these studies. The onset of LIDs literally refers to the time dyskinesias are experienced by a Parkinson's patient for the first time. LIDs of minimal severity may be unnoticeable by the patients or incorporated into socially acceptable movements. Hence, questioning each patient on whether he/she has been experiencing any involuntary movements over the past few months is likely to be invaluable for precisely estimating the onset of LIDs. The time dyskinesias are first noted at the Movement disorders clinics has been taken into account in these studies to *approximate* the onset of LIDs. This is unlikely to reflect the actual onset of LIDs, as Parkinson's patients attend their clinical appointments from home not being instructed to take their medicines under a certain levodopa protocol. Hence, each Parkinson's patient is unlikely to be in an "on" dopaminergic medication state at each clinical appointment, unless this has been arranged between the Specialist and the patient beforehand.

It should be noted that Parkinson's patients who participated in these studies were diagnosed by the same clinical team, were reviewed clinically at least every six months by the same clinical team, and were prescribed doses of levodopa and other dopaminergic medicines based on their individual needs. The longitudinal studies of *Chapter 4* and *6*, were designed to assess putaminal SERT, DAT availabilities at only two time points. Notwithstanding the clinical management of these patients was consistent, the interval between the multiple clinical assessments could not have been matched to the interval between scanning. Hence, with this set of data, it is quite difficult to estimate in detail the serotonergic and dopaminergic decline rate in this Parkinson's cohort. In absence of longitudinal ^{11}C–DASB PET data in early and advanced Parkinson's patients and controls, the current set of data can propose that striatal serotonergic terminals are relatively preserved in moderate–to–advanced Parkinson's but cannot demonstrate the rate of decline. The same point applies also for the estimation of the DAT decline rate (as measured by DAT–specific imaging) and the lack of longitudinal data from controls. In the studies of this thesis, the six–month interval between the clinical assessments was thought to be appropriate for detecting (or not) the appearance of LIDs. Taking into account feasibility measures, the interval between baseline and follow–up scans was similarly thought to be appropriate for detecting (any) changes in the dopaminergic and the serotonergic terminals over time.

A longitudinal PET imaging study designed to assess the changes of striatal SERT and DAT across the different stages of Parkinson's progression and in controls of various age groups would clarify whether the observed minor changes are due to Parkinson's

and not due to ageing or simply due to partial volume effects. The best way to determine precisely the onset of LIDs would be through appropriate clinical monitoring of patients at risk for developing LIDs who are being treated with standardised levodopa doses throughout the day for several weeks or months. Unless appropriate clinical monitoring has been arranged to specifically determine the onset of LIDs for each patient over a certain period of treatment, the timing of dyskinesia onset relative to PET/SPECT imaging is practically impossible to calculate. At length, a prospective study with the same aims of the studies of *Chapters 3* and *4*, could be designed to match participants to study procedures as best as possible; nonetheless, the data collected for these two studies were collected retrospectively and this point could not have been addressed.

It should be clearly noted that from a PET/SPECT methodology point of view, the studies presented here were not conducted following a pharmacological challenge for dopamine release but, while all participants were in an "off" medication state. Still, quantification of specific binding *in vivo* through PET/SPECT represents here only an approximation of the available target and that ^{123}I–Ioflupane specific to non–specific binding, ^{11}C–PE2I $BP_{ND}$ and ^{11}C–DASB PE2I $BP_{ND}$ are only reflective of the *in vivo* DAT and SERT densities, respectively. DAT and SERT are both appropriate *in vivo* markers of dopaminergic and serotonergic terminals' integrity; hence, the changes (if any) in the DAT– and SERT–specific to non–specific binding values over time should be viewed only as reflective of changes (if any) in the integrity of dopaminergic and serotonergic terminals. Theoretically, tracking such changes in the striatum of the

living Parkinson's brain would require multiple PET/SPECT scans with several radioligands for each individual and at multiple time points. This set of imaging data would be meaningful if in parallel to imaging, multiple clinical assessments were performed including the administration of increasing doses of levodopa. An ideal clinical and imaging study in the Parkinson's brain relative to the development of LIDs, should have been possible through multiple PET or SPECT imaging of both pre– and postsynaptic terminals' markers before and after respective levodopa challenges and over time. However, such a study would be impractical to perform with Parkinson's patients taking into consideration the discomfort and inconvenience of performing multiple scanning in "off" and "on" medication state, the conduct of several clinical ratings over time and of course the total exposure to ionising radiation for each individual.

Manual delination of ROIs or VOIs is subject to unintentional errors with considerable inter- and intra-operator variability. On the other hand, an automated anatomy-based analysis using standardised ROIs defined on MRI template images may not be always able to provide the best fitting. The imaging methods being used in the studies of this thesis have been developed well before these studies were designed and have been validated through several other PET and SPECT studies over the past years. Undoubtedly, methods should be always under review and subject to process improvements and updates.

The main findings of the two cross–sectional studies in *Chapters 5* and *6* are grouped in the discussion of this thesis. Nonetheless, the two Parkinson's cohorts were entirely different and the methods for assessing striatal DAT density for the SERT–to–DAT binding ratios were different between the two cross–sectional studies. The two cross–sectional studies are grouped as they have great similarities in the study design and their group of participants had relatively similar clinical characteristics. With regards to the methods, in the study of *Chapter 5*, DAT density was estimated *in vivo* through ^{123}I–Ioflupane SPECT while in the study of *Chapter 6*, DAT density was assessed using ^{11}C–PE2I PET. PET is more sensitive than SPECT and ^{11}C–PE2I has higher affinity for the DAT. Nonetheless, ^{11}C–PE2I $BP_{ND}$ values does not equal to ^{123}I–Ioflupane specific to non–specific binding values. Similarly to $BP_{ND}$ (derived from PET data), specific to non–specific binding ratios (derived from SPECT data) have been proposed to be a reliable estimate of $BP=B_{max}/KD$. Hence, though not entirely accurate, both ^{123}I–Ioflupane specific to non–specific binding ratio values and ^{11}C–PE2I BPND values are viewed as acceptable here to reflect DAT–specific binding and equally acceptable for the calculation of the SERT–to–DAT binding ratios. The above point represents a limitation of the study design which could have been better addressed by performing DAT–specific imaging with PET only. However, funds in place for the study of *Chapter 5* allowed at the time the conduct of SPECT and PET scans. Later on, additional funds became available for study of *Chapter 6*, which allowed me to test the same hypothesis using PET only.

Finally, LIDs are by definition *levodopa*-induced dyskinesias. The studies presented here could have included analyses of imaging data in relation to dopamine receptor agonists' therapeutics and explore the understanding on the topic further; however, this would have extended the studies far beyond the purpose of this thesis.

## 7.3 Clinical relevance and future plans

Current available treatments for managing LIDs in advanced disease may be fairly efficient, however, several limitations apply (reviewed in Section 1.8). Continuous levodopa infusion and DBS may be efficient in managing LIDs in advanced disease, nonetheless, they are limited to symptomatic relief in cases whereas medication management is poor. Notwithstanding that amantadine is an inexpensive and widely effective drug, long term efficacy of amantadine in managing LIDs is doubtful. In addition, further evidence for the exact mechanism of amantadine in the central nervous system is needed to encourage the development of novel NMDA glutamate–receptor drugs.

Drugs with direct serotonergic action have shown able to improve LIDs in Parkinson's patients (Politis et al., 2014); however, long term efficacy of drugs with direct serotonergic actions as anti–dyskinetic agents in humans is not known. Given the evidence from the studies conducted for this thesis, it could questioned whether long term treatment of dyskinetic patients with selective serotonergic agents could control adequately the severity of LIDs. A previous clinical trial in LIDs (Politis et al., 2014), showed that buspirone had anti–dyskinetic effects when administered prior to

levodopa without counteracting levodopa's main effects. In this study, the role of buspirone in attenuating LIDs was further supported by PET imaging findings that buspirone administration normalised levels of dopamine release in the striatum (Politis et al., 2014). However, the doses of buspirone administered in this acute study (20 to 30 mg) may not be practical for daily administration in Parkinson's disease patients because of side effects (merely drowsiness and nausea). Also, buspirone in higher doses has a moderate affinity for the dopamine D2 receptors, thus implicating its beneficial effect. Hence, it would be most interesting to study the effect of highly selective serotonergic drugs in the long term as well as to reassess levodopa dosing in earlier stages of the disease.

Towards this, I set up and started the conduct of a clinical and imaging study in Parkinson's disease patients with LIDs with lower doses of buspirone which was unfortunately terminated early during the acute phase of it. The clinical trial was designed to have two phases: (a) a cross–over, dose–finding (two different doses of buspirone to be tested), placebo–controlled, double–blinded study and (b) a chronic double–blinded, placebo controlled clinical trial with buspirone administered prior to levodopa. Depending on the results of the acute study, patients would continue with buspirone (on one of the lowest efficient dose of the acute study) on a chronic clinical trial for six weeks. In addition, a subgroup of patients treated with buspirone would be assessed through PET imaging for the effect of buspirone in normalising dopamine release in the striatum. In this study, I hypothesised that buspirone will reduce levels

of synaptic dopamine generated from the serotonergic terminals after oral levodopa administration and this would be associated with a reduction in the severity of LIDs.

The above study had secured funding from the Michael J Fox Foundation, USA for the acute arm of the clinical trial. It received favourable approvals from the East Midland Research Ethics Committee, the Imperial College Joint Research Compliance Office, the Administration of Radioactive Substances Advisory Committee and the Medicines & Healthcare products Regulatory Agency. 20 Parkinson's patients with a history of LIDs were screened for the acute clinical trial. 10 Parkinson's patients did not fulfil one or more of the exclusion criteria. 2 eligible patients finally decided not to take part in the study. 8 Parkinson's patients with LIDs (3M:5F) participated in the acute clinical trial. All participants received buspirone either 0.10mg/kg or 0.20mg/kg prior to levodopa. All participants also received placebo prior to levodopa. During a routine monitoring visit from the Sponsor it was discussed whether to perform an interim analysis to assess the efficacy of Buspirone in order to apply for extending the recruitment period. It was agreed that the unblinded clinician would perform the interim analysis of collected data (N=8 participants). The outcome of the interim analysis revealed minor safety issues (induction of minor adverse effects) and was inconclusive for the efficacy of buspirone over placebo. The unblinded clinician discussed this with the Principal Investigator, who then discussed this with the Sponsor and the Funder of the study. It was commonly agreed to terminate the acute clinical trial and subsequently to early terminate the study. Collected data are still

being kept blinded over discussions on the probability of continuing the study. To this end, no data are shown here from this clinical trial.

For the near future, I am planning to continue the longitudinal PET study described in *Chapter 6* and include a larger number of non–dyskinetic Parkinson's with variable clinical characteristics patients. The aims of this larger study would be to estimate the decline rate of striatal dopaminergic and serotonergic terminals and then explore if there is a clear relation between the two individually, and between distinct clinical groups. In addition, I am planning to look into differences of imaging data taking into account the differences (if any) in disease duration and the amount of administered levodopa doses, as indicated elsewhere (Cilia et al., 2014).

# Funding

# Bibliography

listed in alphabetical order by the name of the first author

Ahlskog JE, Muenter MD. Frequency of levodopa-related dyskinesias and motor fluctuations as estimated from the cumulative literature. Mov Disord. 2001; 16(3):448-58.

Ahmed I, Bose SK, Pavese N, Ramlackhansingh A, Turkheimer F, Hotton G, et al. Glutamate NMDA receptor dysregulation in Parkinson's disease with dyskinesias. Brain. 2011; 134(Pt 4):979-86.

Beck AT, Ward CH, Mendelson M, Mock J, Erbaugh J. An inventory for measuring depression. Arch Gen Psychiatry. 1961; 4:561-71.

Bézard E, Tronci E, Pioli EY, Li Q, Porras G, Björklund A, et al. Study of the antidyskinetic effect of eltoprazine in animal models of levodopa-induced dyskinesia. Mov Disord 2013; 28: 1088-96.

Bernheimer H, Birkmayer W, Hornykiewicz O. Distribution of 5-hydroxytryptamine (serotonin) in the human brain and its behavior in patients with Parkinson's syndrome. Klin Wochenschr. 1961; 39:1056-9.

Blakely RD, Berson HE, Fremeau RT Jr, Caron MG, Peek MM, Prince HK et al. Cloning and expression of a functional serotonin transporter from rat brain. Nature. 1991; 354(6348):66-70.

Blakely RD, Ramamoorthy S, Qian Y, Schroeter S, Bradley C. Regulation of antidepressant-sensitive serotonin transporters. In: Reith MEA, editor. Neurotransmitter Transporters: Structure, Function, and Regulation. Totowa, NJ: Humana Press; 1997. pp. 29–72.

Booij J, Tissingh G, Boer GJ, Speelman JD, Stoof JC, Janssen AG et al. [123I]FP-CIT SPECT shows a pronounced decline of striatal dopamine transporter labelling in early and advanced Parkinson's disease. J Neurol Neurosurg Psychiatry. 1997; 62(2):133-40.

Booij J, Busemann Sokole E, Stabin MG, Janssen AG, de Bruin K, van Royen EA. Human biodistribution and dosimetry of [123I]FP-CIT: a potent radioligand for imaging of dopamine transporters. Eur J Nucl Med. 1998; 25(1):24–30.

Booij J, de Jong J, de Bruin K, Knol R, de Win MM, van Eck-Smit BL. Quantification of striatal dopamine transporters with 123I-FP-CIT SPECT is influenced by the selective serotonin reuptake inhibitor paroxetine: a double-blind, placebo-controlled, crossover study in healthy control subjects. J Nucl Med. 2007; 48(3):359–366.

Braak H, Del Tredici K, Rub U, de Vos RAI, Jansen Steur ENH, Braak E. Staging of brain pathology related to sporadic Parkinson's disease. Neurobiol Aging 2003; 24:197-211.

Bracco F, Battaglia A, Chouza C, Dupont E, Gershanik O, Marti Masso JF, et al. The long-acting dopamine receptor agonist cabergoline in early Parkinson's disease: final results of a 5-year, double-blind, levodopa-controlled study. CNS Drugs. 2004; 18(11):733-46.

British National Formulatory, 2015a.
http://www.evidence.nhs.uk/formulary/bnf/current/4-central-nervous-system/49-drugs-used-in-parkinsonism-and-related-disorders/491-dopaminergic-drugs-used-in-parkinsons-disease/levodopa

British National Formulatory, 2015b.
http://www.evidence.nhs.uk/formulary/bnf/current/4-central-nervous-system/49-drugs-used-in-parkinsonism-and-related-disorders/491-dopaminergic-drugs-used-in-parkinsons-disease/dopamine-receptor-agonists.

Brix G, Zaers J, Adam LE, Bellemann ME, Ostertag H, Trojan H, et al. Performance evaluation of a whole-body PET scanner using the NEMA protocol. National Electrical Manufacturers Association. J Nucl Med. 1997; 38(10):1614-23.

Brooks DJ, Salmon EP, Mathias CJ, Quinn N, Leenders KL, Bannister R, et al. The relationship between locomotor disability, autonomic dysfunction, and the integrity of the striatal dopaminergic system in patients with multiple system atrophy, pure autonomic failure, and Parkinson's disease, studied with PET. Brain. 1990; 113 ( Pt 5):1539-52.

Brooks DJ. Molecular imaging of dopamine transporters. Ageing Res Rev. 2016; 30:114-21.

Buongiorno M, Antonelli F, Cámara A, Puente V, de Fabregues-Nebot O, Hernandez-Vara J, et al. Long-term response to continuous duodenal infusion of levodopa/carbidopa gel in patients with advanced Parkinson disease: The Barcelona registry. Parkinsonism Relat Disord. 2015; 21(8):871-6.

Cáceres-Redondo MT, Carrillo F, Lama MJ, Huertas-Fernández I, Vargas-González L, Carballo M, et al. Long-term levodopa/carbidopa intestinal gel in advanced Parkinson's disease. J Neurol. 2014; 261(3):561-9.

Carta M, Carlsson T, Kirik D, Björklund A. Dopamine released from 5-HT terminals is the cause of L-DOPA-induced dyskinesia in parkinsonian rats. Brain 2007; 130: 1819-33.

Cenci MA. Presynaptic Mechanisms of l-DOPA-Induced Dyskinesia: The Findings, the Debate, and the Therapeutic Implications. Front Neurol. 2014; 5:242.

Chalon S, Garreau L, Emond P, Zimmer L, Vilar MP, Besnard J-C, et al. Pharmacological characterization of (E)-N-(3-iodoprop-2-enyl)-2β-carbomethoxy-3β-(4'-methylphenyl)nortropane as a selective and potent inhibitor of the neuronal dopamine transporter. J Pharmacol Exp 1999; 291:648–654.

Chang LT. A method of attenuation correction in radionuclide computed tomography. 1978; IEEE Trans Nucl Sci 25: 638-643.

Charcot JM. De la paralysie agitante. In Oeuvres Complètes (t 1) Leçons sur les maladies du système nerveux. 1877. Paris. A Delahaye. pp. 155–188.

Cilia R, Akpalu A, Sarfo FS, Cham M, Amboni M, Cereda E, et al. The modern pre-levodopa era of Parkinson's disease: insights into motor complications from sub-Saharan Africa. Brain. 2014; 137(Pt 10):2731-42.

Chaudhuri KR, Odin P, Antonini A, Martinez-Martin P. Parkinson's disease: the non-motor issues. Parkinsonism Relat Disord. 2011; 17(10):717-23.

Ciliax BJ, Heilman C, Demchyshyn LL, Pristupa ZB, Ince E, Hersch SM, et al. The dopamine transporter: immunochemical characterization and localization in brain. J Neurosci 1995; 15: 1714-23.

Conti MM, Ostock CY, Lindenbach D, Goldenberg AA, Kampton E, Dell'isola R, et al. Effects of prolonged selective serotonin reuptake inhibition on the development and expression of L-DOPA-induced dyskinesia in hemi-parkinsonian rats. Neuropharmacology 2014; 77: 1-8.

Cortés R, Soriano E, Pazos A, Probst A, Palacios JM. Autoradiography of antidepressant binding sites in the human brain: localization using [3H]imipramine and [3H]paroxetine. Neuroscience. 1988; 27(2):473-96.

Cotzias GC, Van Woert MH, Schiffer LM. Aromatic amino acids and modification of parkinsonism. N Engl J Med 1967; 276:374–379.

Cotzias GC, Papavasiliou PS, Gellene R. Modification of Parkinsonism--chronic treatment with L-dopa. N Engl J Med. 1969; 280(7):337-45.

Crum WR, Hartkens T, Hill DL. Non-rigid image registration: theory and practice. Br J Radiol. 2004; 77 Spec No 2:S140-53.

de la Fuente-Fernández R, Lu JQ, Sossi V, Jivan S, Schulzer M, Holden JE, et al. Biochemical variations in the synaptic level of dopamine precede motor fluctuations in Parkinson's disease: PET evidence of increased dopamine turnover. Ann Neurol 2001; 49: 298-303.

de la Fuente-Fernández R, Sossi V, Huang Z, Furtado S, Lu JQ, Calne DB et al. Levodopa-induced changes in synaptic dopamine levels increase with progression of Parkinson's disease: implications for dyskinesias. Brain 2004; 127: 2747-54.

Damier P, Hirsch EC, Agid Y, Graybiel AM. The substantia nigra of the human brain. II. Patterns of loss of dopamine containing neurons in Parkinson's disease. Brain 1999; 122:1437-48.

Darcourt J, Booij J, Tatsch K, Varrone A, Vander Borght T, Kapucu OL, et al. EANM procedure guidelines for brain neurotransmission SPECT using (123)I-

labelled dopamine transporter ligands, version 2. Eur J Nucl Med Mol Imaging. 2010; 37(2):443-50.

Deep-Brain Stimulation for Parkinson's Disease Study Group. Deep-brain stimulation of the subthalamic nucleus or the pars interna of the globus pallidus in Parkinson's disease. N Engl J Med. 2001; 345(13):956-63.

Duvernoy HM. The human brain: surface, blood supply, and three-dimensional sectional anatomy. 2nd edition. Springer. 1999.

Ehringer H and Hornykiewicz O. Distribution of noradrenaline and dopamine (3-hydroxytyramine in the human brain and their behavior in diseases of the extrapyramidal system. Klin Wochenschr. 1960; 38:1236-9.

Ekesbo A, Rydin E, Torstenson R, Sydow O, Låengström B, Tedroff J. Dopamine autoreceptor function is lost in advanced Parkinson's disease. Neurology. 1999; 52(1):120-5.

Elia AE, Dollenz C, Soliveri P, Albanese A. Motor features and response to oral levodopa in patients with Parkinson's disease under continuous dopaminergic infusion or deep brain stimulation. Eur J Neurol. 2012; 19:76–83.

Emond P, Garreau L, Chalon S, Boazi M, Caillet M, Bricard J, et al. Synthesis and ligand binding of nortropane derivatives: N-substituted- 2β-carbomethoxy-3β-(4′-iodophenyl)nortropane and N-(3- iodoprop-2E-enyl)-2β-carbomethoxy-3β-(3′,4′-disubstituted phenyl)nortropane. New affinity and selectivity compounds for the dopamine transporter. J Med Chem 1997; 40:1366– 1372

197

European Medicines Agency. 2011. Summary of product characteristics of DaTSCAN 74 MBq/ml solution for injection. http://www.ema.europa.eu/docs/en_GB/document_library/EPAR_-_Product_Information/human/000266/WC500035355.pdf.

Fahn S, Elton RL, UPDRS program members. Unified Parkinsons Disease Rating Scale. In: Fahn S, Marsden CD, Goldstein M, Calne DB, editors. Recent developments in Parkinsons disease, vol 2. Florham Park, NJ: Macmillan Healthcare Information; 1987. p 153–163.

Fahn S, Oakes D, Shoulson I, Kieburtz K, Rudolph A, Lang A, et al. Levodopa and the progression of Parkinson's disease. N Engl J Med. 2004; 351(24):2498-508.

Fahn S. Does levodopa slow or hasten the rate of progression of Parkinson's disease? J Neurol. 2005; 252:iv37–42.

Fahn S. The medical treatment of Parkinson disease from James Parkinson to George Cotzias. Mov Disord. 2015; 30(1):4-18.

Farde L, Halldin C, Stone-Elander S, Sedvall G. PET analysis of human dopamine receptor subtypes using 11C-SCH 23390 and 11C-raclopride. Psychopharmacology (Berl). 1987; 92(3):278-84.

Farde L, Eriksson L, Blomquist G, Halldin C. Kinetic analysis of central [11C]raclopride binding to D2-dopamine receptors studied by PET--a comparison to the equilibrium analysis. J Cereb Blood Flow Metab. 1989; 9(5):696-708.

Farde L, von Bahr C. Distribution of remoxipride to the human brain and central D2-dopamine receptor binding examined in vivo by PET. Acta Psychiatr Scand Suppl. 1990; 358:67-71.

Fearnley JM, Lees AJ. Ageing and Parkinson's disease: substantia nigra regional selectivity. Brain. 1991; 114:2283-301.

Food and Drug Administration. Center for Drug Evaluation and Research. Silver Spring, Maryland, USA; 2011. http://www.accessdata.fda.gov/drugsatfda_docs/nda/2011/022454sOrig1 s000Lbl.pdf.

Folstein MF, Folstein SE, McHugh PR. "Mini-mental state". A practical method for grading the cognitive state of patients for the clinician. J Psychiatr Res. 1975; 12(3):189-98.

Freed C, Revay R, Vaughan RA, Kriek E, Grant S, Uhl GR, Kuhar MJ. Dopamine transporter immunoreactivity in rat brain. J Comp Neurol 1995; 359:340 –349.

Garnett ES, Firnau G, Nahmias C. Dopamine visualized in the basal ganglia of living man. Nature. 1983; 305(5930):137-8.

Gelb DJ, Oliver E, Gilman S. Diagnostic criteria for Parkinson disease. Arch Neurol. 1999; 56(1):33-9.

Ginovart N, Wilson AA, Meyer JH, Hussey D, Houle S. Positron emission tomography quantification of [(11)C]-DASB binding to the human serotonin transporter: modeling strategies. J Cereb Blood Flow Metab 2001; 21: 1342-53.

Giros B, el Mestikawy S, Bertrand L, Caron MG. Cloning and functional characterization of a cocaine-sensitive dopamine transporter. FEBS Lett. 1991; 295(1-3):149-54.

Giros B, Caron MG. Molecular characterization of the dopamine transporter. Trends Pharmacol Sci. 1993; 14(2):43-9.

Goetz CG, Stebbins GT, Shale HM, Lang AE, Chernik DA, Chmura TA, et al. Utility of an objective dyskinesia rating scale for Parkinson's disease: inter- and intrarater reliability assessment. Mov Disord. 1994; 9(4):390-4.

Goetz CG, Fahn S, Martinez-Martin P, Poewe W, Sampaio C, Stebbins GT, et al. Movement Disorder Society-sponsored revision of the Unified Parkinson's Disease Rating Scale (MDS-UPDRS): Process, format, and clinimetric testing plan. Mov Disord. 2007; 22(1):41-7

Grandas F, Galiano ML, Tabernero C. Risk factors for levodopa-induced dyskinesias in Parkinson's disease. J Neurol 1999; 246: 1127-33.

Gunn RN, Lammertsma AA, Hume SP, Cunningham VJ. Parametric imaging of ligand-receptor binding in PET using a simplified reference region model. Neuroimage. 1997; 6: 279-87.

Gunn RN, Coello C, Searle GE. Molecular Imaging And Kinetic Analysis Toolbox (MIAKAT) - A Quantitative Software Package for the Analysis of PET Neuroimaging Data. J Nucl Med. 2016; 57 supp.: 2 1928.

Guy W. ECDEU Assessment Manual for Psychopharmacology: Revised (DHEW publication number ADM 76-338). Rockville, MD, US Department of Health, Education and Welfare, Public Health Service, Alcohol, Drug Abuse and Mental Health Administration, NIMH Psychopharmacology Research Branch, Division of Extramural Research Programs. 1976: 534–7.

Hall H, Farde L, Sedvall G. Human dopamine receptor subtypes--in vitro binding analysis using 3H-SCH 23390 and 3H-raclopride. J Neural Transm. 1988; 73(1):7-21.

Hall H, Halldin C, Guilloteau D, Besnard J-C, Emond P, Chalon S, et al. Specific visualization of the dopamine transporter in the human brain post-mortem with thenew selective ligand [125I]PE2I. Neuroimage 1999; 9:108–116.

Halldin C, Erixon-Lindroth N, Pauli S, Chou YH, Okubo Y, Karlsson P, et al. [(11)C]PE2I: a highly selective radioligand for PET examination of the dopamine transporter in monkey and human brain. Eur J Nucl Med Mol Imaging. 2003; 30(9):1220-30.

Hamilton M. A rating scale for depression. J Neurol Neurosurg Psychiatry. 1960; 23:56-62.

Hammers A, Allom R, Koepp MJ, Free SL, Myers R, Lemieux L, et al. Three-dimensional maximum probability atlas of the human brain, with particular reference to the temporal lobe. Hum Brain Mapp. 2003; 19(4):224-47.

Heiss WD, Herholz K. Brain receptor imaging. J Nucl Med. 2006; 47(2):302-12.

Hersch SM, Yi H, Heilman CJ, Edwards RH, Levey AI. Subcellular localization and molecular topology of the dopamine transporter in the striatum and substantia nigra. J Comp Neurol 1997; 388:211–227.

Hinson VK, Goetz CG, Leurgans S, Fan W, Nguyen T, Hsu A. Reducing dosing frequency of carbidopa/levodopa: double-blind crossover study comparing twice-daily bilayer formulation of carbidopa/levodopa (IPX054) versus 4 daily doses of standard carbidopa/levodopa in stable Parkinson disease patients. Clin Neuropharmacol. 2009; 32(4):189-92.

Hoehn MM, Yahr MD. Parkinsonism: onset, progression and mortality. Neurology. 1967;17(5):427-42.

Hoffman BJ, Mezey E, Brownstein MJ. Cloning of a serotonin transporter affected by antidepressants. Science. 1991; 254(5031):579-80.

Holden M, Hill DL, Denton ER, Jarosz JM, Cox TC, Rohlfing T, et al. Voxel similarity measures for 3-D serial MR brain image registration. IEEE Trans Med Imaging. 2000; 19(2): 94-102.

Holden M. A review of geometric transformations for nonrigid body registration. IEEE Trans Med Imaging. 2008; 27(1):111-28.

Holloway RG, Shoulson I, Fahn S, Kieburtz K, Lang A, Marek K, et al. Pramipexole vs levodopa as initial treatment for Parkinson disease: a 4-year randomized controlled trial. Arch Neurol. 2004; 61(7):1044-53.

Hong JY, Oh JS, Lee I, Sunwoo MK, Ham JH, Lee JE, et al. Presynaptic dopamine depletion predicts levodopa-induced dyskinesia in de novo Parkinson disease. Neurology. 2014; 82(18):1597-604.

Hornykiewicz O. The tropical localization and content of noradrenalin and dopamine (3-hydroxytyramine) in the substantia nigra of normal persons and patients with Parkinson's disease. Wien Klin Wochenschr. 1963; 75:309-12.

Houle S, Ginovart N, Hussey D, Meyer JH, Wilson AA. Imaging the serotonin transporter with positron emission tomography: initial human studies with [11C]DAPP and [11C]DASB. Eur J Nucl Med. 2000; 27(11):1719-22.

Hughes AJ, Daniel SE, Kilford L, Lees AJ. Accuracy of clinical diagnosis of idiopathic Parkinson's disease: a clinico-pathological study of 100 cases. J Neurol Neurosurg Psychiatry. 1992; 55(3):181-4.

Ichise M, Meyer JH, Yonekura Y. An introduction to PET and SPECT neuroreceptorquantification models. J Nucl Med. 2001; 42(5):755-63.

Ichise M, Liow JS, Lu JQ, Takano A, Model K, Toyama H, et al. Linearized reference tissue parametric imaging methods: application to [11C]DASB positron emission tomography studies of the serotonin transporter in human brain. J Cereb Blood Flow Metab. 2003; 23(9):1096-112.

Innis RB, Cunningham VJ, Delforge J, Fujita M, Gjedde A, Gunn RN, et al. Consensus nomenclature for in vivo imaging of reversibly binding radioligands. J Cereb Blood Flow Metab. 2007; 27(9):1533-9.

Ishibashi K, Ishii K, Oda K, Kawasaki K, Mizusawa H, Ishiwata K et al. Regional analysis of age-related decline in dopamine transporters and dopamine D2-like receptors in human striatum. Synapse. 2009; 63(4):282-90.

Jucaite A, Odano I, Olsson H, Pauli S, Halldin C, Farde L. Quantitative analyses of regional [11C]PE2I binding to the dopamine transporter in the human brain: a PET study. Eur J Nucl Med Mol Imaging. 2006; 33(6):657-68.

Kannari K, Shen H, Arai A, Tomiyama M, Baba M. Reuptake of L-DOPA-derived extracellular dopamine in the striatum with dopaminergic denervation via serotonin transporters. Neurosci Lett 2006; 402: 62-5.

Kim JH, Chang WS, Jung HH, Chang JW2. Effect of Subthalamic Deep Brain Stimulation on Levodopa-Induced Dyskinesia in Parkinson's Disease. Yonsei Med J. 2015; 56(5):1316-21.

Kish SJ, Furukawa Y, Chang LJ, Tong J, Ginovart N, Wilson A, et al. Regional distribution of serotonin transporter protein in postmortem human brain: is the cerebellum a SERT-free brain region? Nucl Med Biol 2005; 32: 123-8.

Kish SJ, Tong J, Hornykiewicz O, Rajput A, Chang LJ, Guttman M, et al. Preferential loss of serotonin markers in caudate versus putamen in Parkinson's disease. Brain 2008; 131: 120-31.

Koch W, Radau PE, Hamann C, Tatsch K. Clinical testing of an optimized software solution for an automated, observer-independent evaluation of dopamine transporter SPECT studies. J Nucl Med. 2005; 46: 1109-18.

Koeppe RA, Frey KA, Kuhl DE, Kilbourn MR. Assessment of extrastriatal vesicular monoamine transporter binding site density using stereoisomers of [11C]dihydrotetrabenazine. J Cereb Blood Flow Metab. 1999; 19(12):1376-84.

Koopman KE, la Fleur SE, Fliers E, Serlie MJ, Booij J. Assessing the optimal time point for the measurement of extrastriatal serotonin transporter binding with 123I-FP-CIT SPECT in healthy, male subjects. J Nucl Med. 2012; 53, 1087-1090.

Kostic V, Przedborski S, Flaster E, Sternic N. Early development of levodopa-induced dyskinesias and response fluctuations in young-onset Parkinson's disease. Neurology. 1991; 41(2 ( Pt 1)):202-5.

Krack P, Pollak P, Limousin P, Hoffmann D, Benazzouz A, Le Bas JF, et al. Opposite motor effects of pallidal stimulation in Parkinson's disease. Ann Neurol. 1998; 43(2):180-92.

Kuikka JT, Bergström KA, Ahonen A, Länsimies E. The dosimetry of iodine-123 labelled 2 beta-carbomethoxy-3 beta-(4-iodophenyl)tropane. Eur J Nucl Med. 1994; 21(1):53-6.

Laakso A, Bergman J, Haaparanta M, Vilkman H, Solin O, Hietala J. [18F]CFT [(18F)WIN 35,428], a radioligand to study the dopamine transporter with PET: characterization in human subjects. Synapse. 1998; 28(3):244-50.

Lammertsma AA, Bench CJ, Hume SP, Osman S, Gunn K, Brooks DJ, et al. Comparison of methods for analysis of clinical [11C]raclopride studies. J Cereb Blood Flow Metab. 1996; 16(1):42-52.

Lammertsma AA, Hume SP. Simplified reference tissue model for PET receptor studies. Neuroimage. 1996; 4(3Pt 1):153-8.

Laruelle M, Vanisberg MA, Maloteaux JM. Regional and subcellular localization in human brain of [3H] paroxetine binding, a marker of serotonin uptake sites. Biol Psychiatry 1988; 24:299-309.

Laruelle M, Wallace E, Seibyl JP, Baldwin RM, Zea-Ponce Y, Zoghbi SS, et al. Graphical, kinetic, and equilibrium analyses of in vivo [123I] beta-CIT binding to dopamine transporters in healthy human subjects. J Cereb Blood Flow Metab. 1994; 14(6):982-94.

Lee CS, Kim SJ, Oh SJ, Kim HO, Yun SC, Doudet D, et al. Uneven age effects of [(18)F]FP-CIT binding in the striatum of Parkinson's disease. Ann Nucl Med. 2014; 28(9):874-9.

Lee JY, Seo SH, Kim YK, Yoo HB, Kim YE, Song IC, et al. Extrastriatal dopaminergic changes in Parkinson's disease patients with impulse control disorders. J Neurol Neurosurg Psychiatry. 2014; 85(1):23-30.

Lee JY, Seo S, Lee JS, Kim HJ, Kim YK, Jeon BS. Putaminal serotonergic innervation: monitoring dyskinesia risk in Parkinson disease. Neurology. 2015; 85(10):853-60.

Leenders KL, Palmer AJ, Quinn N, Clark JC, Firnau G, Garnett ES, et al. Brain dopamine metabolism in patients with Parkinson's disease measured with positron emission tomography. J Neurol Neurosurg Psychiatry 1986; 49: 853-60.

Leentjens AF, Verhey FR, Lousberg R, Spitsbergen H, Wilmink FW. The validity of the Hamilton and Montgomery-Asberg depression rating scales as screening and diagnostic tools for depression in Parkinson's disease. Int J Geriatr Psychiatry. 2000a; 15(7):644-9.

Leentjens AF, Verhey FR, Luijckx GJ, Troost J. The validity of the Beck Depression Inventory as a screening and diagnostic instrument for depression in patients with Parkinson's disease. Mov Disord. 2000b; 15(6):1221-4.

Levy R, Dostrovsky JO, Lang AE, Sime E, Hutchison WD, Lozano AM. Effects of apomorphine on subthalamic nucleus and globus pallidus internus neurons in patients with Parkinson's disease. J Neurophysiol. 2001; 86(1):249-60.

Li X, Zhuang P, Li Y. Altered Neuronal Firing Pattern of the Basal Ganglia Nucleus Plays a Role in Levodopa-Induced Dyskinesia in Patients with Parkinson's Disease. Front Hum Neurosci. 2015; 9:630.

Lin KJ, Weng YH, Wey SP, Hsiao IT, Lu CS, Skovronsky D, et al. Whole-body biodistribution and radiation dosimetry of 18F-FP-(+)-DTBZ (18F-AV-133): a novel vesicular monoamine transporter 2 imaging agent. J Nucl Med. 2010; 51(9):1480-5.

Logan J, Fowler JS, Volkow ND, Wang GJ, Ding YS, Alexoff DL. Distribution volume ratios without blood sampling from graphical analysis of PET data. J Cereb Blood Flow Metab 1996; 16: 834-40.

Lu JQ, Ichise M, Liow JS, Ghose S, Vines D, Innis RB. Biodistribution and radiation dosimetry of the serotonin transporter ligand 11C-DASB determined from human whole-body PET. J Nucl Med. 2004; 45(9):1555–9.

Lundkvist C, Halldin C, Swahn CG, Hall H, Karlsson P, Nakashima Y, et al. [O-methyl-11C]beta-CIT-FP, a potential radioligand for quantitation of the dopamine transporter: preparation, autoradiography, metabolite studies, and positron emission tomography examinations. Nucl Med Biol. 1995; 22(7):905–913.

Maeda T, Nagata K, Yoshida Y, Kannari K. Serotonergic hyperinnervation into the dopaminergic denervated striatum compensates for dopamine conversion from exogenously administered l-DOPA. Brain Res 2005; 1046: 230-3.

Maratos EC, Jackson MJ, Pearce RK, Cannizzaro C, Jenner P. Both short- and long-acting D-1/D-2 dopamine agonists induce less dyskinesia than L-DOPA in the MPTP-lesioned common marmoset (Callithrix jacchus). Exp Neurol. 2003; 179(1):90-102.

Masson J, Sagne C, Hamon M, El Mestikawy S. Neurotransmitter transporters in the central nervous system. Pharmacol Rev 1999; 51:439–464.

Marek K, Innis R, van Dyck C, Fussell B, Early M, Eberly S, et al. [123I]beta-CIT SPECT imaging assessment of the rate of Parkinson's disease progression. Neurology. 2001; 57(11):2089-94.

Mazziotta JC, Toga AW, Evans A, Fox P, Lancaster J. A probabilistic atlas of the human brain: theory and rationale for its development. The International Consortium for Brain Mapping (ICBM). Neuroimage. 1995; 2(2):89-101.

McGonigle P, Molinoff PB. Receptors and signal transduction: classification and quantitation. In: Siegel GJ, Agranoff BW, Albers RW, Molinoff PB, et al. Basic Neurochemistry. Lippincott–Raven; 1994:209 –230.

Merello M, Nouzeilles MI, Cammarota A, Leiguarda R. Effect of memantine (NMDA antagonist) on Parkinson's disease: a double-blind crossover randomized study. Clin Neuropharmacol. 1999; 22(5):273-6.

Metman LV, Del Dotto P, LePoole K, Konitsiotis S, Fang J, Chase TN. Amantadine for levodopa-induced dyskinesias: a 1-year follow-up study. Arch Neurol. 1999; (11):1383-6.

Meyer JH, Ichise M. Modeling of receptor ligand data in PET and SPECT imaging: a review of major approaches. J Neuroimaging. 2001; 11(1):30-9.

Meyer PT, Sattler B, Winz OH, Fundke R, Oehlwein C, Kendziorra K, et al. Kinetic analyses of [123I]IBZM SPECT for quantification of striatal dopamine D2 receptor binding: a critical evaluation of the single-scan approach. Neuroimage. 2008; 42(2):548-58.

Mintun MA, Raichle ME, Kilbourn MR, Wooten GF, Welch MJ. A quantitative model for the in vivo assessment of drug binding sites with positron emission tomography. Ann Neurol. 1984; 15(3):217-27.

Montastruc JL, Rascol O, Senard JM, Rascol A. A randomised controlled study comparing bromocriptine to which levodopa was later added, with levodopa

alone in previously untreated patients with Parkinson's disease: a five year follow up. J Neurol Neurosurg Psychiatry. 1994; 57(9):1034-8.

Montgomery AJ, Thielemans K, Mehta MA, Turkheimer F, Mustafovic S, Grasby PM. Correction of head movement on PET studies: comparison of methods. J Nucl Med. 2006; 47(12):1936-44.

Morton RJ, Guy MJ, Clauss R, Hinton PJ, Marshall CA, Clarke EA. Comparison of different methods of DatSCAN quantification. Nucl Med Commun. 2005; 26(12):1139-46.

Mukherjee J, Christian BT, Dunigan KA, Shi B, Narayanan TK, Satter M, et al. Brain imaging of 18F-fallypride in normal volunteers: blood analysis, distribution, test-retest studies, and preliminary assessment of sensitivity to aging effects on dopamine D-2/D-3 receptors. Synapse. 2002; 46(3):170-88.

Muñoz A, Li Q, Gardoni F, Marcello E, Qin C, Carlsson T, et al. Combined 5-HT1A and 5-HT1B receptor agonists for the treatment of L-DOPA-induced dyskinesia. Brain 2008; 131: 3380-94.

Nelson N. The family of Na+/Cl- neurotransmitter transporters. J Neurochem 1998; 71:1785–1803.

Neumeyer JL, Wang S, Gao Y, Milius RA, Kula NS, Campbell A, et al. N-omega-fluoroalkyl analogs of (1R)-2 beta-carbomethoxy-3 beta-(4-iodophenyl)-tropane (beta-CIT): radiotracers for positron emission tomography and single photon emission computed tomography imaging of dopamine transporters. J Med Chem. 1994; 37(11):1558-61.

Nevalainen N, Af Bjerkén S, Gerhardt GA, Strömberg I. Serotonergic nerve fibers in L-DOPA-derived dopamine release and dyskinesia. Neuroscience 2014; 260: 73-86.

Ng KY, Chase TN, Colburn RW, Kopin IJ. Dopa-induced release of cerebral monoamines. Science. 1970; 170:76-7.

Ng KY, Colburn RW, Kopin IJ. Effects of L-dopa on efflux of cerebral monoamines from synaptosomes. Nature. 1971; 230:331–2.

Nutt JG, Holford NH. The response to levodopa in Parkinson's disease: imposing pharmacological law and order. Ann Neurol. 1996; 39(5):561-73.

Østergaard K, Sunde N, Dupont E. Effects of bilateral stimulation of the subthalamic nucleus in patients with severe Parkinson's disease and motor fluctuations. Mov Disord. 2002; 17(4):693-700.

Oertel WH, Wolters E, Sampaio C, Gimenez-Roldan S, Bergamasco B, Dujardin M, et al. Pergolide versus levodopa monotherapy in early Parkinson's disease patients: The PELMOPET study. Mov Disord. 2006; 21(3):343-53.

Olanow WC, Kieburtz K, Rascol O, Poewe W, Schapira AH, Emre M, et al. Factors predictive of the development of Levodopa-induced dyskinesia and wearing-off in Parkinson's disease. Mov Disord 2013; 28: 1064-71.

Olanow CW, Kieburtz K, Odin P, Espay AJ, Standaert DG, Fernandez HH et al. Continuous intrajejunal infusion of levodopa-carbidopa intestinal gel for patients with advanced Parkinson's disease: a randomised, controlled, double-blind, double-dummy study. Lancet Neurol. 2014; 13(2):141-9.

Oliveira FP, Tavares JM. Medical image registration: a review. Comput Methods Biomech Biomed Engin. 2014; 17(2):73-93.

Ory–Magne F, Corvol JC, Azulay JP, Bonnet AM, Brefel-Courbon C, Damier P, et al. Withdrawing amantadine in dyskinetic patients with Parkinson disease: the AMANDYSK trial. Neurology. 2014; 82(4):300-7.

Pahwa R, Tanner CM, Hauser RA, Sethi K, Isaacson S, Truong D. Amantadine extended release for levodopa-induced dyskinesia in Parkinson's disease (EASED Study). Mov Disord. 2015; 30(6):788-95.

Papa SM, Desimone R, Fiorani M, Oldfield EH. Internal globus pallidus discharge is nearly suppressed during levodopa-induced dyskinesias. Ann Neurol. 1999; 46(5):732-8.

Parkinson J. An essay on the shaking palsy. London. Whittingham and Rowland for Sherwood, Neely and Jones; 1817.

Parkinson Study Group. Dopamine transporter brain imaging to assess the effects of pramipexole vs levodopa on Parkinson disease progression. JAMA. 2002; 287(13):1653-61.

Parkinson's UK. Parkinson's prevalence in the United Kingdom in 2009. http://www.parkinsons.org.uk/sites/default/files/parkinsonsprevalenceuk_0.pdf

Pavese N, Evans AH, Tai YF, Hotton G, Brooks DJ, Lees AJ, et al. Clinical correlates of levodopa-induced dopamine release in Parkinson disease: a PET study. Neurology 2006; 67: 1612-7.

Piccini P, Brooks DJ, Björklund A, Gunn RN, Grasby PM, Rimoldi O, et al. Dopamine release from nigral transplants visualized in vivo in a Parkinson's patient. Nat Neurosci 1999; 2: 1137-40.

Piccini P, Pavese N, Brooks DJ. Endogenous dopamine release after pharmacological challenges in Parkinson's disease. Ann Neurol. 2003a; 53(5):647-53.

Piccini P. Dopamine transporter: basic aspects and neuroimaging. Mov Disord 2003b; 18 (Suppl 7): S3–8.

Pickut BA, van der Linden C, Dethy S, Van De Maele H, de Beyl DZ. Intestinal levodopa infusion: the Belgian experience. Neurol Sci. 2014; 35(6):861-6.

Pirker W, Holler I, Gerschlager W, Asenbaum S, Zettinig G, Brücke T. Measuring the rate of progression of Parkinson's disease over a 5-year period with beta-CIT SPECT. Mov Disord. 2003; 18(11):1266-72.

Politis M, Wu K, Loane C, Kiferle L, Molloy S, Brooks DJ, et al. Staging of serotonergic dysfunction in Parkinson's disease: an in vivo 11C-DASB PET study. Neurobiol Dis 2010; 40: 216-21.

Politis M, Wu K, Loane C, Brooks DJ, Kiferle L, Turkheimer FE, et al. Serotonergic mechanisms responsible for levodopa-induced dyskinesias in Parkinson's disease patients. J Clin Invest 2014; 124: 1340-9.

Pristupa ZB, McConkey F, Liu F, Man HY, Lee FJ, Wang YT, Niznik HB. Protein kinase-mediated bidirectional trafficking and functional regulation of the human dopamine transporter. Synapse 1998; 30:79–87.

Radau PE, Linke R, Slomka PJ, Tatsch K. Optimization of automated quantification of 123I-IBZM uptake in the striatum applied to parkinsonism. J Nucl Med. 2000; 41(2):220-7.

Radau PE, Slomka PJ, Julin P, Svensson L, Wahlund LO. Evaluation of linear registration algorithms for brain SPECT and the errors due to hypoperfusion lesions. Med Phys. 2001; 28(8):1660-8.

Rakshi JS, Uema T, Ito K, Bailey DL, Morrish PK, Ashburner J, et al. Frontal, midbrain and striatal dopaminergic function in early and advanced Parkinson's disease A 3D [(18)F]dopa-PET study. Brain. 1999; 122 ( Pt 9):1637-50.

Rascol O, Brooks DJ, Korczyn AD, De Deyn PP, Clarke CE, Lang AE. A five-year study of the incidence of dyskinesia in patients with early Parkinson's disease who were treated with ropinirole or levodopa. N Engl J Med. 2000; 342(20):1484-91.

Ribeiro MJ, Ricard M, Lièvre MA, Bourgeois S, Emond P, Gervais P, et al. Whole-body distribution and radiation dosimetry of the dopamine transporter radioligand [(11)C]PE2I in healthy volunteers. Nucl Med Biol. 2007; 34(4):465-70.

Rorden C, Brett M. Stereotaxic display of brain lesions. Behav Neurol. 2000; 12(4): 191-200.

Russmann H, Ghika J, Combrement P, Villemure JG, Bogousslavsky J, Burkhard PR, et al. L-dopa-induced dyskinesia improvement after STN-DBS depends upon medication reduction. Neurology 2004; 63:153-5.

Scherfler C, Nocker M. Dopamine transporter SPECT: how to remove subjectivity? Mov Disord. 2009; 24 Suppl 2:S721–S724.

Schrag A, Quinn N. Dyskinesias and motor fluctuations in Parkinson's disease. A community-based study. Brain 2000; 123: 2297-305.

Seki C, Ito H, Ichimiya T, Arakawa R, Ikoma Y, Shidahara M, et al. Quantitative analysis of dopamine transporters in human brain using [11C]PE2I and positron emission tomography: evaluation of reference tissue models. Ann Nucl Med. 2010; 24(4):249-60.

Shimada S, Kitayama S, Lin CL, Patel A, Nanthakumar E, Gregor P, et al. Cloning and expression of a cocaine-sensitive dopamine transporter complementary DNA. Science. 1991; 254(5031):576-8.

Shingai Y, Tateno A, Arakawa R, Sakayori T, Kim W, Suzuki H, et al. Age-related decline in dopamine transporter in human brain using PET with a new radioligand [$^{18}$F]FE-PE2I. Ann Nucl Med. 2014; 28(3):220-6.

Siessmeier T, Zhou Y, Buchholz HG, Landvogt C, Vernaleken I, Piel M, et al. Parametric mapping of binding in human brain of D2 receptor ligands of different affinities. J Nucl Med. 2005; 46(6):964-72.

Simonin C, Tir M, Devos D, Kreisler A, Dujardin K, Salleron J, et al. Reduced levodopa-induced complications after 5 years of subthalamic stimulation in Parkinson's disease: a second honeymoon. J Neurol. 2009;256(10):1736-41.

Smith SM. Fast robust automated brain extraction. Hum Brain Mapp. 2002; 17(3):143-55.

Snow BJ, Macdonald L, Mcauley D, Wallis W. The effect of amantadine on levodopa-induced dyskinesias in Parkinson's disease: a double-blind, placebo-controlled study. Clin Neuropharmacol. 2000; 23(2):82-5.

Sossi V, de la Fuente-Fernández R, Schulzer M, Adams J, Stoessl J. Age-related differences in levodopa dynamics in Parkinson's: implications for motor complications. Brain 2006; 129: 1050-8.

Studholme C, Hill DLG, Hawkes DJ. An overlap invariant entropy measure of 3D medical image alignment. Pattern Recognition 1999; 32: 71−86.

Suwijn SR, Berendse HW, Verschuur CV, Winogrodzka A, de Bie RM, Booij J. SERT-to-DAT ratios in early Parkinson's disease do not correlate with the development of dyskinesias. EJNMMI Res 2013; 3: 44.

Svenningsson P, Rosenblad C, Af Edholm Arvidsson K, Wictorin K, Keywood C, Shankar B, et al. Eltoprazine counteracts l-DOPA-induced dyskinesias in Parkinson's disease: a dose-finding study. Brain. 2015; 138(Pt 4):963-73.

Tanaka H, Kannari K, Maeda T, Tomiyama M, Suda T, Matsunaga M. Role of serotonergic neurons in L-DOPA-derived extracellular dopamine in the striatum of 6-OHDA-lesioned rats. Neuroreport 1999; 10: 631-4.

Tedroff J, Pedersen M, Aquilonius SM, Hartvig P, Jacobsson G, Långström B. Levodopa-induced changes in synaptic dopamine in patients with Parkinson's disease as measured by [11C]raclopride displacement and PET. Neurology 1996; 46: 1430-6.

Timpka J, Fox T, Fox K, Honig H, Odin P, Martinez-Martin P et al. Improvement of dyskinesias with l-dopa infusion in advanced Parkinson's disease. Acta Neurol Scand. Acta Neurol Scand. 2016; 133(6):451-8.

Towey DJ, Bain PG, Nijran KS. Automatic classification of 123I-FP-CIT (DaTSCAN) SPECT images. Nucl Med Commun. 2011; 32(8):699-707.

215

Troiano AR, de la Fuente-Fernandez R, Sossi V, Schulzer M, Mak E, Ruth TJ et al. PET demonstrates reduced dopamine transporter expression in PD with dyskinesias. Neurology. 2009; 72(14):1211-6.

Tziortzi AC, Searle GE, Tzimopoulou S, Salinas C, Beaver JD, Jenkinson M, et al. Imaging dopamine receptors in humans with [11C]-(+)-PHNO: dissection of D3 signal and anatomy. Neuroimage. 2011; 54(1):264-77.

Varrone A, Tóth M, Steiger C, Takano A, Guilloteau D, Ichise M, et al. Kinetic analysis and quantification of the dopamine transporter in the nonhuman primate brain with 11C-PE2I and 18F-FE-PE2I. J Nucl Med. 2011; 52(1):132-9.

Varanese S, Howard J, Di Rocco A. NMDA antagonist memantine improves levodopa-induced dyskinesias and "on-off" phenomena in Parkinson's disease. Mov Disord. 2010; 25(4):508-10.

Verhagen Metman L, Del Dotto P, van den Munckhof P, Fang J, Mouradian MM, Chase TN. Amantadine as treatment for dyskinesias and motor fluctuations in Parkinson's disease. Neurology. 1998; 50(5):1323-6.

Volkow ND, Wang GJ, Fowler JS, Logan J, Schlyer D, Hitzemann R, et al. Imaging endogenous dopamine competition with [11C]raclopride in the human brain. Synapse. 1994; 16(4):255-62.

Volkow ND, Wang GJ, Gatley SJ, Fowler JS, Ding YS, Logan J, et al. Temporal relationships between the pharmacokinetics of methylphenidate in the human brain and its behavioral and cardiovascular effects. Psychopharmacology (Berl). 1996; 123(1):26-33.

Wickremaratchi MM, Knipe MD, Sastry BS, Morgan E, Jones A, Salmon R, et al. The motor phenotype of Parkinson's disease in relation to age at onset. Mov Disord 2011; 26: 457-63.

Willeit M, Ginovart N, Kapur S, Houle S, Hussey D, Seeman P, et al. High-affinity states of human brain dopamine D2/3 receptors imaged by the agonist [11C]-(+)-PHNO. Biol Psychiatry. 2006; 59(5):389-94.

Wilson AA, Ginovart N, Schmidt M, Meyer JH, Threlkeld PG, Houle S. Novel radiotracers for imaging the serotonin transporter by positron emission tomography: Synthesis, radiosynthesis, and in vitro and ex vivo evaluation of 11C-labeled 2-(phenylthio)araalkylamines. 2000a; J Med Chem 43:3103–3110.

Wilson AA, Garcia A, Jin L, Houle S. Radiotracer synthesis from [11C]-iodomethane: a remarkably simple captive solvent method. 2000b; Nucl Med Biol 27:529–532.

Wictorin K, Widner H. Memantine and reduced time with dyskinesia in Parkinson's Disease. Acta Neurol Scand. 2016; 133(5):355-60.

Wolf E, Seppi K, Katzenschlager R, Hochschorner G, Ransmayr G, Schwingenschuh P. Long-term antidyskinetic efficacy of amantadine in Parkinson's disease. Mov Disord. 2010; 25(10):1357-63.

Worrall DM, Williams DC. Sodium ion-dependent transporters for neurotransmitters: a review of recent developments. Biochem J. 1994; 297:425– 436.

Yokoi T, Soma T, Shinohara H, Matsuda H. Accuracy and reproducibility of co-registration techniques based on mutual information and normalized mutual information for MRI and SPECT brain images. Ann Nucl Med. 2004; 18(8):659-67.

Zhao YJ, Wee HL, Chan YH, Seah SH, Au WL, Lau PN, et al. Progression of Parkinson's disease as evaluated by Hoehn and Yahr stage transition times. Mov Disord. 2010; 25(6):710-6.

Zhou FC, Tao-Cheng JH, Segu L, Patel T, Wang Y. Serotonin transporters are located on the axons beyond the synaptic junctions: anatomical and functional evidence. Brain Res 1998; 805:241-54.

# Appendices

## Appendix I – Queen Square Brain Bank diagnostic criteria for idiopathic Parkinson's disease (Hughes et al., 1992)

Step 1. Diagnosis of Parkinsonian Syndrome

• Bradykinesia (slowness of initiation of voluntary movement with progressive reduction in speed and amplitude of repetitive actions)

• And at least one of the following:
> • muscular rigidity
> • 4-6 Hz rest tremor
> • postural instability not caused by primary visual, vestibular, cerebellar, or proprioceptive dysfunction

Step 2 Exclusion criteria for Parkinson's disease

• history of repeated strokes with stepwise progression of parkinsonian features
• history of repeated head injury
• history of definite encephalitis
• oculogyric crises
• neuroleptic treatment at onset of symptoms
• more than one affected relative
• sustained remission
• strictly unilateral features after 3 years
• supranuclear gaze palsy
• cerebellar signs
• early severe autonomic involvement
• early severe dementia with disturbances of memory, language, and praxis
• Babinski sign
• presence of cerebral tumor or communication hydrocephalus on imaging study
• negative response to large doses of levodopa in absence of malabsorption
• MPTP exposure

Step 3 supportive prospective positive criteria for Parkinson's disease

(Three or more required for diagnosis of definite Parkinson's disease)
• Unilateral onset
• Rest tremor present
• Progressive disorder
• Persistent asymmetry affecting side of onset most
• Excellent response (70-100%) to levodopa
• Severe levodopa-induced chorea
• Levodopa response for 5 years or more
• Clinical course of ten years or more

# Appendix II

## Unified Parkinson's disease rating scale (UPDRS)
(Goetz et al., 2007)

## Part I
Intellectual Impairment
0 – none
1 – mild (consistent forgetfulness with partial recollection of events with no other difficulties)
2 – moderate memory loss with disorientation and moderate difficulty handling complex problems
3 – severe memory loss with disorientation to time and often place, severe impairment with problems
4 – severe memory loss with orientation only to person, unable to make judgments or solve problems. Requires much help with personal care. Cannot be left alone at all.

Thought Disorder
0 – none
1 – vivid dreaming
2 – "benign" hallucination with insight retained
3 – occasional to frequent hallucination or delusions without insight, could interfere with daily activities
4 – persistent hallucination, delusions, or florid psychosis. Not able to care for self.

Depression
0 – not present
1 – periods of sadness or guilt greater than normal, never sustained for more than a few days or a week
2 – sustained depression for >1 week
3 – sustained depression with vegetative symptoms (insomnia, anorexia, abulia, weight loss)
4 – sustained depression with vegetative symptoms with suicidal thought or intent

Motivation/Initiative
0 – normal
1 – less assertive than usual, more passive
2 – loss of initiative or disinterest in elective (nonroutine) activities
3 – loss of initiative or disinterest in day to say (routine) activities
4 – withdrawn, complete loss of motivation

## Part II
Speech
0 – normal
1 – mildly affected, no difficulty being understood
2 – moderately affected, sometimes asked to repeat statements
3 – severely affected, frequently asked to repeat statements
4 – unintelligible most of the time

Salivation
0 – normal
1 – slight but definite excess of saliva in mouth; may have nighttime drooling
2 – moderately excessive saliva; may have minimal drooling
3 – marked excess of saliva with some drooling
4 – marked drooling, requires constant tissue or handkerchief

Swallowing
0 – normal
1 – rare choking
2 – occasional choking
3 – requires soft food
4 – requires NG tube or gastronomy feeding

Handwriting
0 – normal
1 – slightly small or slow
2 – moderately slow or small; all words are legible
3 – severely affected; not all words are legible
4 – the majority of the words are not legible

Cutting food and handing Utensils
0 – normal
1 – somewhat slow and clumsy, but no help needed
2 – can cut most foods, although clumsy and slow; some help needed
3 – food must be cut by someone, but can still feed slowly
4 – needs to be fed

Dressing
0 – normal
1 – somewhat slow, but no help needed
2 – occasional assistance with buttoning, getting arms in sleeves
3 – considerable help required, but can do some things alone
4 – helpless

Hygiene
0 – normal
1 – somewhat slow but no help needed
2 – needs help to shower or bathe; or very slow in hygienic care
3 – requires assistance for washing, brushing teeth, combing hair, going to bathroom
4 – foley catheter or other mechanical aids

Turning in Bed/ Adjusting Bed Clothes
0 – normal
1 – somewhat slow and clumsy, but no help needed
2 – can turn alone or adjust sheets but, with great difficulty
3 – can initiate, but not turn or adjust sheets alone
4 – helpless

Falling (unrelated to freezing)

0 – none
1 – rare falling
2 – occasional falls, less than once per day
3 – falls on average of once daily
4 – falls more than once daily

Freezing when walking
0 – normal
1 – rare freezing when walking, may have have start–hesitation
2 – occasional freezing when walking,
3 – frequent freezing, occasionally falls from freezing
4 – frequent falls from freezing

Walking
0 – normal
1 – mild difficulty, may not swing arms or may tend to drag legs
2 – moderate difficultly, but requires little or no assistance
3 – severe disturbance of walking, requiring assistance
4 – cannot walk at all, even with assistance

Tremor
0 – absent
1 – slight and infrequently present
2 – moderate; bothersome to patient
3 – severe; interfere with many activities
4 – marked; interferes with most activities

Sensory complaints Related to Parkinsonism
0 – none
1 – occasionally has numbness, tingling, and mild aching
2 – frequently has numbness, tingling, or aching; not distressing
3 – frequently painful sensations
4 – excruciating pain

# Part III

Speech
0 – normal
1 – slight loss of expression, diction, volume
2 – monotone, slurred but understandable, moderate impaired
3 – marked impairment, difficult to understand
4 – unintelligible

Facial Expression
0 – Normal
1 – slight hypomymia, could be poker face
2 – slight but definite abnormal diminution in expression
3 – mod. hypomimia, lips parted some of time
4 – masked or fixed face, lips parted 1/4 of inch or more with complete loss of expression

Tremor at Rest
Face
0 – absent
1 – slight and infrequent
2 – mild and present most of time
3 – moderate and present most of time
4 – marked and present most of time

Right Upper Extremity
0 – absent
1 – slight and infrequent
2 – mild and present most of time
3 – moderate and present most of time
4 – marked and present most of time

Left Upper Extremity
0 – absent
1 – slight and infrequent
2 – mild and present most of time
3 – moderate and present most of time
4 – marked and present most of time

Right Lower Extremity
0 – absent
1 – slight and infrequent
2 – mild and present most of time
3 – moderate and present most of time
4 – marked and present most of time

Left Lower Extremity
0 – absent
1 – slight and infrequent
2 – mild and present most of time
3 – moderate and present most of time
4 – marked and present most of time

Action or Postural Tremor
Right Upper Extremity
0 – absent
1 – slight, present with action
2 – moderate, present with action
3 – moderate present with action and posture holding
4 – marked, interferes with feeding

Left Upper Extremity
0 – absent
1 – slight, present with action
2 – moderate, present with action
3 – moderate present with action and posture holding
4 – marked, interferes with feeding

Rigidity
Neck
0 – absent
1 – slight or only with activation
2 – mild/moderate
3 – marked, full range of motion
4 – severe
Right Upper Extremity
0 – absent
1 – slight or only with activation
2 – mild/moderate
3 – marked, full range of motion
4 – severe
Left Upper Extremity
0 – absent
1 – slight or only with activation
2 – mild/moderate
3 – marked, full range of motion
4 – severe
Right Lower Extremity
0 – absent
1 – slight or only with activation
2 – mild/moderate
3 – marked, full range of motion
4 – severe

Left Lower Extremity
0 – absent
1 – slight or only with activation
2 – mild/moderate
3 – marked, full range of motion
4 – severe

Finger taps
Right
0 – normal
1 – mild slowing, and/or reduction in amplitude
2 – moderately impaired; definite and early fatiguing, may have occasional arrests
3 – severely impaired; frequent hesitations and arrests
4 – can barely perform
Left
0 – normal
1 – mild slowing, and/or reduction in amplitude
2 – moderately impaired; definite and early fatiguing, may have occasional arrests
3 – severely impaired; frequent hesitations and arrests
4 – can barely perform

Hand Movements (open and close hands in rapid succession)
Right
0 – normal

1 – mild slowing, and/or reduction in amplitude
2 – moderately impaired; definite and early fatiguing, may have occasional arrests
3 – severely impaired, frequent hesitations and arrests
4 – can barely perform
Left
0 – normal
1 – mild slowing, and/or reduction in amplitude
2 – moderately impaired; definite and early fatiguing, may have occasional arrests
3 – severely impaired; frequent hesitations and arrests
4 – can barely perform

Rapid Alternating Movements (pronation and supination)
Right
0 – normal
1 – mild slowing, and or reduction in amplitude
2 – moderately impaired; definite and early fatiguing, may have occasional arrests
3 – severely impaired; frequent hesitations and arrests
4 – can barely perform
Left
0 – normal
1 – mild slowing, and/or reduction in amplitude
2 – moderately impaired; definite and early fatiguing, may have occasional arrests
3 – severely impaired; frequent hesitations and arrests
4 – can barely perform

Leg Agility (tap heel on ground, amplitude should be 3 inches)
Right
0 – normal
1 – mild slowing, and/or reduction in amplitude
2 – moderately impaired; definite and early fatiguing, may have occasional arrests
3 – severely impaired; frequent hesitations and arrests
4 – can barely perform
Left
0 – normal
1 – mild slowing, and/or reduction in amplitude
2 – moderately impaired; definite and early fatiguing, may have occasional arrests
3 – severely impaired; frequent hesitations and arrests
4 – can barely perform

Arising From Chair (patient arises with arms folded across chest)
0 – normal
1 – slow, may need more than one attempt
2 – pushes self up from arms or seat
3 – tends to fall back, may need multiple tries but can arise without assistance
4 – unable to arise without help

Posture
0 – normal erect
1 – slightly stooped, could be normal for older person
2 – definitely abnormal, moderately stooped, may lean to one side

3 – severely stooped with kyphosis
4 – marked flexion with extreme abnormality of posture

Gait
0 – normal
1 – walks slowly, may shuffle with short steps, no festination or propulsion
2 – walks with difficulty, little or no assistance, some festination, short steps or propulsion
3 – severe disturbance, frequent assistance
4 – cannot walk

Postural Stability (retropulsion test)
0 – normal
1 – recovers unaided
2 – would fall if not caught
3 – falls spontaneously
4 – unable to stand

Body Bradykinesia/ Hypokinesia
0 – none
1 – minimal slowness, could be normal, deliberate character
2 – mild slowness and poverty of movement, definitely abnormal, or decreased amplitude of movement
3 – moderate slowness, poverty, or small amplitude
4 – marked slowness, poverty, or amplitude

# Part IV

A. Dyskinesias

Duration: What proportion of the waking day are dyskinesias present? (Historical information.)
0 – none
1 – 1–25% of day
2 – 26–50% of day
3 – 51–75% of day
4 – 76–100% of day


Disability: How disabling are the dyskinesias? (Historical information; may be modified by office examintation)
0 – not disabling
1 – mildly disabling
2 – moderately disabling
3 – severely disabling
4 – completely disabled

Painful Dyskinesias: How painful are the dyskinesias?
0 – no painful dyskinesias
1 – slight
2 – moderate

3 – severe
4 – marked

Presence of Early Morning Dystonia (Historical information.)
0 – no
1 – yes


B. Clinical Fluctuations

Are "off" periods predictable?
0 – no
1 – yes

Are "off" periods unpredictable?
0 – no
1 – yes

Do "off" periods come on suddenly, within a few seconds?
0 – no
1 – yes

What proportion of the waking day is the patient "off" on average?
0 – none
1 – 1–25% of day.
2 – 26–50% of day.
3 – 51–75% of day.
4 – 76–100% of day.

C. Other Complications

Does the patient have anorexia, nausea, or vomiting?
0 – no
1 – yes

Any sleep disturbances, such as insomnia or hypersomnolence?
0 – no
1 – yes

Does the patient have symptomatic orthostasis? (Record the patient's blood pressure, height and weight on the scoring form)
0 – no
1 – yes

# Appendix III

## Hoehn & Yahr staging scale
(Hoehn and Yahr. 1967)

| Stages | |
|---|---|
| 1 | Unilateral involvement only usually with minimal or no functional disability |
| 2 | Bilateral or midline involvement without impairment of balance |
| 3 | Bilateral disease: mild to moderate disability with impaired postural reflexes; physically independent |
| 4 | Severely disabling disease; still able to walk or stand unassisted |
| 5 | Confinement to bed or wheelchair unless aided |

# Appendix IV

## Calculation of levodopa equivalent doses
(as in Politis et al., 2014)

Calculation of dopaminergic–levodopa equivalent dose ($LED_{Total}$):

---

**$LED_{Total}$\* (mg) =** (1 X levodopa) + (0.77 X levodopa CR) + (1.43 X levodopa + entacapone) + (1.11 X levodopa CR + entacapone) + (20 X ropinirole) + (20 X ropinirole PR + (100 X pramipexole) + (30 X rotigotine) + (10 X bromocriptine) + (8 X apomorphine) + (100 X pergolide) + (67 X cabergoline)

---

\*In levodopa / carbidopa or benserazide hydrochloride, only levodopa is calculated; PR, CR stands for controlled/prolonged release preparations

---

Calculation of levodopa (only) equivalent dose ($LED_{Ldopa}$):

---

**$LED_{Ldopa}$\* (mg) =** (1 X levodopa) + (0.77 X levodopa CR) + (1.43 X levodopa + entacapone) + (1.11 X levodopa CR + entacapone)

---

\*In levodopa / carbidopa or benserazide hydrochloride, only levodopa is calculated; CR stands for controlled release preparations

---

Calculation of dopamine–receptor agonist equivalent dose ($LED_{Dag}$):

---

**$LED_{Dag}$\* (mg) =** (20 X ropinirole) + (20 X ropinirole PR + (100 X pramipexole) + (30 X rotigotine) + (10 X bromocriptine) + (8 X apomorphine) + (100 X pergolide) + (67 X cabergoline)

---

\*In levodopa / carbidopa or benserazide hydrochloride, only levodopa is calculated; PR stands for prolonged release preparations

---

229

# Appendix V
## Abnormal Involuntary Movements Scale (AIMS) (Guy. 1976)

| Complete Examination Procedure (attachment d.) before making ratings | | 0 = None<br>1 = Minimal, may be extreme normal<br>2 = Mild<br>3 = Moderate<br>4 = Severe | | | |
|---|---|---|---|---|---|
| MOVEMENT RATINGS: Rate highest severity observed. Rate movements that occur upon activation one <u>less</u> than those observed spontaneously. Circle movement as well as code number that applies. | | date/time | date/time | date/time | date/time |
| Facial and Oral Movements | 1. Muscles of Facial Expression<br>   e.g. movements of forehead, eyebrows periorbital area, cheeks, including frowning blinking, smiling, grimacing | 0 1 2 3 4 | 0 1 2 3 4 | 0 1 2 3 4 | 0 1 2 3 4 |
| | 2. Lips and Perioral Area<br>   e.g., puckering, pouting, smacking | 0 1 2 3 4 | 0 1 2 3 4 | 0 1 2 3 4 | 0 1 2 3 4 |
| | 3. Jaw e.g. biting, clenching, chewing, mouth opening, lateral movement | 0 1 2 3 4 | 0 1 2 3 4 | 0 1 2 3 4 | 0 1 2 3 4 |
| | 4. Tongue Rate only increases in movement both in and out of mouth. NOT inability to sustain movement. Darting in and out of mouth. | 0 1 2 3 4 | 0 1 2 3 4 | 0 1 2 3 4 | 0 1 2 3 4 |
| Extremity Movements | 5. Upper (arms, wrists, hands, fingers) Include choreic movements (i.e., rapid, objectively purposeless, irregular, spontaneous) athetoid movements (i.e., slow, irregular, complex, serpentine). DO NOT INCLUDE TREMOR (i.e., repetitive, regular, rhythmic) | 0 1 2 3 4 | 0 1 2 3 4 | 0 1 2 3 4 | 0 1 2 3 4 |
| | 6. Lower (legs, knees, ankles, toes)<br>   e.g., lateral knee movement, foot tapping, heel dropping, foot squirming, inversion and eversion of foot. | 0 1 2 3 4 | 0 1 2 3 4 | 0 1 2 3 4 | 0 1 2 3 4 |
| Trunk Movements | 7. Neck, shoulders, hips e.g., rocking, twisting, squirming, pelvic gyrations | 0 1 2 3 4 | 0 1 2 3 4 | 0 1 2 3 4 | 0 1 2 3 4 |
| Global Judgments | 8. Severity of abnormal movements overall | 0 1 2 3 4 | 0 1 2 3 4 | 0 1 2 3 4 | 0 1 2 3 4 |
| | 9. Incapacitation due to abnormal Movements | 0 1 2 3 4 | 0 1 2 3 4 | 0 1 2 3 4 | 0 1 2 3 4 |
| | 10. Patient's awareness of abnormal movements. Rate only patient's report<br>No awareness 0<br>Aware, no distress 1<br>Aware, mild distress 2<br>Aware, moderate distress 3<br>Aware, severe distress 4 | 0<br>1<br>2<br>3<br>4 | 0<br>1<br>2<br>3<br>4 | 0<br>1<br>2<br>3<br>4 | 0<br>1<br>2<br>3<br>4 |
| Dental Status | 11. Current problems with teeth and/or Dentures | Yes/No | Yes/No | Yes/No | Yes/No |
| | 12. Are dentures usually worn? | Yes/No | Yes/No | Yes/No | Yes/No |
| | 13. Edentia? | Yes/No | Yes/No | Yes/No | Yes/No |
| | 14. Do movements disappear in sleep? | Yes/No | Yes/No | Yes/No | Yes/No |

# Appendix VI

## Rush dyskinesia rating scale
(Goetz et al., 1994)


1. View the patient walk, drink from a cup, put on a coat and button clothing.

2. Rate the severity of dyskinesias. These may include chorea, dystonia, and other dyskinetic movements in combination. Rate the patient's worst function.

3. Check which dyskinesia you see (more than one response possible, please tick or list).

4. Check the type of dyskinesia that is causing the most disability on the tasks seen on the tape (only one response permitted).

Severity rating code

0 – absent;
1 – minimal severity no interference with voluntary motor acts;
2 – dyskinesias may impair voluntary movements but patient is normally capable of undertaking most motor acts;
3 – intense interference with movement control and daily life activities are greatly limited;
4 – violent dyskinesias; incompatible with any normal motor task.

| Severity of worst dyskinesia observed | Dyskinesias present (more than one choice possible) | | | Most disabling dyskinesia (choose one) | | |
|---|---|---|---|---|---|---|
| | Chorea (C) | Dystonia (D) | Other (List) | C | D | Other |

# Appendix VII

# The Hamilton Depression Rating Scale (HAM–D)
(Hamilton. 1960)

The HAM–D is designed to rate the severity of depression in patients.

1. Depressed mood (Gloomy attitude, pessimism about the future, feeling of sadness, tendency to weep)
0 – absent
1 – sadness, etc.
2 – occasional weeping
3 – frequent weeping
4 – extreme symptoms

2. Feelings of guilt
0 – absent
1 – self-reproach, feels he/she has let people down
2 – ideas of guilt
3 – present illness is a punishment; delusions of guilt
4 – hallucinations of guilt

3. Suicide
0 – absent
1 – feels life is not worth living
2 – wishes he/she were dead
3 – suicidal ideas or gestures
4 – attempts at suicide

4. Insomnia: initial (Difficulty in falling asleep)
0 – absent
1 – occasional
2 – frequent

5. Insomnia: middle (Complains of being restless and disturbed during the night. Waking during the night)
0 – absent
1 – occasional
2 – frequent

6. Insomnia: delayed (Waking in early hours of the morning and unable to fall asleep again)
0 – absent
1 – occasional
2 – frequent

7. Work and interest
0 – no difficulty
1 – feelings of incapacity, listlessness, indecision and vacillation
2 – loss of interest in hobbies, decreased social activities

3 – productivity decreased
4 – unable to work. Stopped working because of present illness only (absence from work
    after treatment or recovery may rate a lower score)

8. Retardation (slowness of thought, speech, and activity; apathy; stupor)
0 – absent
1 – slight retardation at interview
2 – obvious retardation at interview
3 – interview difficult
4 – complete stupor

9. Agitation (restlessness associated with anxiety)
0 – absent
1 – fidgetiness
2 – playing with hands, hair, etc
3 – moving about, can't sit still
4 – hand wringing, nail biting, hair–pulling, biting of lips

10. Anxiety – psychic
0 – no difficulty
1 – subject tension and irritability
2 – worrying about minor matters
3 – apprehensive attitude apparent in face or speech
4 – fears expressed without questioning

11. Anxiety – somatic
0 – absent
1 – mild
2 – moderate
3 – severe
4 – incapacitating

12. Somatic symptoms – gastrointestinal (loss of appetite, heavy feeling in abdomen;
constipation)
0 – absent
1 – mild; loss of appetite but eating without encouragement from others. Food intake about
    normal
2 – severel difficulty eating without urging from others. Marked reduction of appetite and
    food intake

13. Somatic symptoms – general (heaviness in limbs, back or head; diffuse backache; loss of
energy and fatiguability)
0 – absent
1 – mild; heabiness in limbs, back or head. Backaches, headache, muscle aches. Loss of
    energy and fatigability
2 – severe; any clear–cut symptom rates 2

14. Genital symptoms (loss of libido, impaired sexual performance, menstrual disturbances)
0 – absent
1 – mild

2 – severe

15. Hypohondriachis
0 – not present
1 – self-absorption (bodily)
2 – preoccupation with health
3 – frequent complaints, requests for help, etc.
4 – hypochondriacal delusions

16. Weight loss (when rating by history)
0 – no weight loss
1 – probably weight loss associated with present illness
2 – obvious or severe

17. Insight (insight must be interpreted in terms of patient's understanding and background)
0 – acknowledges being depressed and ill
1 – partial or doubtfull loss of insight
2 – loss of insight

18. Diurinal variation
A. Whether symptoms are worse in morning or evening. If NO diurnal variation, make none
0 – no variation
1 – worse in AM
2 – worse in PM
B. When present, mark the severity of the variation. Mark "none" if NO variation
0 – none
1 – mild
2 – severe

19. Depersonalisation and derealisation (feelings of unreality, nihilistic ideas)
0 – absent
1 – mild
2 – moderate
3 – severe
4 – incapacitating

20. Paranoid symptoms (not with a depressive quality)
0 – none
1 – suspicious
2 – ideas of reference
3 – delusions of reference and persecution
4 – hallucinations, persecutory

21. Obsessional symptoms (obsessive thoughts and compulsions against which the patient
     struggles)
0 – absent
1 – mild
2 – severe

Total score_____

# Appendix VIII

## Beck Depression Inventory (BDI)
(Beck et al., 1961)
(this depression inventory can be self–scored)

Inventory Item 1.
0 – I do not feel sad.
1 – I feel sad
2 – I am sad all the time and I can't snap out of it.
3 – I am so sad and unhappy that I can't stand it.

Inventory Item 2.
0 – I am not particularly discouraged about the future.
1 – I feel discouraged about the future.
2 – I feel I have nothing to look forward to.
3 – I feel the future is hopeless and that things cannot improve.

Inventory Item 3.
0 – I do not feel like a failure.
1 – I feel I have failed more than the average person.
2 – As I look back on my life, all I can see is a lot of failures.
3 –I feel I am a complete failure as a person.

Inventory Item 4.
0 – I get as much satisfaction out of things as I used to.
1 – I don't enjoy things the way I used to.
2 – I don't get real satisfaction out of anything anymore.
3 – I am dissatisfied or bored with everything.

Inventory Item 5.
0 – I don't feel particularly guilty
1 – I feel guilty a good part of the time.
2 – I feel quite guilty most of the time.
3 – I feel guilty all of the time.

Inventory Item 6.
0 – I don't feel I am being punished.
1 – I feel I may be punished.
2 – I expect to be punished.
3 – I feel I am being punished.

Inventory Item 7.
0 – I don't feel disappointed in myself.
1 – I am disappointed in myself.
2 – I am disgusted with myself.
3 – I hate myself.

Inventory Item 8.
0 – I don't feel I am any worse than anybody else.
1 – I am critical of myself for my weaknesses or mistakes.
2 – I blame myself all the time for my faults.
3 – I blame myself for everything bad that happens.

Inventory Item 9.
0 – I don't have any thoughts of killing myself.
1 – I have thoughts of killing myself, but I would not carry them out.
2 – I would like to kill myself.
3 – I would kill myself if I had the chance.

Inventory Item 10.
0 – I don't cry any more than usual.
1 – I cry more now than I used to.
2 – I cry all the time now.
3 – I used to be able to cry, but now I can't cry even though I want to.

Inventory Item 11.
0 – I am no more irritated by things than I ever was.
1 – I am slightly more irritated now than usual.
2 – I am quite annoyed or irritated a good deal of the time.
3 – I feel irritated all the time.

Inventory Item 12.
0 – I have not lost interest in other people.
1 – I am less interested in other people than I used to be.
2 – I have lost most of my interest in other people.
3 – I have lost all of my interest in other people.

Inventory Item 13.
0 – I make decisions about as well as I ever could.
1 – I put off making decisions more than I used to.
2 – I have greater difficulty in making decisions more than I used to.
3 – I can't make decisions at all anymore.

Inventory Item 14.
0 – I don't feel that I look any worse than I used to.
1 – I am worried that I am looking old or unattractive.
2 – I feel there are permanent changes in my appearance that make me look unattractive
3 – I believe that I look ugly.

Inventory Item 15.
0 – I can work about as well as before.
1 – It takes an extra effort to get started at doing something.
2 – I have to push myself very hard to do anything.
3 – I can't do any work at all.

Inventory Item 16.
0 – I can sleep as well as usual.

1 – I don't sleep as well as I used to.
2 – I wake up 1-2 hours earlier than usual and find it hard to get back to sleep.
3 – I wake up several hours earlier than I used to and cannot get back to sleep.

Inventory Item 17.
0 – I don't get more tired than usual.
1 – I get tired more easily than I used to.
2 – I get tired from doing almost anything.
3 – I am too tired to do anything.

Inventory Item 18.
0 – My appetite is no worse than usual.
1 – My appetite is not as good as it used to be.
2 – My appetite is much worse now.
3 – I have no appetite at all anymore.

Inventory Item 19.
0 – I haven't lost much weight, if any, lately.
1 – I have lost more than five pounds.
2 – I have lost more than ten pounds.
3 – I have lost more than fifteen pounds.

Inventory Item 20.
0 – I am no more worried about my health than usual.
1 – I am worried about physical problems like aches, pains, upset stomach, or constipation.
2 – I am very worried about physical problems and it's hard to think of much else.
3 – I am so worried about my physical problems that I cannot think of anything else.
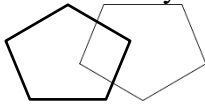
Inventory Item 21.
0 – I have not noticed any recent change in my interest in sex.
1 – I am less interested in sex than I used to be.
2 – I have almost no interest in sex.
3 – I have lost interest in sex completely.

# Appendix IX

## Mini–Mental State Examination
(Folstein et al., 1975)

Instructions: Ask the questions in the order listed. Score one point for each correct response within each question or activity.

| Maximum score | Patient's Score | Questions |
|---|---|---|
| 5 | / / / / | i. What is the year? Season? Date? Day of the week? Month? |
| 5 | / / / / | ii. Where are we now: State? County? Town/city? Hospital? Floor? |
| 3 | / / / | iii. The examiner names three unrelated objects clearly and slowly, then asks the patient to name all three of them. The patient's response is used for scoring. The examiner repeats them until patient learns all of them, if possible. Number of trials: __ |
| 5 | / / / / | iv. "I would like you to count backward from 100 by sevens." (93, 86, 79, 72, 65, …) Stop after five answers.  Alternative: "Spell WORLD backwards." (D-L-R-O-W) |
| 3 | / / / | v. "Earlier I told you the names of three things. Can you tell me what those were?" |
| 2 | / | vi. Show the patient two simple objects, such as a wristwatch and a pencil, and ask the patient to name them. |
| 1 | | vii. "Repeat the phrase: 'No ifs, ands, or buts.'" |
| 3 | / / / | viii. "Take the paper in your right hand, fold it in half, and put it on the floor." (The examiner gives the patient a piece of blank paper.) |
| 1 | | ix. "Please read this and do what it says." (Written instruction is "Close your eyes.") |
| 1 | | x. "Make up and write a sentence about anything." (This sentence must contain a noun and a verb.) |
| 1 | | xi. "Please copy this picture." (The examiner gives the patient a blank piece of paper and asks him/her to draw the symbol below.  All 10 angles must be present and two must intersect). |
| 30 | TOTAL | |